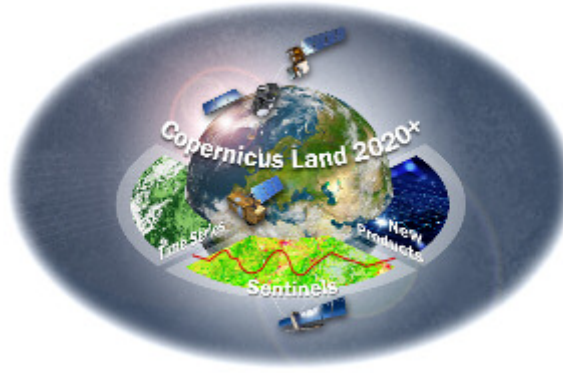


Horizon 2020
Space Call - Earth Observation: EO-3-2016: Evolution of Copernicus services
Grant Agreement No. 730008

ECoLaSS

Evolution of Copernicus Land Services based on Sentinel data



D12.1

"D42.1a - Prototype Report: Consistent HR Layer Time Series/Incremental Updates (Issue 1)"

Issue/Rev.: 1.0

Date Issued: 23.07.2018

submitted by:



in collaboration with the consortium partners:



submitted to:



European Commission – Research Executive Agency

This project has received funding from the European Union's Horizon 2020 Research and Innovation Programme, under Grant Agreement No. 730008.

CONSORTIUM PARTNERS

NO.	PARTICIPANT ORGANISATION NAME	SHORT NAME	CITY, COUNTRY
1	GAF AG	GAF	Munich, Germany
2	Systèmes d'Information à Référence Spatiale SAS	SIRS	Villeneuve d'Ascq, France
3	JOANNEUM RESEARCH Forschungsgesellschaft mbH	JR	Graz, Austria
4	Université catholique de Louvain, Earth and Life Institute (ELI)	UCL	Louvain-la-Neuve, Belgium
5	German Aerospace Center (DLR), German Remote Sensing Data Center (DFD), Weßling	DLR	Weßling, Germany

CONTACT:

GAF AG
Arnulfstr. 199 – D-80634 München – Germany
Phone: ++49 (0)89 121528 0 – FAX: ++49 (0)89 121528 79
E-mail: copernicus@gaf.de – Internet: www.gaf.de

DISCLAIMER:

The contents of this document are the copyright of GAF AG and Partners. It is released by GAF AG on the condition that it will not be copied in whole, in section or otherwise reproduced (whether by photographic, reprographic or any other method) and that the contents thereof shall not be divulged to any other person other than of the addressed (save to the other authorised officers of their organisation having a need to know such contents, for the purpose of which disclosure is made by GAF AG) without prior consent of GAF AG. Nevertheless single or common copyrights of the contributing partners remain unconditionally unaffected.

DOCUMENT RELEASE SHEET

	NAME, FUNCTION	DATE	SIGNATURE
Author(s):	David Herrmann (GAF), Giovanni Buzzo (GAF), Linda Moser (GAF), Christophe Sannier (SIRS), Alexandre Pennec (SIRS)	20.07.2018	
Review:	Markus Probeck (GAF) Sophie Villerot (SIRS)	21.07.2018	
Approval:	Linda Moser (GAF)	23.07.2018	
Acceptance:	Massimo Ciscato (REA)		
Distribution:	Public		

DISSEMINATION LEVEL

DISSEMINATION LEVEL		
PU	Public	<input checked="" type="checkbox"/>
CO	Confidential: only for members of the consortium (including the Commission Services)	

DOCUMENT STATUS SHEET

ISSUE/REV	DATE	PAGE(S)	DESCRIPTION / CHANGES
1.0	23.07.2018	76	First Issue of the Prototype Report on Consistent HR Layer Time Series and Incremental Updates

APPLICABLE DOCUMENTS

ID	DOCUMENT NAME / ISSUE DATE
AD01	Horizon 2020 Work Programme 2016 – 2017, 5 iii. Leadership in Enabling and Industrial Technologies – Space. Call: EO-3-2016: Evolution of Copernicus services. Issued: 13.10.2015
AD02	Guidance Document: Research Needs Of Copernicus Operational Services. Final Version issued: 30.10.2015
AD03	Proposal: Evolution of Copernicus Land Services based on Sentinel data. Proposal acronym: ECoLaSS, Proposal number: 730008. Submitted: 03.03.2016
AD04	Grant Agreement – ECoLaSS. Grant Agreement number: 730008 – ECoLaSS – H2020-EO-2016/H2020-EO-2016, Issued: 18.10.2016
AD05	D3.1 : D21.1a – Service Evolution Requirements Report (Issue 1), Issued: 09.08.2017
AD06	D7.1 : D32.1a - Methods Compendium: Time Series Preparation (Issue 1), Issued: 28.02.2018
AD07	D8.1 : D33.1a - Methods Compendium: Time Series Analysis for Thematic Classification (Issue 1), Issued: 29.03.2018
AD08	D9.1 : D34.1a - Methods Compendium: Time Series Analysis for Change Detection (Issue 1), Issued: 29.03.2018
AD09	D10.1 : D35.1- Methods Compendium: HRL Time Series Consistency for HRL Product Updates (Issue 1), Issued: 14.05.2018

EXECUTIVE SUMMARY

The Horizon 2020 (H2020) project, “Evolution of Copernicus Land Services based on Sentinel data” (ECoLaSS) addresses the H2020 Work Programme 5 iii. Leadership in Enabling and Industrial technologies - Space, specifically the Topic EO-3-2016: Evolution of Copernicus services. ECoLaSS is being conducted from 2017–2019 and aims at developing and prototypically demonstrating selected innovative products and methods for future next-generation operational Copernicus Land Monitoring Service (CLMS) products of the pan-European and Global Components. This will contribute to demonstrating operational readiness of the products finally suggested for implementation, and shall allow the key CLMS stakeholders (i.e. mainly the Entrusted European Entities (EEE), such as the European Environment Agency (EEA) and the Joint Research Centre (JRC)), to take informed decisions on potential procurement of the next generation of Copernicus Land services from 2020 onwards.

To achieve this goal, ECoLaSS makes full use of dense time series primarily of Sentinel-2 optical Earth Observation (EO) data as well as Sentinel-1 Synthetic Aperture Radar (SAR) data. Rapidly evolving scientific developments as well as user requirements are continuously analysed, in support of a future pan-European roll-out of new/improved CLMS products, and the potential transfer to global applications.

This Deliverable **D12.1a: “D42.1 - Prototype Report: Consistent HR Layer Time Series/Incremental Updates** constitutes a prototype report of the Work Package (WP) 42 which is working on developing improved status layers and proposed incremental update prototypes for the High Resolution Layer (HRL) Imperviousness and HRL Forest. The applied methodologies build directly on the methods and processing lines developed in Task 3, especially WP 33 “Time Series Analysis for Thematic Classification” and WP 34 “Time Series Analysis for Change Detection”. The demonstration of incremental updates is oriented towards the update frequency proposed in WP 35 “HRL Time Series Consistency for HRL Product (incremental) Updates”.

This document is structured as follows: After a short introduction on the purpose and scope of this WP, the HRL incremental update feasibility is analysed in chapter 2. Besides layer-specific background information, user requirements are taken into account which are relevant for the proposed prototypes. Chapter 3 provides an overview of the relevant demonstration sites in which the prototypes are finally implemented. In chapter 4 an overview of the applied methods is given. These have been developed and assessed in Task 3 and have been transferred to and applied in specific demonstration sites to implement the respective prototypes. The main results and outcomes are presented in chapter 5. First, input data, general pre-processing steps and the layer-specific prototype setup are presented, followed by the classification and validation results of the improved status layers for Imperviousness and Forest, which are analysed and discussed in detail. Subsequently, the selected change detection approaches and the incremental updates resulting thereof are presented, together with dedicated assessments, conclusions and proposed specifications. Finally, chapter 6 concludes the findings and provides an outlook on the activities and research aspects suggested for the second project phase.

The ECoLaSS project follows a two-phased approach of two times 18 months duration. This deliverable constitutes the first issue at month 18, in which preliminary results are presented. In the second 18-month project cycle, a second issue of this deliverable will be published, containing all relevant updates.

Table of Contents

1	INTRODUCTION	1
2	HRL INCREMENTAL UPDATE NEEDS AND FEASIBILITY.....	2
3	DEMONSTRATION SITES.....	5
3.1	DEMONSTRATION SITE SOUTH-WEST	6
3.2	DEMONSTRATION SITE NORTH	7
4	OVERVIEW OF APPLIED METHODS.....	9
4.1	METHODS FOR IMPLEMENTING A PROTOTYPE ON IMPERVIOUSNESS	9
4.1.1	Derivation of biophysical variables.....	9
4.1.2	Active learning Classification approach based on DAP profiles.....	10
4.2	METHODS FOR IMPLEMENTING A PROTOTYPE ON FOREST.....	11
5	PROTOTYPE IMPLEMENTATION.....	13
5.1	PROTOTYPE OF A POTENTIAL FUTURE HRL IMPERVIOUSNESS.....	13
5.1.1	Data and Processing Setup	13
5.1.1.1	Input Data	13
5.1.1.2	Pre-processing	14
5.1.1.3	Experimental Setup.....	16
5.1.2	Classification Results and Validation	25
5.1.2.1	Thematic accuracy	25
5.1.2.2	Discussion of the validation results	25
5.1.3	Change Detection and Incremental Update Results and Validation	28
5.2	PROTOTYPE OF A POTENTIAL FUTURE HRL FOREST	30
5.2.1	Data and Processing Setup	30
5.2.1.1	Input Data	30
5.2.1.2	Pre-processing	35
5.2.1.3	Experimental Setup.....	35
5.2.2	Classification Results and Validation	40
5.2.3	Change Detection and Incremental Update Results and Validation	52
5.3	PROTOTYPE SPECIFICATIONS	67
6	CONCLUSIONS AND OUTLOOK.....	73
REFERENCES.....		75

List of Figures

Figure 3-1: Biogeographic Regions of Europe (2015) and European ECoLaSS Demonstration Sites <i>(Map: © European Environment Agency; administrative boundaries: © EuroGeographics)</i>	5
Figure 3-2: Demonstration site South-West, with CLC 2012 background layer (<i>© EEA, © EuroGeographics for the administrative boundaries</i>).....	7
Figure 3-3: Demonstration site North with CLC 2012 background layer (<i>© EEA, © EuroGeographics for the administrative boundaries</i>)	8
Figure 4-1: Example of SSUs organised in a 5x5 10m grid.....	11
Figure 5-1: Theia Level-2A data production extent. (21.07.2018) Source: http://www.cesbio.ups-tlse.fr/multitemp/?page_id=7501	14
Figure 5-2: Reference calibration samples overlaid on the change mask.....	17
Figure 5-3: NDVI Sentinel-2 based maximum feature.....	18
Figure 5-4: SAR statistical features (NB: the 4 features have different value ranges and scaling)	19
Figure 5-5: Sentinel-2 based initial built-up and non-built-up mask for 2017	20
Figure 5-6: Sentinel-1 based initial built-up and non-built-up mask for 2017	21
Figure 5-7: Post-classification processing.....	23
Figure 5-8: Final HRL Imperviousness 2017 prototype for the South-West demonstration site.....	23
Figure 5-9: Final HRL Imperviousness Change 2015-2017 prototype for the South-West demonstration site	25
Figure 5-10: Case of omission (yellow dots) in isolated built-up features in the IMD 2017 prototype.....	26
Figure 5-11: Examples of commission errors in the IMD 2017 prototype	27
Figure 5-12: Example of calibration points for the newly detected built-up in 2017	28
Figure 5-13: Example of omission errors in 2015 (undetected built-up in 2015)	29
Figure 5-14: Example of commission errors in 2017, false built-up in 2017	29
Figure 5-15: Sentinel-2 coverage of the ECoLaSS demonstration site North in Sweden. (<i>contains modified Copernicus Sentinel data [2017]; © EuroGeographics for the administrative boundaries</i>).....	30
Figure 5-16: No. of Sentinel-2 scenes with maximum 60% cloud cover from 15-March to 15-August 2017 in the demonstration site North.....	31
Figure 5-17: Cloud cover percentages (y axis) per scene count (x axis) for relevant MGRS tiles	32
Figure 5-18: Sentinel-2 Data Score Layer (S2DSL): Number of cloud-free Sentinel-2 observations per pixel	33
Figure 5-19: Forest sample layer derived from the integrated Copernicus High Resolution Layers 2015 (<i>© EuroGeographics for the administrative boundaries</i>).....	34
Figure 5-20: Selected time features based on the BRIGHTNESS index (mean: upper right, 50% percentile: lower left, 75% percentile: lower right). Non-tree areas are illustrated in grey. Sentinel-2 is visualized for comparison (upper left). (<i>produced using modified Copernicus Sentinel data [2017]</i>)	39
Figure 5-21: Selected time features based on NDVI (maximum: upper right; 50% percentile: lower left) and NDWI (75% percentile: lower right). Non-tree areas are illustrated in grey. Sentinel-2 is visualized for comparison (upper left). (<i>produced using modified Copernicus Sentinel data [2017]</i>)	39
Figure 5-22: Internal evaluation model for the TCM 2017 classification	40
Figure 5-23: Feature importance of calculated time features for the TCM classification	41
Figure 5-24: Classified Tree Cover Mask 2017 in 10m spatial resolution (<i>© EuroGeographics for the administrative boundaries</i>)	42
Figure 5-25: Internal evaluation model for the DLT 2017 classification	43
Figure 5-26: Feature importance of calculated time features for the DLT 2017 classification.....	44
Figure 5-27: Improved Dominant Leaf Type 2017 in 10m spatial resolution (<i>© EuroGeographics for the administrative boundaries</i>).....	45
Figure 5-28: Statistics of the Dominant Leaf Type 2017 per Sentinel-2 tile and the whole demonstration site.....	46
Figure 5-29: Comparison of VHR_IMAGE_2015 (left) and the improved DLT 2017 in 10m spatial resolution (right) (<i>© Digital Globe, Inc. 2015, all rights reserved. Produced using modified Copernicus Sentinel data [2017]</i>)	47

Figure 5-30: Comparison of the 20m DLT 2015 (left) and the improved DLT 2017 in 10m spatial resolution (right). Corresponding Sentinel-2 scenes are presented in false-colour infrared (band combination: NIR-RED-GREEN). (© European Union, Copernicus Land Monitoring Service 2015, European Environment Agency (EEA))	47
Figure 5-31: Comparison of the 20m DLT 2015 (left) and the improved DLT 2017 in 10m spatial resolution (right). Corresponding Sentinel-2 scenes are presented in false-colour infrared (band combination: NIR-RED-GREEN). (© European Union, Copernicus Land Monitoring Service 2015, European Environment Agency (EEA))	48
Figure 5-32: Spatial extents of the 20m DLT 2015 (left) and 10m DLT 2017 (right) for the demonstration site North.....	48
Figure 5-33: VHR_IMAGE_2015 coverage for the demonstration site North; complemented by VHR1 data from the D2_MG2b_ECOL_011a dataset (highlighted in yellow) (© EuroGeographics for the administrative boundaries).....	49
Figure 5-34: Distribution of validation samples for the DLT 2017	51
Figure 5-35: Pixel-based raw (yet unfiltered) changes in tree cover caused by both, geometric imprecisions, edge effects and forest management activities.....	53
Figure 5-36: Distribution of the 24 AOIs for qualitative assessment of suitable MMUs for forest loss © EuroGeographics for the administrative boundaries	54
Figure 5-37: Different MMUs ranging from 0.5 ha (beige), 1 ha (yellow), 2 ha (green) and 3 ha (light blue) to 5 ha (dark blue)	54
Figure 5-38: Pixel-based and MMU filtered Tree Cover Change product	55
Figure 5-39: Examples of forest loss provided by the prototypic Incremental Update layer. Left: 20m Sentinel-2A scene from June 2016; right: Sentinel-2B scene from July 2017.....	56
Figure 5-40: Incremental Update Layer Tree Cover Change 2015-2017 in 20m spatial resolution (© EuroGeographics for the administrative boundaries)	57
Figure 5-41: Final statistics of the TCC layer per Sentinel-2 tile and for the whole demonstration site North.....	58
Figure 5-42: Detected losses within TCC layer in red (left) and number of cloud-free observations (right)	59
Figure 5-43: Distribution of validation segments for the TCC layer.....	60
Figure 5-44: Example for omission and commission errors of forest loss within the same plot in the TCC layer. Left: 20m Sentinel-2A scene from June 2016; right: Sentinel-2B scene from June 2017.	61
Figure 5-45: Example 1: Forest cover loss in demonstration site North: a) VHR_IMAGE_2015; b) D2_MG2b_ECOL_011a; c) D2_MG2b_ECOL_011a overlaid with improved 10m DLT 2017.....	63
Figure 5-46: Example 2: Forest cover loss in demonstration site North: a) VHR_IMAGE_2015; b) D2_MG2b_ECOL_011a; c) D2_MG2b_ECOL_011a overlaid with improved 10m DLT 2017.....	64
Figure 5-47: Example 3: Forest cover loss in demonstration site North: a) VHR_IMAGE_2015; b) D2_MG2b_ECOL_011a; c) D2_MG2b_ECOL_011a overlaid with improved 10m DLT 2017.....	65
Figure 5-48: Example 4: Forest cover loss in demonstration site North: a) VHR_IMAGE_2015; b) D2_MG2b_ECOL_011a; c) D2_MG2b_ECOL_011a overlaid with improved 10m DLT 2017.....	66

List of Tables

Table 3-1: Description of the ECoLaSS demonstration sites	6
Table 5-1: Used Sentinel-2 reflectance bands (adapted from Suhet, 2015).....	14
Table 5-2: SAR annual statistical features.....	18
Table 5-3: Specifications of the ‘classified change’ layer	24
Table 5-4: Confusion matrix of the internal validation of the IMD 2017 in demo site South-West (area-weighted).....	25
Table 5-5: Proportional distribution of detected changes within the IMC layer	28
Table 5-6: Land Cover statistics of the derived HRL 2015 sample layer.....	34
Table 5-7: Sample distribution of the initial training dataset.	35
Table 5-8: Set of calculated time features relevant for TCM and DLT 2017 classification.....	37
Table 5-9: Accuracy assessment results for the improved Primary Status Layer DLT 2017.....	50
Table 5-10: Initial accuracy assessment results for the Incremental Update Layer TCC	60
Table 5-11: Final accuracy assessment results for the Incremental Update Layer TCC.....	62
Table 5-12: Detailed specifications for the improved primary status layer Imperviousness 2017.....	68
Table 5-13: Detailed specifications for the Incremental Update Layer Imperviousness Change Classified.....	69
Table 5-14: Detailed specifications for the improved primary status layer Dominant Leaf Type 2017.....	70
Table 5-15: Detailed specifications for the Incremental Update Layer Tree Cover Change	71

Abbreviations

AD	Applicable Document
AL	Active Learning
AOI	Areas of Interest
ATCOR	Atmospheric and Topographic Correction
CI	Confidence Interval
CLC	CORINE Land Cover
CLMS	Copernicus Land Monitoring Service
CNES	Centre national d'études spatiales
CRM	Crop Mask
CRT	Crop Type
DAP	Differential Attribute Profile
DEM	Digital Elevation Model
DLT	Dominant Leaf Type
DMP	Differential Morphological Profile
DWH	Data Warehouse
ECoLaSS	Evolution of Copernicus Land Services based on Sentinel data
EEA	European Environment Agency
EEA-39	The 33 EEA member states plus the 6 cooperating Wets Balkan countries
EEE	Entrusted European Entities
EO	Earth Observation
EPSG	European Petroleum Survey Group
ESA	European Space Agency
EU	European Union
ETRS89	European Terrestrial Reference System 1989
FADSL	Forest Additional Support Layer
FOR	Forest
FP7	7 th Framework Programme for research of the EU
FRE	Flat Reflectance
FTS	Fast Track Service
GeoTIFF	Georeferenced TIFF (file format)
GHSL	Global Human Settlement Layer
GIO	GMES Initial Operations
GIS	Geographic Information System
GMES	Global Monitoring for Environment and Security
GRA	Grassland
H2020	Horizon 2020
HR	High Resolution
HRL	High Resolution Layer
IMC	Imperviousness Change Classified
IMD	Imperviousness Density
IMP	Imperviousness
INSPIRE	Infrastructure for Spatial Information in Europe
IRECI	Inverted Red-edge Chlorophyll Index
IRS	Indian Remote Sensing satellite
ISO	International Organisation for Standardisation
ITT	Invitation to Tender
JRC	Joint Research Centre
LC	Land Cover
LM	Land Monitoring
LU	Land Use
LUCAS	Land Use/Cover Area frame statistical Survey

LZW	Lempel-Ziv-Welch (data compression algorithm)
MACCS	Multi-sensor Atmospheric Correction and Cloud Screening
MAJA	MACCS-ATCOR Joint Algorithm
MAX	Maximum
MEAN	Arithmetic mean value
MGRS	Military Grid Reference System
MIN	Minimum
MMU	Minimum Mapping Unit
MSGI	Metadata Standard for Geographic Information
MUSCATE	Multi-satellite, multi-sensor ground segment for multi-temporal data
NDVI	Normalized Difference Vegetation Index
NDVImax	Normalized Difference Vegetation Index maximal
NDWI	Normalized Difference Water Index
OA	Overall Accuracy
OSM	Open Street Map
PSU	Primary Sampling Units
RF	Random Forest
RSG	Remote Sensing Software Graz
S-1	Sentinel-1
S-2	Sentinel-2
S2DSL	Sentinel-2 Data Score Layer
SAR	Synthetic Aperture Radar
SCL	Scene Classification Layer
SPOT	Satellite Pour l'Observation de la Terre
SRE	Surface Reflectance
SRTM	Shuttle Radar Topography Mission
SSU	Secondary Sampling Units
STD	Standard Deviation
SVM	Support Vector Machines
SWF	Small Woody Features
TCC	Tree Cover Change
TCD	Tree Cover Density
TCM	Tree Cover Mask
TIFF	Tagged Image File Format
USGS	United States Geological Survey
UTM	Universal Transverse Mercator
VH	Vertical transmit/Horizontal receive (polarisation)
VHR	Very High Resolution
VHR1	Very High Resolution 1 where resolution <=1m
VHR2	Very High Resolution 2 where 1m < resolution <=4m
VV	Vertical transmit/Vertical receive (polarisation)
WaW	Water and Wetness
WGS84	World Geodetic System 1984
WP	Work Package
XML	Extensible Markup Language

1 Introduction

The Horizon 2020 (H2020) project, “Evolution of Copernicus Land Services based on Sentinel data” (ECoLaSS) addresses the H2020 Work Programme 5 iii. Leadership in Enabling and Industrial technologies - Space, specifically the Topic EO-3-2016: Evolution of Copernicus services. ECoLaSS is being conducted from 2017–2019 and aims at developing and prototypically demonstrating selected innovative products and methods for future next-generation operational Copernicus Land Monitoring Service (CLMS) products of the pan-European and Global Components. This will contribute to demonstrating operational readiness of the products finally suggested for implementation, and shall allow the key CLMS stakeholders (i.e. mainly the Entrusted European Entities (EEE) EEA and JRC) to take informed decisions on potential procurement of the next generation of Copernicus Land services from 2020 onwards.

To achieve this goal, ECoLaSS makes full use of dense time series primarily of Sentinel-2 optical EO data as well as Sentinel-1 Synthetic Aperture Radar (SAR) data. Rapidly evolving scientific developments as well as user requirements are continuously analysed, in support of a future pan-European roll-out of new/improved CLMS products, and the potential transfer to global applications.

This Deliverable **D12.1a: “D42.1 - Prototype Report: Consistent HR Layer Time Series/Incremental Updates** aims to demonstrate the feasibility of future consistent time series as well as incremental update products with a focus on Imperviousness and Forest which have the longest time series history. These improved HRL prototypes are implemented in specific demonstration sites in Europe. This work is part of **WP 42** of Task 4: “Thematic Proof-of-Concept/Prototype on Continental/Global Scale”. This report will be accompanied by the Deliverable **D12.3: “P.42.2a - Data Sets of HR Layer Incremental Updates”**. This report serves as documentation of the prototype datasets.

In the ECoLaSS project a prototype is defined as a thematic proof-of-concept implementation of an improved or newly defined potential future Copernicus Land layer, building on the methods and processing lines developed in Task 3. The consortium has selected representative demonstration sites both in Europe and Africa, covering various bio-geographic regions and biomes. All prototype products and services are being prototypically implemented in a selection of these sites in the frame of the Task 4 WPs. In ECoLaSS, proofs-of-concept / prototype demonstrations are carried out with respect to five topics of relevance: (i) Time series derived indicators and variables, (ii) Incremental Updates of HR Layers, (iii) Improved permanent grassland identification, (iv) Crop area and crop status / parameters monitoring, and (v) New LC/LU products.

After first methods had been tested by the Task 3 WPs (cf. Deliverables D31.1a, D32.1a, D33.1a, D34.1a, D35.1a) in various test sites and algorithms were described, the demonstration activities of Task 4 have commenced to set up the developed processing lines in demonstration sites and derive first prototype versions. This deliverable focusses on the two time series consistency/incremental update prototypes on **Imperviousness** and **Forest** as part of **WP 42**.

This report comprises a Chapter on the background to an Imperviousness and Forest Prototype and associated requirements (Chapter 2); a description of the Demonstration Sites where the prototypes are implemented (Chapter 3); an overview of the methodologies carried over from the testing and benchmarking in Task 3 (Chapter 4); followed by a Chapter on the prototype implementation itself, the results and validation, including a description of the dataset (Chapter 5); and a summary and outlook (Chapter 6).

2 HRL Incremental Update Needs and Feasibility

This section discusses the feasibility of incremental updates of the HR Layers, with a focus on preserving a consistent product time series. At present, the investigations focus on the two most mature HRLs with the longest time series, i.e. Imperviousness and Forest. In future investigations, exploring the potential for incremental updates may become relevant specifically also for the HRL Grassland, for which currently only the 2015 implementation (with the current product specifications) has been published recently. However, at present, the direction to be taken appears largely dependent on the HRL 2018 operational ITT which EEA is expected to launch in late summer 2018. Likewise, the HR Layer Water & Wetness 2015 has just recently been published by the EEA, and this significantly differs in its definition from the other HRLs, making use of continuous radar based observations over seven consecutive years. Conceptualising a change product for this HRL will be a challenge of its own, and will also largely depend on the direction which EEA will take in the upcoming operational HRL 2018 ITT. The HRL on Small Woody Features is anyway out of scope for incremental updates due to much higher spatial (VHR) resolution and associated longer EO coverage repetition cycles. For these reasons, the report currently addresses the HRLs Imperviousness and Forest.

The IMD layer was the first HRL to be produced for the reference year 2006. However, at that time it was described as a “soil sealing database for Europe” and delivered as part of the GMES (Global Monitoring for Environment and Security, former name of Copernicus) Fast Track Service on Land Monitoring (Land FTS LM). It was produced during 2006-2008 from multi-sensor and bi-temporal, orthorectified satellite imagery. The production of IMD2006 covered 38 European countries (32 EEA Member States and 6 West-Balkan countries) and was implemented in two phases:

- an initial soil sealing product based on the EEA specification, and
- a soil sealing enhancement product based on evaluation of the initial product by some Member States.

The production approach used an automatic algorithm based on calibrated NDVI. The main deliverable was a raster dataset of continuous degree of soil sealing ranging from 0 – 100 % in full spatial resolution (20 m x 20 m) with no MMU (Minimum Mapping Unit, i.e. the minimum number of pixels to form a patch) and with the associated metadata. A derived product, a raster dataset of continuous degree of soil sealing ranging from 0 - 100% in aggregated spatial resolution (100 m x 100 m) in European projection was generated.

Since the production of the HRL IMD 2006, a time series of imperviousness has been delivered for the reference years 2009, under the FP7 geoland2 project, and 2012, under the GMES Initial Operations (GIO). For each of these iterations, the results contain two products: a status layer for each reference year (e.g. IMD2012), as well as an imperviousness density change layer between reference years (e.g. IMC2009-2012), and based on the already existing imperviousness product for that previous reference year. It is worth noting that there have been revisions to the previous years' IMD products during updating and the IMC time series has been reworked. The update for 2012 and 2015 was produced as part of the operational Copernicus Land Monitoring Service (CLMS), on the same procedure and for the same product types. A re-analysis of all existing Imperviousness Degree (IMD 2006, 2009 and 2012) and Imperviousness Change products (IMC 2006-2009, 2009-2012, 2006-2012) was also conducted during the production of IMD2015.

The most recent HRL IMD 2015 production was conducted through semi-automatic classification of calibrated biophysical parameters, derived from multi-temporal high-resolution optical satellite images from the reference period 2015 +/- 1 year. The result for the pan-European IMD2015 product shows a producer's accuracy of 84.58% and a user's accuracy of 90.14%, as determined by visual checks of open source VHR images in combination with the multi-temporal, multi-seasonal EO database (e.g. Sentinel-2, Landsat). The production of the IMD2015 was achieved in a very short time (15-18 months) thanks to multi-sensors and multi-temporal time series data available through the European Space Agency's (ESA)

Data Warehouse (DWH) (mainly SPOT, IRS-P6, Sentinel-2A and Landsat). The availability of time-series along with Landsat-8 for gap filling permitted to shorten the production phase compared to 2012. But the user's point of view (as expressed by various stakeholders, cf. WP 21 results) typically is to rather have the products available as close as possible to the reference year of image acquisition and thus in an even more shortened time. The reduction of the production time is tied to the question of the input data and their availability for all areas in sufficient quantity and reliable quality at the beginning of the project. The higher spatial resolution of the time series used for IMD2015 leads to generate products in the actual resolution of 20m (compared to former used data from the ESA DWH such as IRS with a nominal resolution of 23.5m or Landsat 8 with a nominal resolution of 30m). It is noticeable that the use of full S-2 time series will also lead to an improvement of the currently applied spatial resolution from 20m to 10m.

The HRL Forest at the status of the reference year 2015 consists of two pixel-based primary status layers at 20m spatial resolution: the Dominant Leaf Type (DLT), providing information on the corresponding leaf type (broadleaved or coniferous) per pixel, and the Tree Cover Density (TCD), providing information on the proportional tree (crown) coverage per pixel. These two status layers are fully identical in their spatial extents and are currently produced for the EEA-39 area in a 3-year update cycle for certain reference years (2012, 2015, 2018, etc.), whereas the reference year is defined as comprising +/- 1 year. Both products represent the main input data source for any derived layers of the HRL Forest product portfolio and enable users to apply any (national) forest definition (when being further processed to a desired TCD and MMU), whichever fits best to the specific needs.

However, the data situation of the reference year 2012 and 2015 differs significantly in terms of temporal data availability, available sensors and, connected to both: data quality. Whereas in 2012, a mono-temporal optical EO data coverage from 2011 to 2013 had been used in form of the European Space Agency's (ESA) Data Warehouse (DWH) dataset MG2b_CORE_01 (also referred to as HR_IMAGE_2012, consisting of SPOT-4, SPOT-5, IRS-P6, IRS-ResourceSat-2 and RapidEye data), multi-temporal time series data became available for the 2015 production with the launch of Sentinel-2A and the utilization of the Landsat archive of the United States Geological Survey (USGS), strongly focussing on the acquisition year 2016 (i.e. reference year 2015 +1). Consequently, the production workflow of the HRLs 2015 was already adopted towards the processing of mass data and thematic analysis of multi-temporal EO data, resulting in high quality products, which are partially not directly comparable with the derived 2012 products due to their specific lineage (e.g. mono-temporal data basis, radiometric resolution, data quality issues (haze, cloud cover, phenology), distribution in geographical production units (lots), etc.).

Even though significant improvements in the production speed were achieved in the 2015 production (15-18 months) compared to 2012 (40 months), users argue that the time span between production start and final provision to the end-users should be shortened, and that product specifications could be improved in terms of spatial and temporal resolution (cf. WP 21). It has to be noted, that the HRL Forest 2015 has already strongly benefitted from a generally good data situation, with more than 80% of the image acquisitions having taken place within one year. ECoLaSS is able to explore taking the full advantage of the complete Sentinel-2A+B time series, which provides a significantly improved temporal resolution, supporting an improved tree cover and leaf type mapping as well as change detection approaches.

Even though the HRLs 2015 on Imperviousness and Forest are of high quality, requirements for improved products have been voiced by users and stakeholders in WP21 and WP 51 as well as in terms of ongoing Copernicus developments. Moreover, ECoLaSS aims to demonstrate the feasibility of HRL incremental updates. The recognised potential for improvement of the methodological approaches for both Layers which can be summarised as follows:

- an improved level of automation to allow a faster production and
- shorter monitoring intervals (e.g. for future yearly incremental updates);
- improving the thematic classification accuracy

- fully exploiting optical Sentinel-2 and SAR Sentinel-1 time series instead of using limited temporal EO data coverages or pre-selected, best-suited EO data scenes
- applying an integrated SAR/optic time series data analysis to benefit from the multi-sensor characteristics and ability for gap filling of clouds
- improving the status layer's spatial detail from 20m spatial resolution to 10m. Product definitions consequently might have to be adapted, such as e.g. the Minimum Mapping Unit
- refine the change detection approach to detect both increase and decrease of Imperviousness or Forest areas

The tested methods for the Imperviousness and Forest prototypes, addressing the abovementioned user demands, are presented in the next chapters, alongside with investigations on the feasibility for future operational implementation of such prototypes.

3 Demonstration Sites

The incremental update prototypes investigated by WP 42 (i.e. Imperviousness and Forest) are implemented in selected representative demonstration sites which cover various bio-geographic regions and biomes, as shown in the following.

The selected demonstration sites (60,000/90,000km² per demonstration site) spatially contain the 5 test sites used by Task 3. The demonstration sites are relevant in Task 4 for demonstrating the proposed candidates for a Copernicus Land Service Evolution roll-out on a larger scale. As shown in Figure 3-1, the pre-selected demonstration sites are covering the Atlantic and Continental zones (Source EEA: <http://www.eea.europa.eu/data-and-maps/data/biogeographical-regions-europe-3#tab-gis-data>) of the member and associated states of the EEA-39, and are determined by the position of Sentinel-2 tiles of the official tiling grid. These selected ECoLaSS demonstration sites are located in the North of Europe, in the Alpine/Central region, in the West, in the South-West and in the South-East of Europe.

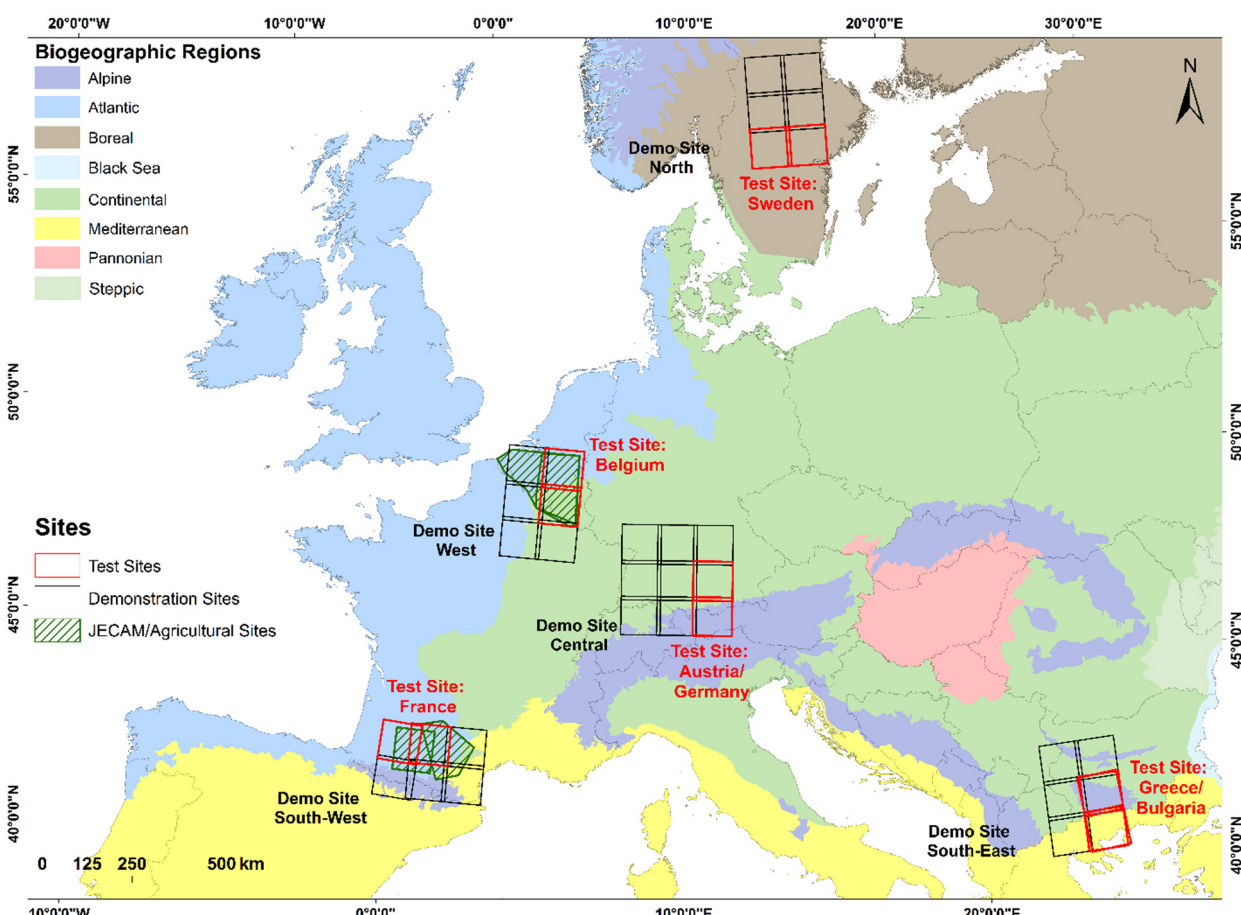


Figure 3-1: Biogeographic Regions of Europe (2015) and European ECoLaSS Demonstration Sites
 (Map: © European Environment Agency; administrative boundaries: ©EuroGeographics)

A short description of these prototype sites is given in Table 3-1 below. The land cover figures are derived from CORINE Land Cover (CLC) 2012 data with a Minimum Mapping Unit (MMU) of 25 ha. Therefore, strong generalisation effects have to be assumed.

Table 3-1: Description of the ECoLaSS demonstration sites

Location	Biogeographical region(s)	Countries	Distribution of CORINE land cover classes 2012 (Level 1) per prototype site *
Northern Europe	Boreal	Sweden	Artificial areas: 1.38 %, Agricultural areas: 10.54 %, Forest and semi-natural areas: 70.61 %, Wetlands: 4.25 %, Water bodies: 13.22 %
Alpine / Central Europe	Continental, Alpine	Germany, Austria, Switzerland, Italy and France	Artificial areas: 5.86 %, Agricultural areas: 42.96 %, Forest and semi-natural areas: 49.95 %, Wetlands: 0.24 %, Water bodies: 0.98 %
West Europe	Atlantic, Continental	Belgium, France, Luxembourg, Netherlands	Artificial areas: 7.81 %, Agricultural areas: 53.75 %, Forest and semi-natural areas: 13.15 %, Wetlands: 0.25 %, Water bodies: 25.04 %
South-East Europe	Mediterranean, Continental, Alpine	Serbia, Macedonia, Greece, Bulgaria	Artificial areas: 3.03%, Agricultural areas: 37.00 %, Forest and semi-natural areas: 53.95 %, Wetlands: 0.17 %, Water bodies: 5.71 %
South-West Europe	Atlantic, Mediterranean, Alpine	France, Spain	Artificial areas: 3.26 %, Agricultural areas: 46.73 %, Forest and semi-natural areas: 49.20 %, Wetlands: 0.01 %, Water bodies: 0.40 %

* The figures for “Agricultural areas” comprise both, arable land and grassland

All prototype products and services have been prototypically implemented in one or more demonstration sites in the first Reporting Period, and will be complemented to a total of three demonstration sites in Reporting Period 2. In the first Reporting Period, the Imperviousness prototype has been implemented in the South-West demonstration site (which covers the Mediterranean, Atlantic and Alpine biogeographic regions), and the Forest prototype in the North demonstration site (which covers the Boreal zone). Since these two demonstration sites constitute the more relevant ones for WP 42, they are shortly described in the following sections.

3.1 Demonstration Site South-West

The Demonstration Site South-West (an area of approx. 65,000 km²), covering southern France and some parts of northern Spain, includes the primary test site for the method developments in Task 3 related to the improvement of the HRL Imperviousness (IMP). It serves to demonstrate the implementation of the prototype of a potential future HRL Imperviousness, as part of WP 42, in the first Reporting Period. In the second project phase, the demonstration sites Central and Belgium will be added.

The landscape in the demonstration site South-West is composed of different biogeographic regions such as Mediterranean, Alpine and Atlantic. Three Sentinel-2 tiles are dominated by mountain landscapes, a mix of bare soils and natural grasslands, due to the presence of the Pyrenees. The 31TCJ tile is dominated by a strong proportion of impervious surfaces, because of Toulouse, a major French city. Toulouse is the 4th city in France in terms of urban and demographic expansions and is the most dynamic city of the South-West region. The presence of the city leads the region to be the second most attractive and dynamic region in France. The plains surrounding the city are mainly rurally dominated areas composed of croplands mixed with grassland and an increasing amount of forest with the proximity of the coastal region. But rurally dominated areas also show a dynamic increase of population and a dynamic situation of settlements due to the proximity of Toulouse. So the region shows a real tendency towards urban expansion in the surroundings of Toulouse and in the rural parts of the region with small cities like Montauban, Auch, Carcassonne, Tarbes, Castres or Albi. In general, the Mediterranean area in the East of the demonstration site is a patchwork of cropland, dry grassland and vineyards. There is also a small portion of the Landes forest in the North-West of the demonstration site. The unique situation of the region in terms of urban dynamic is the reason for the selection of this site for the Imperviousness prototype.

A more detailed map of the characteristics of the selected demonstration site South-West as used for the Imperviousness prototype is provided in Figure 3-2 below.

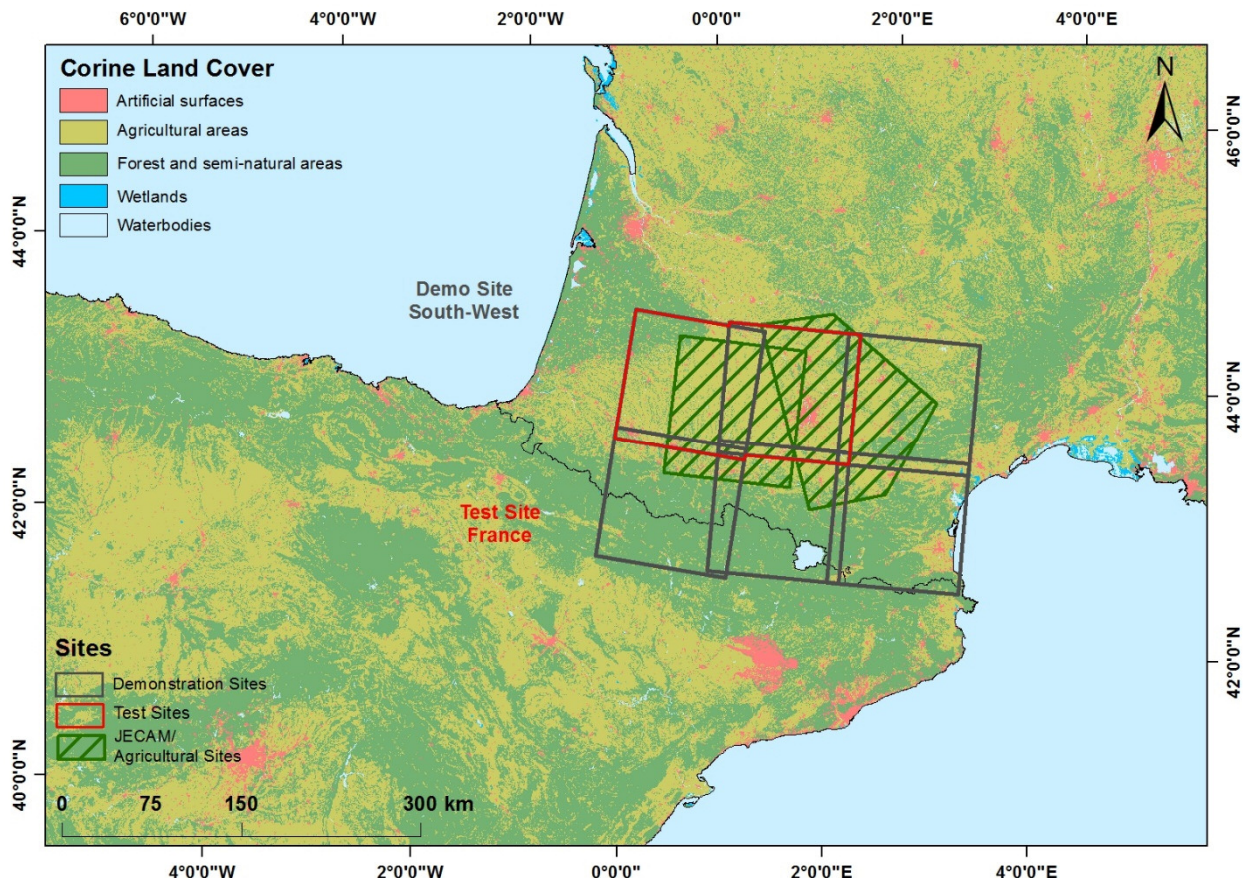


Figure 3-2: Demonstration site South-West, with CLC 2012 background layer
 (© EEA, ©EuroGeographics for the administrative boundaries)

3.2 Demonstration Site North

The demonstration site North in southern Sweden includes the primary test site for the method developments in Task 3 related to the improvement of the HRL Forest (FOR). It serves to demonstrate the implementation of a prototype on a potential future HRL Forest status layer, and the incremental update thereof, as part of WP 42, in the first Reporting Period. In the second project phase the demonstration sites Central and South-East will be added.

The site has a spatial extent of approx. 65,000 km² and is dominated by forests and water bodies. In some central parts and in the South, larger agricultural areas are included. The forested land is intersected by lakes and smaller water bodies, as well as by peat bogs and grassland.

The particular challenges of the demonstration site North are related to:

- a typically medium to high cloud cover throughout the year;
- the existence of very large tree and forest stands within the area;
- extensive forest management practices with clear cuts frequently > 0.5 ha, resulting in a fragmented pattern of forest stand ages and densities due to frequent tree harvesting;
- a generally difficult differentiation between the two dominant leaf types (broadleaved / coniferous) due to:
 - the influence of soil moisture and water content (small water bodies and peat bogs);
 - over-radiation effects of vital vegetative undergrowth (e.g. grassland and bushes) in less dense coniferous tree/forest stands.

A map of the selected demonstration site North for the Forest prototype is provided in Figure 3-3 below.

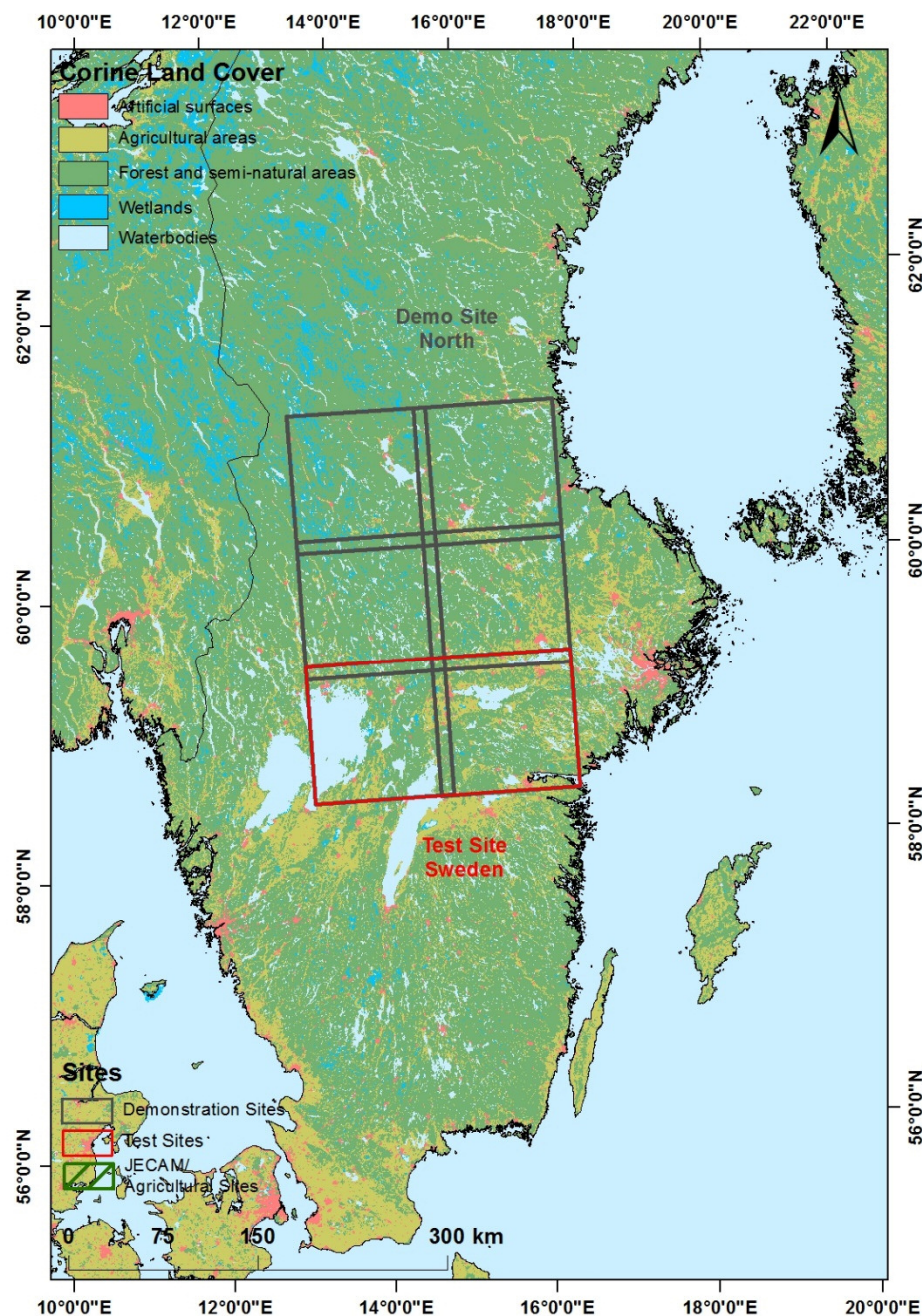


Figure 3-3: Demonstration site North with CLC 2012 background layer
(© EEA, © EuroGeographics for the administrative boundaries)

4 Overview of Applied Methods

In the following, a brief overview on the methods applied to derive the prototypes on Imperviousness and Forest is given. Further details and background information are provided in [AD07] and [AD08] as outcomes of Task 3.

4.1 Methods for Implementing a Prototype on Imperviousness

This section shows an overview of the methods implemented for the Imperviousness prototypes Imperviousness Degree (IMD) and Imperviousness Change Classified (IMC) following the outcomes of the Task 3. Further details and background information are provided in the three Deliverables on “D33.1a - Methods Compendium: Time Series Analysis for Thematic Classification” [AD07] and “D34.1a - Methods Compendium: Time Series Analysis for Change Detection” [AD08], as well as “D35.1- Methods Compendium: HRL Time Series Consistency for HRL Product Updates” [AD09], as outcomes of Task 3.

4.1.1 Derivation of biophysical variables

Many spectral indices and biophysical variables have been defined in the past three decades. Some have been and are still widely used, such as the Normalized Difference Vegetation Index (NDVI), while others have been proposed as alternatives only in the recent years. In the WP 31, main spectral indices are listed focusing on vegetation and built-up discrimination in order to explore their potential contribution to the evolution of CLMS products.

In the frame of the Task 4, it has been chosen to focus on the NDVI, adapted for the Sentinel-2 sensor as defined by Henrich et al. (2012). Further details on the NDVI are provided in WP31. However, although multispectral information such as from the NDVI is essential to discriminate landscape elements, it has limitations in the detection of built-up area and calculation of imperviousness density. An effective detection could require advanced feature computing able to discriminate objects:

- **Texture / Structure:** Texture and structure analysis consists in extracting information on the spatial arrangement of pixels. Amongst numerous existing techniques, the Sobel filter is particularly interesting. The **Sobel operator** is used in image processing particularly within edge detection algorithms where it creates an image emphasizing edges.
- **Granulometry by Mathematical morphology:** Mathematical morphology is the analysis of the image constructions and their distribution at different scale. It consists in simplifying the image progressively through the preservation of bright elements (with closing operators) or dark elements (opening operators). Amongst numerous existing techniques, the following one is particularly interesting and is implementing for the HRL IMD 2017 Prototype:

Differential Attribute Profiles (DAP)/Haar attributes: Multiscale features often appear as a relevant alternative, with Gabor filters and Differential Morphological Profile (DMP) having achieved great classification performances. However, even such features come with a significant cost. DMP is relying on a series of morphological filters by reconstruction and it has shown for more than a decade its ability to deal with VHSR images (Pesaresi & Benediktsson, 2001). Recently, an alternative multiscale feature, called Differential Attribute Profile (Dalla Mura et al., 2010) has been built upon DMP to achieve more discriminative power, a higher flexibility, for a lower computational cost. DAP is very appealing since it is computed from a tree-based image representation that can be built with very efficient algorithms (see Carlinet et al. (2014) for a review). Once the tree is built, the description of each pixel (or object, node) is straightforward and relies on the analysis of all its ancestors up to the root. As such, it has been embedded in large-scale analysis performed by the Joint Research Center such as the Global Human Settlement Layer (GHSL) (Pesaresi et al., 2013) and European Settlement Map (Florczyk et al., 2015).

4.1.2 Active learning Classification approach based on DAP profiles

Multiple algorithms could be used to map artificial lands. Classification methods range from unsupervised algorithms such as K-means to parametric supervised algorithms to machine learning algorithms such as artificial neural networks (Mas & Flores, 2008), decision trees (Breiman, 1984), Support Vector Machines (SVM) (Mountrakis et al., 2011) and ensembles of classifiers such as Random Forest (Breiman, 2001). A selection of these best algorithms for classification has been tested in the frame of the WP 33.

The automated supervised classification used to derive the built-up mask follows the outcomes of the Task 3 of the project. So the Imperviousness built-up mask layer for 2017 was performed using supervised machine learning methods to create the updated built-up mask for 2017. The production of the built-up mask is achieved with a selection of reference (or training) data. Following the results of the WP31 (separability of the information for thematic classifications) and WP33 (Time Series Analysis for Thematic Classification), the input data selected rely on multispectral information and granulometry by mathematical morphology (Differential Attribute Profiles). Indeed, the active learning algorithm shows great classification performances whilst being very computer efficient, thus substantially reducing processing time overall and dealing with large dataset.

Active Learning (AL) and Differential Attribute Profiles (DAP)

Production of Land Cover maps is usually achieved with a selection of reference (or training) data, supervised classification, and manual map refinement/correction. The classification accuracy is directly related to the quality of the training samples, i.e. their ability to represent the data to be classified. Collecting training samples is done through a costly operation consisting of manually labelling the pixels. Furthermore, such pixels may not be representative of the land cover classes, thus requiring important corrections in the post processing step. To alleviate these issues, active learning has been introduced a couple of decades ago, and used in remote sensing since more than 5 years (Tuia et al., 2009). It works in both interactive and batch mode. In the former case, the user is given some specific pixels to label (e.g. by photo-interpretation), while in the latter case only relevant samples from the training sets will be used (leading to a better modelling of land cover classes as well as a more efficient classification process). It has been a very active field of research (see Tuia et al. (2011) for a review) reaching similar accuracies than supervised classifiers but with only 5 to 10% of the training samples. It is now considered as a well-established framework (Crawford et al., 2013). Recent developments are related to large-scale analysis and domain adaptation (Alajlan et al., 2013) or multiscale classification (Zhang et al., 2016).

Set-up of reference databases for validation

A stratified random sampling approach is used adapting the number of sample units to each stratum. For the HRL IMD 2017 Prototype, a stratification has been applied on a series of omission/commission strata. The number of sample units called Primary Sampling Units (PSUs) per stratum based on LUCAS and densified LUCAS grid ensured a sufficient level of precision at reporting level. Different sampling intensity has been applied and the stratification was defined as follows:

- Commission: impervious class (1-100%) (80 PSUs)
- Omission high probability: no IMP areas and CLC/OSM IMP areas (20 PSUs)
- Omission low probability: Remaining areas (900 PSUs)

The number of primary sample units (PSUs) per stratum should be such to ensure a sufficient level of precision at reporting level. The minimum number of PSUs per stratum is set at 20. The validation exercise covers the whole study area to be valid (e.g. use of low and high probability omission strata for HRL with low sampling intensity in low probability stratum). 1,000 sample units for the prototype product were selected.

Each PSU corresponds to one 0.25ha square. Each PSU is then associated to secondary sampling units (SSUs) corresponding to a 5x5 grid with 10m between each SSU (see Figure 4-1). The idea is that each SSU can then be associated with the corresponding HRL 10m layer pixel.

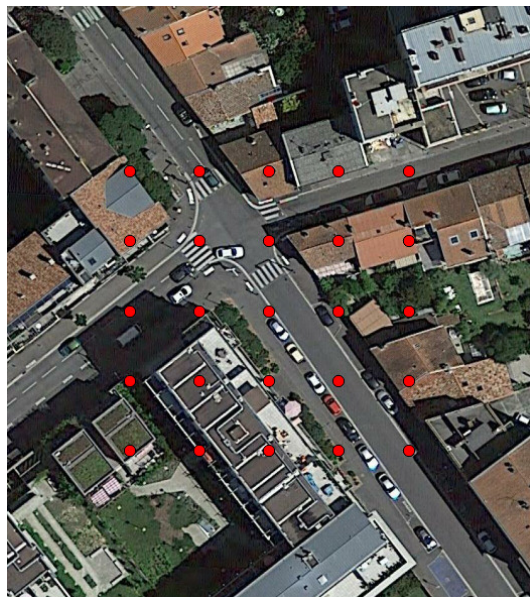


Figure 4-1: Example of SSUs organised in a 5x5 10m grid

In a second stage, the sample units were provided to the interpretation team as separate shapefiles in which the information about the product class was included to perform a plausibility analysis.

Estimation and analyses procedures

Thematic accuracy is presented in the form of an error matrix. Unequal sampling intensity resulting from the stratified systematic sampling approach is accounted for by applying a weight factor to each sample unit. Thematic accuracy is usually assessed based on the construction of confusion or error matrix and associated metrics such as: Overall Accuracy (OA), Producer's Accuracy (related to the omission error), User's Accuracy (related to the commission error).

4.2 Methods for Implementing a Prototype on Forest

According to the outcomes of the Testing and Benchmarking exercise as part of the methods compendium of WP 33 “Time Series Analysis for Thematic Classification” [AD07], the Random Forest (RF) classifier has been selected as the best rated classification algorithm in terms of processing time and achieved accuracy for creation of an improved primary status layer Dominant Leaf Type (DLT) 2017. Spatio-temporal input features that capture important time series properties and patterns are used. An automated reference sampling approach has been applied to derive the necessary sample basis for the classifier. According to the tests carried out in WP 33, the use of Sentinel-2 data from the spring period was expected to provide the best ratio of high classification accuracy and lowest processing cost. First, a 10m Tree Cover Mask (TCM) is calculated from time series features derived from the Sentinel-2. This mask is subsequently intersected with a seamless and independently derived leaf type layer to create the improved DLT 2017 status layer.

In view of a potential future HRL Forest Incremental Update layer, the delineation of forest change/loss is based on the comparison of a pre- and post-change tree cover mask as described in the methods compendium of WP 34 “Time Series Analysis for Change Detection” [AD08]. The TCM 2015 in 20m spatial resolution as derived by the Copernicus HRL Forest Dominant Leaf Type layer 2015 represents the pre-change mask whereas the DLT 2017 classification represents the post-change mask with reference year 2017. The Incremental Update layer resulting thereof, hereinafter explicitly named as Tree Cover Change

(TCC), compares the pre- and post-change mask (TCM 2015 and newly classified TCM 2017 resampled to 20m) to detect areas of forest loss. Due to the very short time interval of mostly < 1 year between the two masks (the HRL 2015 data are mainly from spring and summer 2016 and the ECoLaSS data from spring and summer 2017), this layer concentrates on negative changes (loss) only.

This map-to-map change detection method is fully detached from the input data used for the tree cover/forest mask generation and therefore completely independent from the input data applied for production. Issues in view of the fusion of images from different optical sensors or even the fusion of optical and SAR data can be solved in complete isolation from the change detection.

The presented methodology can incorporate both, Sentinel-1 and Sentinel-2 data without significant adjustments, which provides more flexibility in areas of frequent cloud cover. However, in this project phase, only optical Sentinel-2 data has been utilised. An extension to SAR data is planned for project phase two.

5 Prototype Implementation

This chapter presents the implementation of the prototypes of the improved HRL Imperviousness (section 5.1) and HRL Forest (section 5.2) within the two demonstration sites South-West and North. For each prototype, the following aspects are examined: Data and Processing Setup (sections 5.1.1 & 5.2.1), the Classification Results and Validation (sections 5.1.2 and 5.2.2), and the Change Detection and Incremental Update Results and Validation (sections 5.1.3 & 5.2.3). Finally, the description of the dataset properties and the associated metadata are provided in detailed Prototype Specifications (section 5.3).

5.1 Prototype of a potential Future HRL Imperviousness

This section shows the prototypical implementation of the Imperviousness prototypes, both the improved status layer IMD and the incremental update layer IMC. Firstly, the integrated EO and ancillary data are described (section 5.1.1), followed by explaining the pre-processing steps (section 5.1.2), the demonstration of the classification results of the actual prototype in the demonstration site (section 5.1.3), and the demonstration of the prototypic results of change and incremental updates including the accuracy assessment (section 5.1.4).

5.1.1 Data and Processing Setup

Firstly, the integrated EO and ancillary data are described, followed by explaining the pre-processing steps for optical and SAR data, as well as the experimental setup for the classification and incremental update approach.

5.1.1.1 Input Data

Based on the outcomes of the Task 3, a multi-sensor approach combining Sentinel-1 and Sentinel-2 was initially adopted to perform the classification that finally leads to the impervious prototype.

SAR DATA - SENTINEL-1

The Sentinel-1 sensor system has an overall number of 2 bands (both polarisation signals VV and VH) at 10m pixel spacing. Pre-processing has been performed following the processing chain as detailed in WP32. Selected scenes cover the time frame from 01-January to 15-November 2017 and represent a total of 785 Sentinel-1 images which were used to produce the impervious prototype.

OPTICAL DATA - SENTINEL-2

The South-West demonstration site comprises six adjacent Sentinel-2 tiles (30TYN, 30TYP, 31TCH, 31TCJ, 31TDH, 31TDJ) for which Sentinel-2A+B data in 10m resolution have been processed.

The Sentinel-2 sensor system has an overall number of 12 bands from 10m to 60m spatial resolution. For the ECoLaSS processing, only the 10m and 20m bands are used, which are in total 10 bands. The list of the used bands with their central wavelengths and abbreviations is shown in Table 5-1.

Table 5-1: Used Sentinel-2 reflectance bands (adapted from Suhet, 2015).

Sentinel-2 Bands	Description	Central Wavelength (μm)	Stack number
Band 2	Blue	0.490	1
Band 3	Green	0.560	2
Band 4	Red	0.665	3
Band 5	Vegetation Red Edge (VRE1)	0.705	5
Band 6	Vegetation Red Edge (VRE2)	0.740	6
Band 7	Vegetation Red Edge (VRE3)	0.783	7
Band 8	NIR	0.842	4
Band 8A	Narrow NIR (NNIR)	0.865	8
Band 11	SWIR (SWIR1)	1.610	9
Band 12	SWIR (SWIR2)	2.190	10

The CNES MUSCATE production centre produces the Sentinel-2 Level-2A data in near real time, which are corrected for atmospheric effects using the MACCS-ATCOR Joint Algorithm (MAJA) software. The products are available for download at <https://theia.cnes.fr/atdistrib/rocket/#/home>. The data is acquired in large areas shown in Figure 5-1.

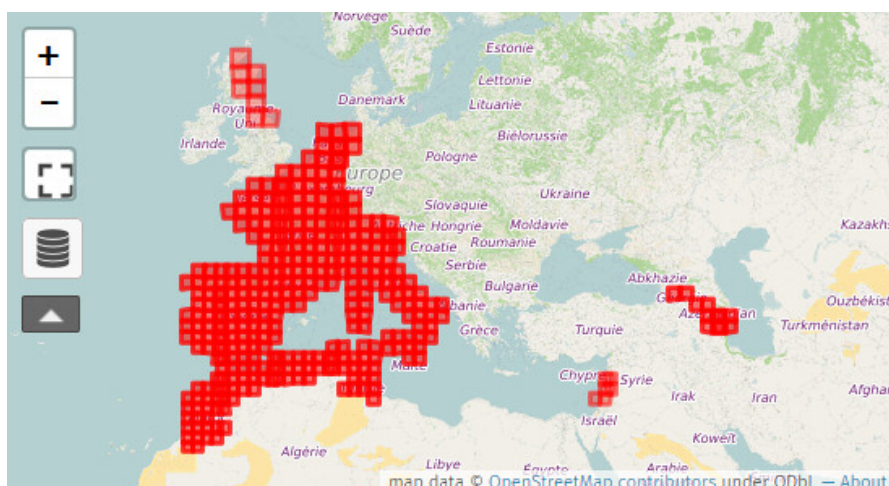


Figure 5-1: Theia Level-2A data production extent. (21.07.2018) Source: http://www.cesbio.ups-tlse.fr/multitemp/?page_id=7501

The Sentinel-2 images are provided as a GeoTiff per spectral band, for the 10m bands (B2, B3, B4, B8) and the 20m bands (B5, B6, B7, B8A, B11 et B12) of Sentinel-2. The data comes along with two types of surface reflectances:

- Surface Reflectance (SRE) which is corrected for atmospheric effects, including adjacency effects
- Flat Reflectance (FRE) which is corrected for atmospheric effects, including adjacency effects and also corrected for terrain effects, which consists in suppressing the apparent reflectance variations. The corrected images look like if the land was flat.

The dataset used for the Imperviousness prototype is based on the Flat Reflectance to take into account the topographic effects as described and tested in the deliverables of the WP32.

Selected scenes cover the time frame from 01-January to 14-November 2017 and represent a total of 319 Sentinel-2A+B images which were used to produce the impervious prototype.

5.1.1.2 Pre-processing

The ECoLaSS South-West demonstration site in France and Spain is comprised of the footprints of six adjacent Sentinel-2 tiles (30TYN, 30TYP, 31TCH, 31TDH, 31 TCJ and 31TDJ) for which Sentinel-2 and

Sentinel-1 data were pre-processed according to the recommendations of the Task 3, as summarised in the subsequent sub-sections.

5.1.1.2.1 Pre-Processing methods for optical time series

As mentioned in the WP 32, the processing methods for optical time images include the generation of spatio-temporally consistent optical images with top of atmosphere reflectance values. Therefore, the following pre-processing steps are available:

- Atmospheric correction,
- Topographic normalisation,
- Cloud, cloud shadow and snow masking.

ATMOSPHERIC CORRECTION

The Sentinel-2 data produced by CNES' Theia Land Data Centre and available for download are corrected for atmospheric effects, including adjacency effects. These atmospheric corrections include compensating the light absorption by air molecules and the light scattering by molecules and aerosols.

Several models may be used to perform atmospheric corrections. In the case of the MAJA software, the MACCS processor is the model used. It pre-computes "Look-up Tables" using an accurate radiative transfer code (Successive Orders of Scattering), that simulates the light propagation through the atmosphere. The MACCS/MAJA method combines different approaches to obtain robust estimates of aerosol optical thickness.

TOPOGRAPHIC NORMALISATION

A topographic correction is necessary if the test sites are characterized by mountainous terrain as it is the case for the South-West Demonstration site. The topography can significantly influence the radiometric properties of the signal received from the satellite (see Wulder and Franklin, 2012). This effect is caused by the different lighting angles resulting from the topography (cf. Gallau et al., 2007). The aim of a topographical correction is to compensate for the differences in reflectance intensity between the areas with varying slope, exposure and inclination and to obtain the radiation values that the sensor would measure in the case of a flat surface.

The Sentinel-2 data using the MAJA software and available for download are corrected from the topographic effects.

CLOUD, CLOUD SHADOW AND SNOW MASKING

The MAJA cloud detection method is based on a number of threshold tests using the cirrus band (B10). Additionally, multi-temporal tests are carried out to detect clouds by measuring a steep increase of the blue surface reflectance. Finally, the correlation of the pixel neighbourhood with previous images is calculated to avoid over detections based on the assumption that two different clouds at the same location on successive dates will not have the same shape. If a large correlation is observed, the pixel is excluded from the cloud mask as it is likely to be a bright land surface.

5.1.1.2.2 Pre-Processing methods for SAR time series

Pre-processing has been performed with the Remote Sensing Software Graz (RSG) module "Space Suite". It comprises the following processing steps:

- Image ingestion: bulk import of original images to RSG .rsx files, orbit update (precise orbits), automated combination of adjacent scenes
- Image pre-processing: definition of image frame extent (based on selected granules), full image resolution, no speckle filtering, no multitemporal filtering, radiometric terrain correction to

gamma naught based on SRTM 4.1 model (Central demonstration site: also tests with sigma naught), combine polarizations in one image stack (band1: VH; band2: VV)

- Orthorectification: based on an interpolated Digital Elevation Model (DEM) (SRTM 4.1), output image resolution is 10m, output image resampling method (nearest neighbour), coordinate system: UTM WGS84
- Calculation of incidence angle map

5.1.1.3 Experimental Setup

The developed processing chain is able to process a large amount of input data within a reasonable amount of time to provide the classification results. The achieved level of automation ensures the effective application of the process to map impervious areas of almost the entirety of Europe.

The workflow/methodological steps for the production of the Imperviousness Prototype is listed hereafter:

1. Set-up of reference databases for calibration
2. Production of the Imperviousness 2017
 - a. Data preparation (Sentinel-1, Sentinel-2)
 - b. Biophysical variables and additional image parameters (NDVI, textural metrics for S-2, time features for S-1)
 - c. Derivation of classification training samples from additional reference data (HR layers)
 - d. Production of initial built-up masks for 2017 by automated supervised classification (Active learning)
 - e. Fusion of S-1/S-2 built-up masks
 - f. Absolute calibration of IMD2017
 - g. Post-processing (filtering, contextual analysis based on change probability)
3. Validation of built-up mask and IMD for 2017
4. Change detection 2015-2017
5. Validation of detected changes

5.1.1.3.1 Set-up of reference databases for calibration

The development of a dataset for calibration of the IMD and IMC prototypes 2017 is needed for two main reasons:

1. To provide a reference dataset for the absolute calibration of the HRL2017 10m status layer Imperviousness degree (1-100%).
2. To provide a reference dataset for the statistical calibration of the changes for the time interval 2015-17 as a basis for the re-processing of the 2015 layers thus ensuring the temporal consistency of the products.

The stratification and sampling approach required to create these two different reference datasets is quite different and therefore they are performed separately.

REFERENCE DATASET FOR ABSOLUTE CALIBRATION OF IMPERVIOUSNESS DEGREE LEVEL (1-100%)

The reference imperviousness density values are collected for selected sample cells (PSU of 1ha) within the Sentinel-2 tiles. Imperviousness degree levels from 1-100% are obtained for each PSU. The sealing Information, built-up vs. non built-up, is collected through Secondary Sampling Units (SSUs – 5x5 grid) within each PSU.

In order to be a representative methodology, the approach chosen combines random and stratified approaches and benefits. The stratification is based on the previous 2015 Imperviousness layer (IMD density value [1-100%]).

REFERENCE DATASET FOR THE STATISTICAL CALIBRATION OF THE CHANGES

One of the key requirement is to ensure the temporal consistency and comparability between the different time intervals and that there should be no spatial inconsistencies between the layers of the different epochs. Due to the semi-automated nature of the HRL production workflow, it is not possible to guarantee that all errors can be removed from the change layer. However, the relative magnitude of actual change versus the errors contained in the change layer for each time interval should be known in order to provide a basis for improving the temporal consistency between each layer. Therefore, there is a need to develop a reference dataset that will be used to determine the relative proportion of actual change versus all the error components described above. To be valid, this calibration dataset should be selected based on a probability sampling approach. Since the focus is on change, the approach will help assess:

- The new built-up for the year 2017;
- The omission errors from 2015 – the undetected built-up pixels of 2015;
- And the commission errors from 2017 – the pixels falsely flagged as built-up in 2017.

Therefore, there is a strong need to develop a reference calibration dataset that will be used to determine the relative proportion of actual change versus all the error components described in the previous paragraph. To be valid, this calibration dataset has been selected based on a probability sampling approach similar, but independent, to that of the validation dataset as implemented in the reports of the Task 3.

The stratification and the sampling design primarily consist of selecting an appropriate sampling frame and a sampling unit. In case of changes, a sampling design based on points is considered most appropriate.



Figure 5-2: Reference calibration samples overlaid on the change mask

5.1.1.3.2 Production of the Imperviousness 2017

DATA PREPARATION (SENTINEL-1, SENTINEL-2)

This step includes all the pre-processing required to prepare the data for the following steps including: downloading, data, extraction, layer stacking, preprocessing, cloud masking for Sentinel-2 or Sentinel-1.

For the purpose of the calibration task, the NDVI is derived per single Sentinel-2 image, then mosaicked to a maximum NDVI as shown in Figure 5-3.

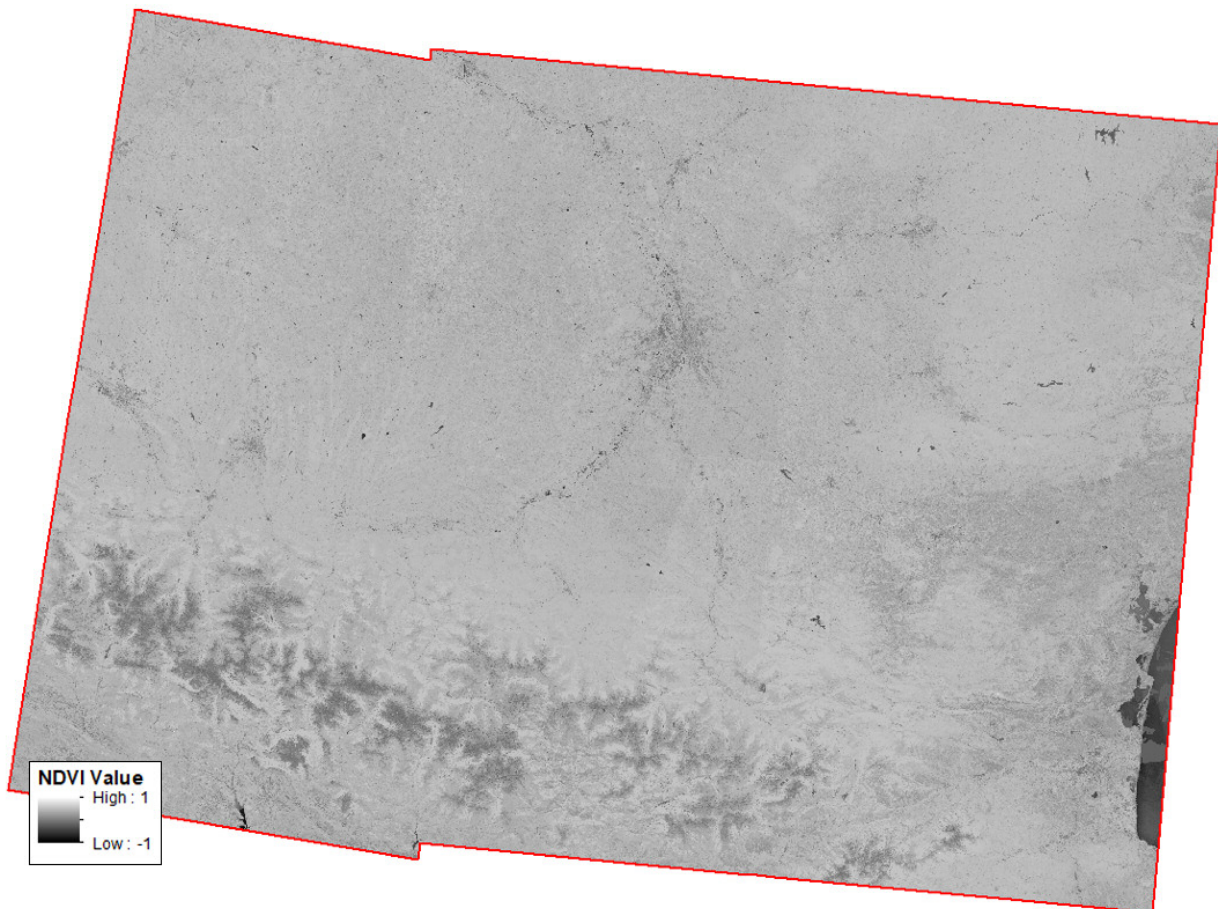


Figure 5-3: NDVI Sentinel-2 based maximum feature

Following annual SAR features are generated using S-1 data and both polarisation signals (VV, VH) including 785 images from 01.01.2017 to 15.11.2017, covering the demonstration site. Examples for such statistical features are presented in Figure 5-4.

Table 5-2: SAR annual statistical features.

feature	description
MIN	Minimum
MAX	Maximum
MEAN	Mean
STD	Standard deviation

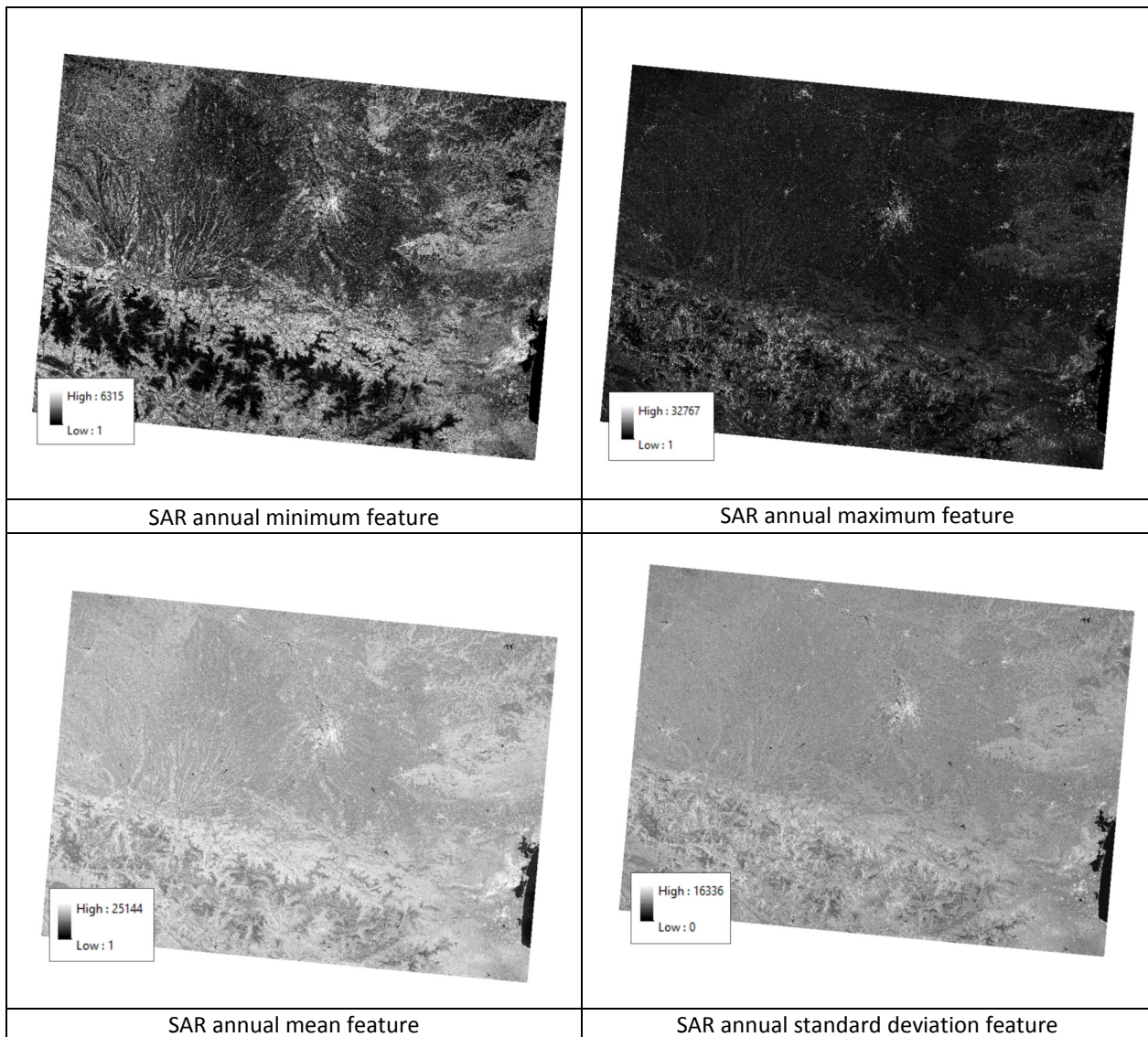


Figure 5-4: SAR statistical features (NB: the 4 features have different value ranges and scaling)

AUTOMATED DERIVATION OF CLASSIFICATION TRAINING SAMPLES

As input for these machine learning algorithms, a set of training data is required. The training data chosen must therefore be representative of the whole study area in order to cover all the reflectance variations of the classes, as well as to go further and take into account the local variability of the environmental classes due to the soil type, moisture, etc. The training sites must be exempt from anomalies and must be a suitable statistical representation of the area. There must be a substantial number of them. That is why, the historical High Resolution Layers have been used as training data:

Reliable training samples have been derived from relevant in-situ sources: historical HRL 2015 Imperviousness, Forest, Grassland, Water and Small Woody Features. In order to best reflect the different imperviousness classes, an automated random point sampling within buffered IMD 2015 has been applied. Samples in non-built-up areas have been selected in different land cover classes such as grassland, bare soil, vegetation and water in order to obtain a representative distribution of non-imperviousness samples.

Based on the spectral information, biophysical indicators and texture parameters at the training sample points, the algorithm ‘learns’ how to classify the features (Tan et al. 2006, Camp-Valls, 2009) and identifies

the most significant combinations of input parameters to differentiate built-up areas from other land cover.

For the purpose of the automated derivation of the training sample, a stratified random approach, based on the HRLs, has been preferred.

PRODUCTION OF INITIAL BUILT-UP AND NON BUILT-UP MASKS FOR 2017

The results of the initial Sentinel-2 based built-up and non-built-up mask are shown in Figure 5-5.

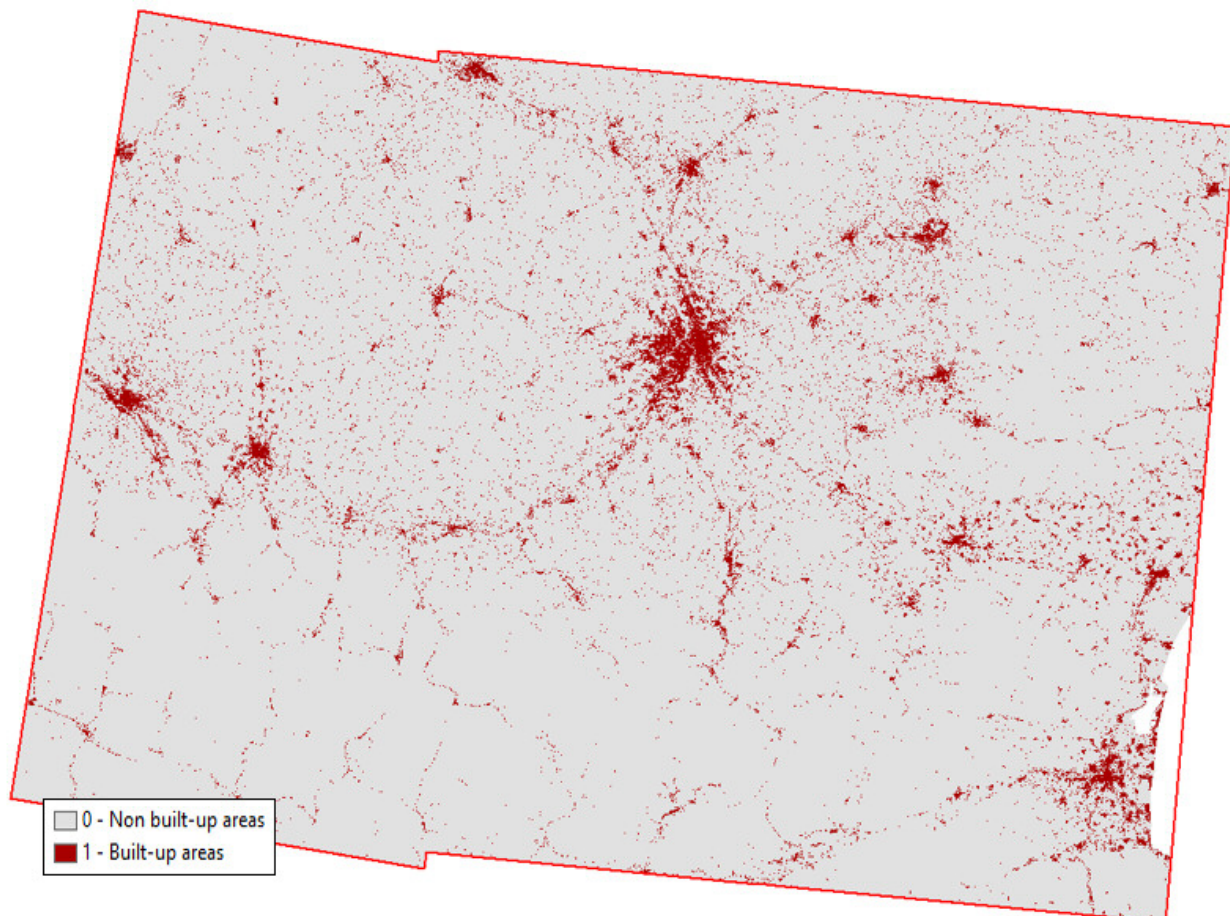


Figure 5-5: Sentinel-2 based initial built-up and non-built-up mask for 2017

Finally, the results from Sentinel-1 (see Figure 5-6) were not as good as from Sentinel-2 and could therefore not be included in the following steps. Investigations will be made to improve the Sentinel-1 based results in phase 2.

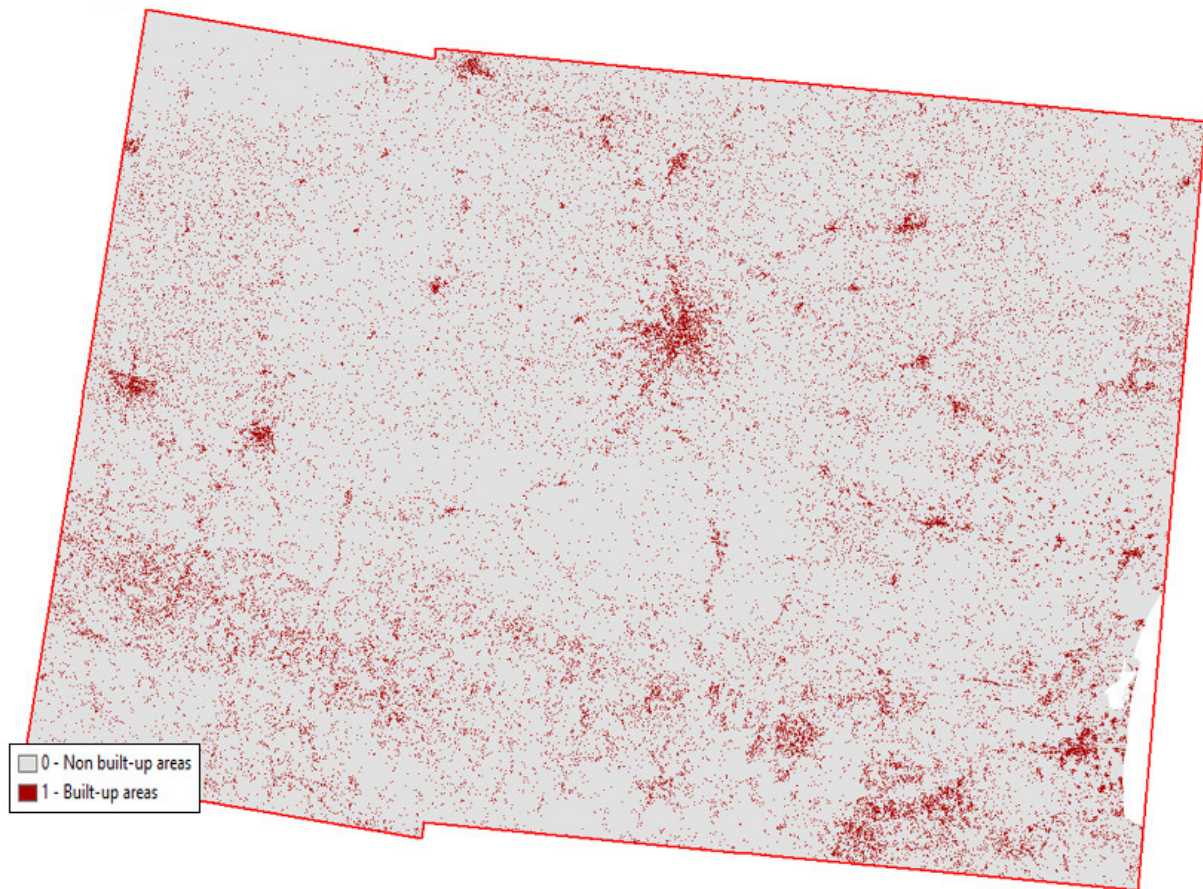


Figure 5-6: Sentinel-1 based initial built-up and non-built-up mask for 2017

Absolute and Relative Calibration of IMD2017

Besides the production of initial built-up and non-built-up masks for 2017 (previous steps described in section 4), one key step in the HRL Imperviousness production is the estimation of the degree of imperviousness and linking these IMD measurements over time. Each single pixel in the built-up mask will be assigned an imperviousness density value of 1 to 100%. The linkage between the biophysical variables and the IMD measurements will be done through an absolute (linking the biophysical variables to IMD) and relative calibration procedure. This combination will improve the accuracy of imperviousness density estimates, correct any over-/underestimation of values and assure comparability and consistency over time.

The reference calibration database serves as calibration input for an absolute calibration of the 2017 IMD measurements. For the prediction of the imperviousness degree, a linear regression method is used to model the relationship between the collected reference samples and meaningful metrics from the biophysical variables (e.g. NDVI_{max}) derived from the seasonal image composites. The established linear equation is applied to transform the input data into imperviousness degree values between 1 – 100%. This will result in absolutely calibrated IMD measurements derived from the 2017 imagery.

Then, the calibrated 20m IMD 2015 status layer will be used as input to adjust the imperviousness density values of 2017 by relative calibration. Indeed, despite the absolute calibration based on a well-established procedure (with the use of a reference calibration dataset), there will always remain some obvious and local issues in the imperviousness density derivation which will lead to wrongly detection changes in the change Layers. The relative approach is so needed to correct these local artefacts

The IMD 2017 values, limited to the newly created 2017 built-up mask, are re-analyzed by an automatic cross-calibration approach: the IMD 2017 values are compared to the IMD 2015 values resampled to 10 meters spatial resolution and further corrected using a rule-based approach. Indeed, a filtering approach is needed to adequately map sealing changes. In 20m spatial resolution, changes of imperviousness density within built-up areas are not that frequent compared to changes of the built-up area. Despite all the calibration efforts in image pre-processing and subsequent adaptation procedures, there will always remain a certain error budget for sealing change detection mainly caused by:

- Persisting spectral differences due to even subtle deviations in illumination, shadow effects, atmospheric conditions and vegetation status, often in conjunction with:
- Geometric misalignments of the IMAGE databases. This occurs quite frequently and often exceeds a range of 1 pixel (>20m).

Hence, in order to derive a reliable and realistic picture of sealing changes (within existing built-up areas), thresholds are applied. Differences of >20% of sealing increase will be considered acceptable if a contiguous area of at least 16 (10m x 10m) pixels is concerned. The threshold of 16 contiguous pixels permits to overcome the scaling issue (10 vs 20m spatial resolution). Differences <= 20% sealing increase will be considered as stable. The special case of imperviousness decrease is rare and, if occurring, it will rather be due to a re-greening (full de-sealing) of an impervious surface than an actual decrease. With regard to this assumption sealing decrease within built-up areas will only be accepted as valid if a remarkable change of 80% decrease takes place. Differences <= 80% sealing decrease will be considered as stable.

POST-PROCESSING

The post-classification (see Figure 5-7) implies post-processing of the layers in order to be spatially consistent, including:

- Post-processing filtering usually used in global urban maps. Indeed, there is a significant portion of noise due to single pixels or isolated pixels (small aggregated group of pixels), which are most likely misclassifications. Such noises should be reduced/removed with post-classification filtering approaches.
- Contextual analysis based on change probability (Lefebvre et al., 2016). The aim is to take into account the built-up pixels in the 2015 built-up mask in order to establish a probability map of changes. The analysis describes each cell's relationship/membership to a source or a set of sources based on probabilities. The assumption made using the contextual analysis is that urbanized areas spread more than they appear randomly in the landscape (Lefebvre et al., 2016).

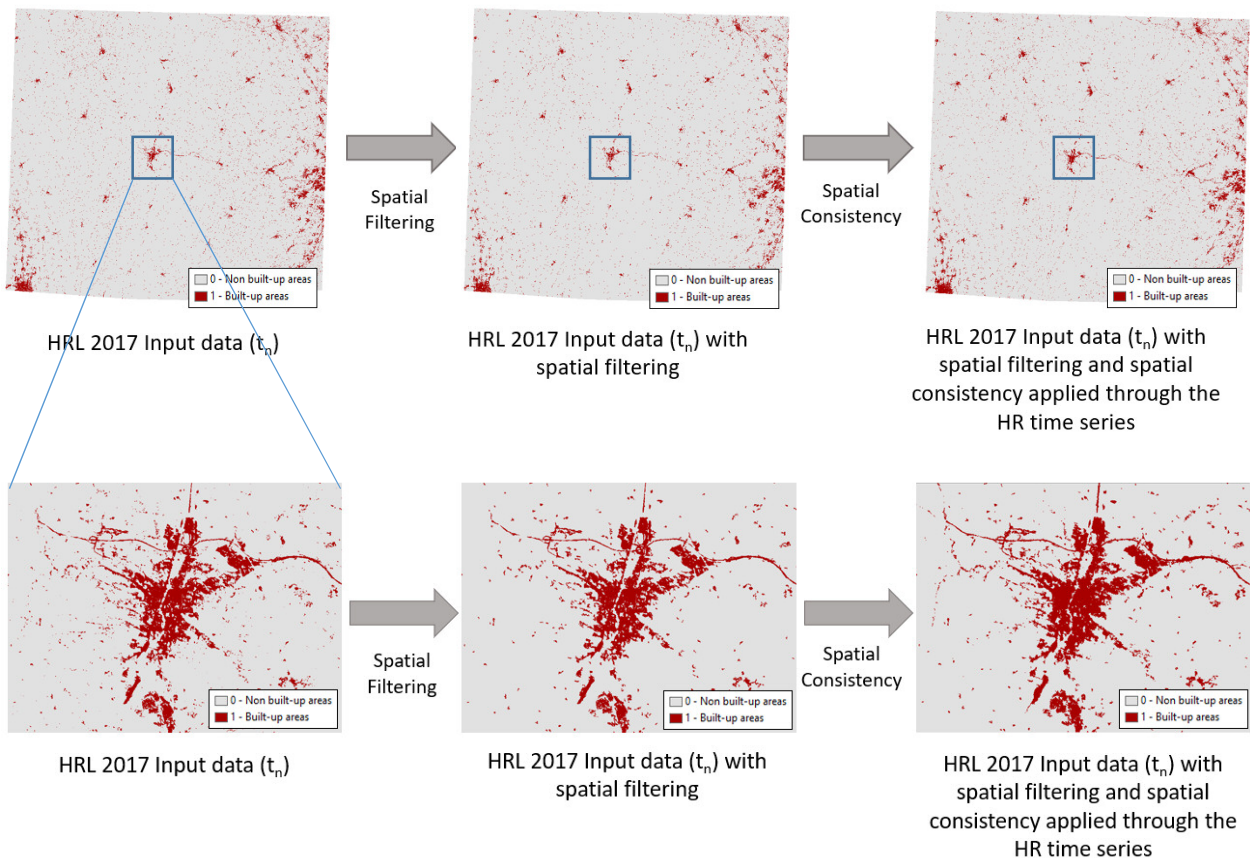


Figure 5-7: Post-classification processing

The final result of the implemented Imperviousness prototype 2017 is shown in Figure 5-8.

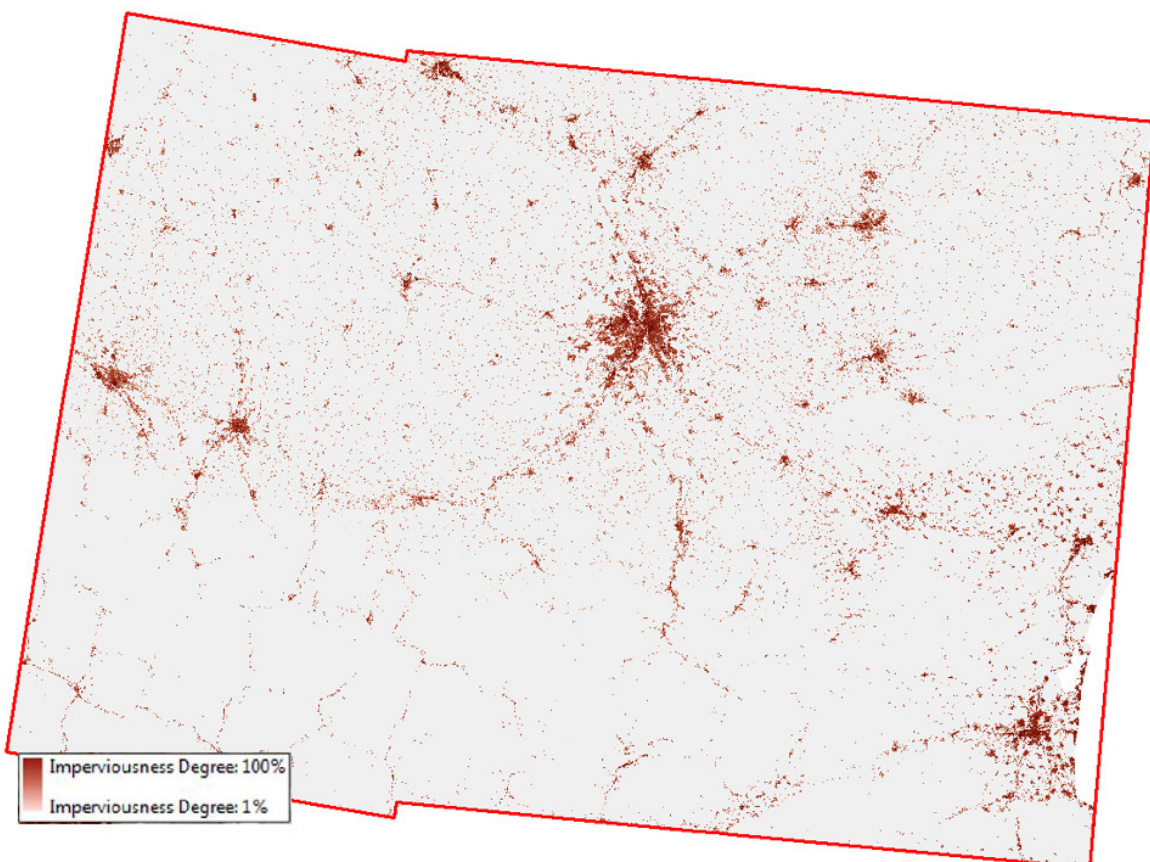


Figure 5-8: Final HRL Imperviousness 2017 prototype for the South-West demonstration site

5.1.1.3.3 Production of the Imperviousness Change 2015-2017

The change detection 2015-2017 is applied based on the HRL IMD 2017 Prototype resampled to 20m and the IMD 2015 from the HRL Imperviousness 2015 produced during the operational HRL production outside this project. It is important to note that this step not only reveals 2015-2017 built-up changes, but, as stated before, it also detects potential omission errors of the built-up mask 2015 as well as potential commission errors of the 2017 built-up mask.

At first, a 20m change layer is calculated by direct subtraction of the 20m imperviousness values but without any further filtering, thereby guaranteeing full consistency of all products. The result displays the total imperviousness degree change values from -100% to +100%, according to the thresholds set at the relative calibration and without any thematic classification applied. In other words, the first-step change layer only consists of a continuous layer with change values from -100% decrease to +100% increase and not a categorisation of changes.

Then, a spatial filtering is applied in order to take into account the different specifications. Indeed, the HRL IMD 2015 data presents a 20-meters spatial resolution whereas the HRL 2017 Prototype, based on Sentinel-2, shows a 10-meters resolution. A minimum mapping unit has been applied on the HRL 2017 Prototype based on a 4 pixels contiguous rule.

To be fully compliant with the actual specification of the products, the derived change layer is then converted into a ‘classified change’ layer. For this purpose, the continuous change values will be thematically aggregated into the following categorical classes according to the rule base defined in Table 5-3 below.

Table 5-3: Specifications of the ‘classified change’ layer

Class Code	Classified change Class name	IMD	
		t1	t2
0	unchanged areas with IMD=0%	0%	0%
1	new cover (increased imperviousness density, 0% IMD at first reference date)	0%	>0%
2	loss of cover (decreasing imperviousness density, 0% IMD at second reference date)	>0%	0
10	unchanged areas (IMD>0% at both reference dates)	>0%	>0%
11	increased IMD (IMD>0% at both reference dates) subject to a 20% threshold for 4px contiguous areas	>0%	>>0%
12	decreased IMD (IMD>0 at both reference dates) subject to a 80% threshold for 4px contiguous areas	>>0%	>0
254	unclassifiable in any of parent status layers	254	254
255	outside area	255	255

The final result of the implementation of the production of the Imperviousness Change Prototype 2015-2017 is presented in the Figure 5-9:

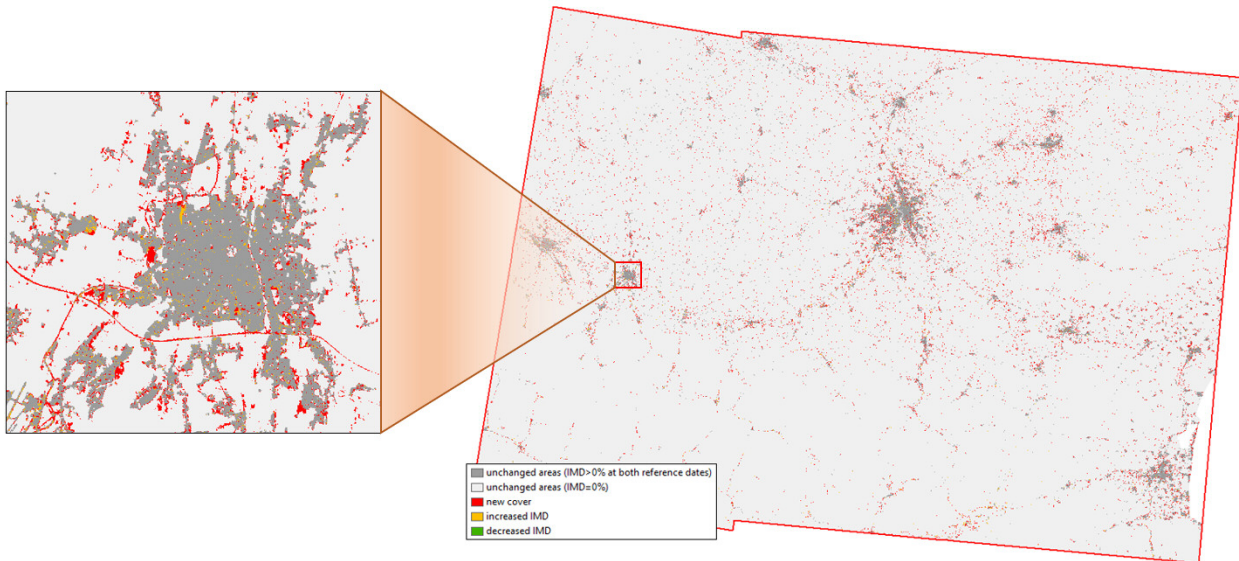


Figure 5-9: Final HRL Imperviousness Change 2015-2017 prototype for the South-West demonstration site

5.1.2 Classification Results and Validation

This chapter depicts the results of the classification as well as their validation. Firstly, the thematic accuracies are summarized (see section 5.1.2.1). The thematic accuracies are followed by a discussion of the validation results (see section 5.1.2.2).

5.1.2.1 Thematic accuracy

The below confusion matrix gives a summary of the internal accuracy assessment of the improved HRL Imperviousness 2017 for the demonstration site (Table 5-4).

Table 5-4: Confusion matrix of the internal validation of the IMD 2017 in demo site South-West (area-weighted)

		REFERENCE		Total			
		0	1				
IMD 2017	0	890.28	7.21	897.49	User	CI95%	Com.
	1	15.30	87.21	102.51	85.07%	1.67%	14.93%
	Total	905.58	94.42	1,000.00	Prod.	92.37%	
		Prod.		92.37%			
		CI95%		1.61%			
		Omi.		7.63%			

5.1.2.2 Discussion of the validation results

Regarding the HRL IMD 2017 prototype, the look and feel assessment shows very satisfying results. Based on the confusion matrix, the internal validation results show very good area-weighted user's and producer's accuracies. The IMD 2017 product shows a very high producer's accuracy (92.37% +/- 1.61%) which is above the requirements threshold. In other words, the validation shows a very limited amount of

omission errors. The user's accuracy is slightly under the required 90% but shows good level of reliability (85.07% +/- 1.67%).

It is important to note that these results are based on the IMD product fully obtained automatically without manual enhancement.

Most of the omission errors concern small and isolated built-up features as exemplarily shown in Figure 5-10 below.



Figure 5-10: Case of omission (yellow dots) in isolated built-up features in the IMD 2017 prototype

Regarding the commission errors, as known from previous HRL IMP productions, the sources of errors are related to the following land use features: arable lands without crops, construction sites, quarries, dry riverbeds (e.g. bare soils). Examples are provided in Figure 5-11.

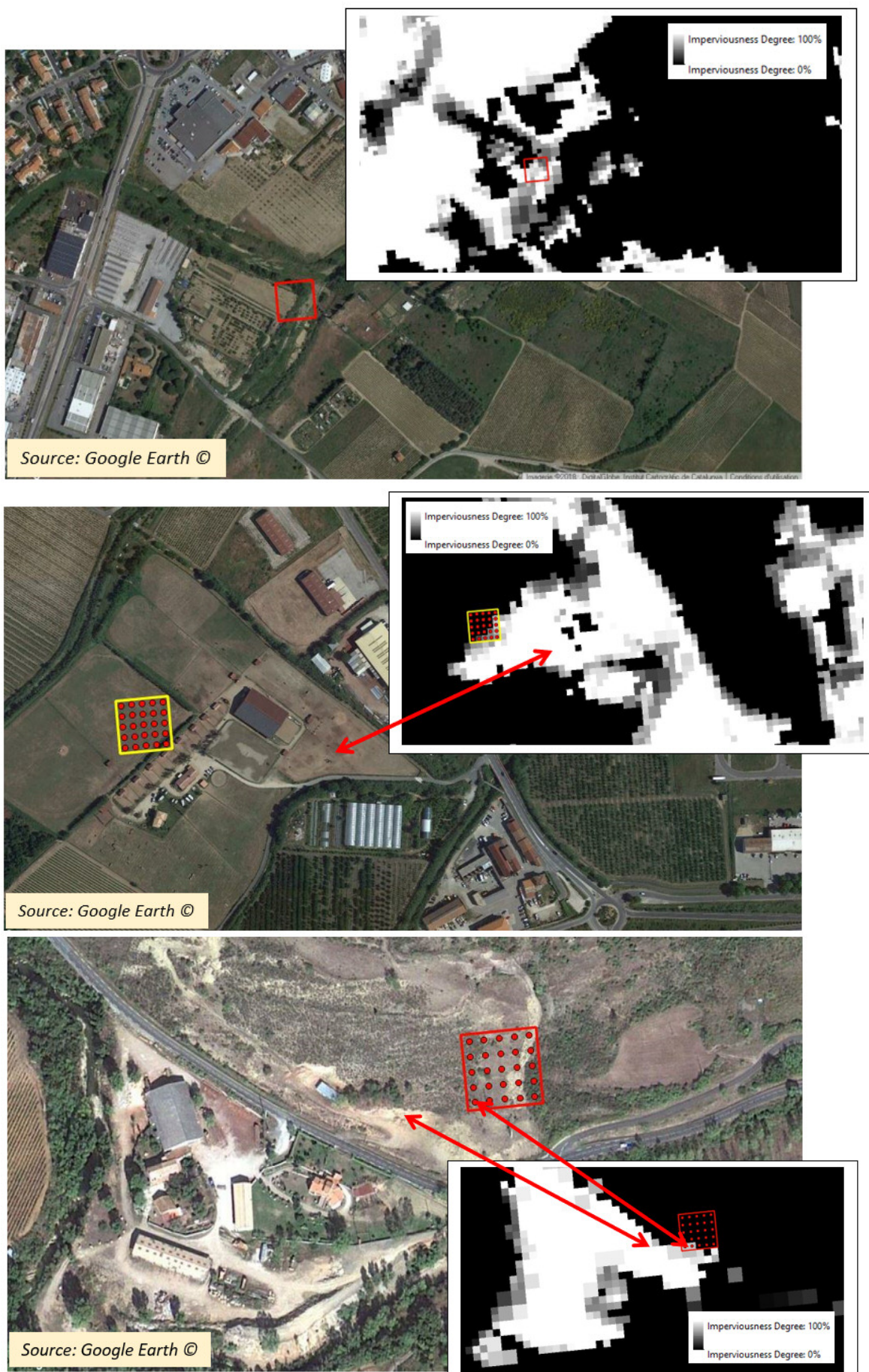


Figure 5-11: Examples of commission errors in the IMD 2017 prototype

5.1.3 Change Detection and Incremental Update Results and Validation

As described before, the benchmarking of the best change detection approach is only done on the basis of the best status layer classification for 2017 based on Sentinel-2 cloud-free images (high resolution spectral and spatial). The implementation has been done on the demonstration site South-West. The change results obtained from the reference calibration dataset are presented in Table 5-5.

Table 5-5: Proportional distribution of detected changes within the IMC layer

% of total change areas	
New built-up 2017	5.80%
Omission errors 2015 (undetected built-up 2015):	78.90%
Commission errors 2017 (false built-up 2017)	15.30%

Based on the calibration dataset, the relative magnitude of actual change is estimated to 5.8% of the total change areas. Thus, the errors concern the remaining 94% of the change areas detected, which is mostly due to the different spatial resolutions, i.e. 10m vs 20m. There is a high amount of omission errors coming from the reference data (2015), impacting the change areas detected.

Although the majority of errors is detected in the reference layer, new errors can also appear in the detection of change between two-time periods. The change layers' errors can be, as mentioned before, due to the following factors:

- Omission of change (quantifiable only in the validation, but not as a delineation from the product);
- Commission errors added for the new period (cf. Figure 5-14);
- Omission errors detected for the previous period (cf. Figure 5-13).

Regarding the latter, it should be noted that the specifications of the HRL 2015 layer are different from the specifications and the input data situation for the HRL 2017, hence a comparison is not fully “fair”. Indeed, for 2015 the product was obtained through a 20-meter spatial resolution production mostly based on Landsat data, whereas the HRL 2017 could draw upon Sentinel-2 and a 10-meter resolution, which explains that most of the omission errors concern small and isolated built-up features (cf. Figure 5-12). It would therefore be a wrong conclusion to consider the reference layer of 2015 being of poor quality.

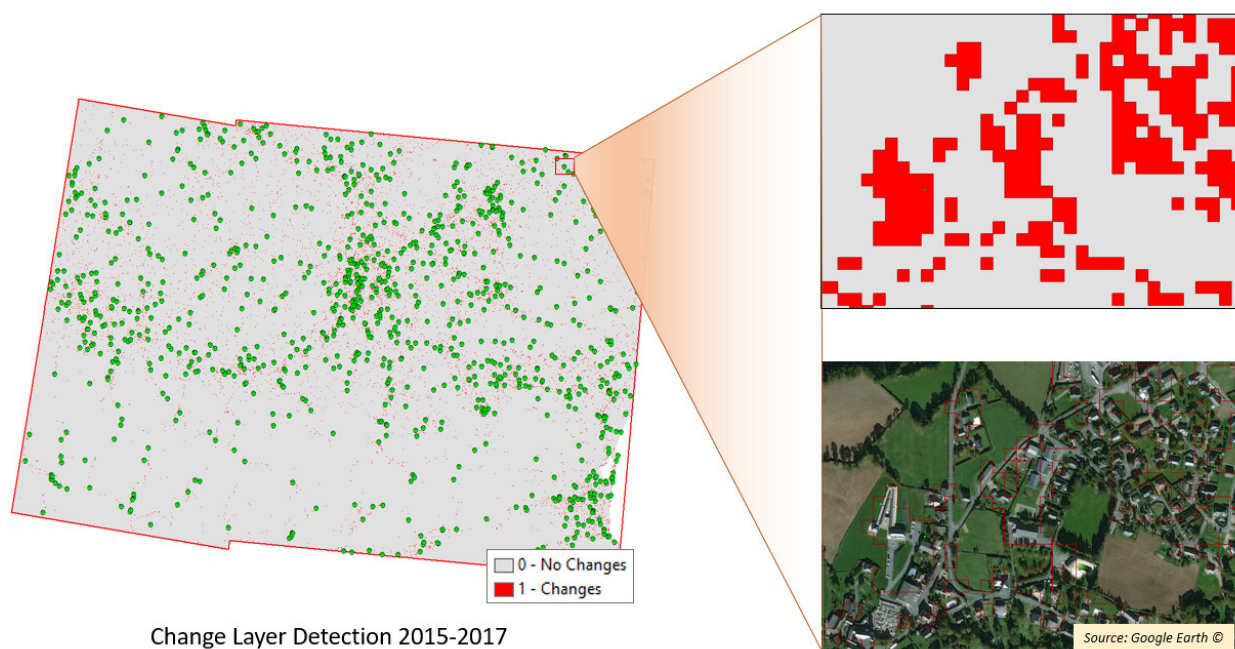


Figure 5-12: Example of calibration points for the newly detected built-up in 2017

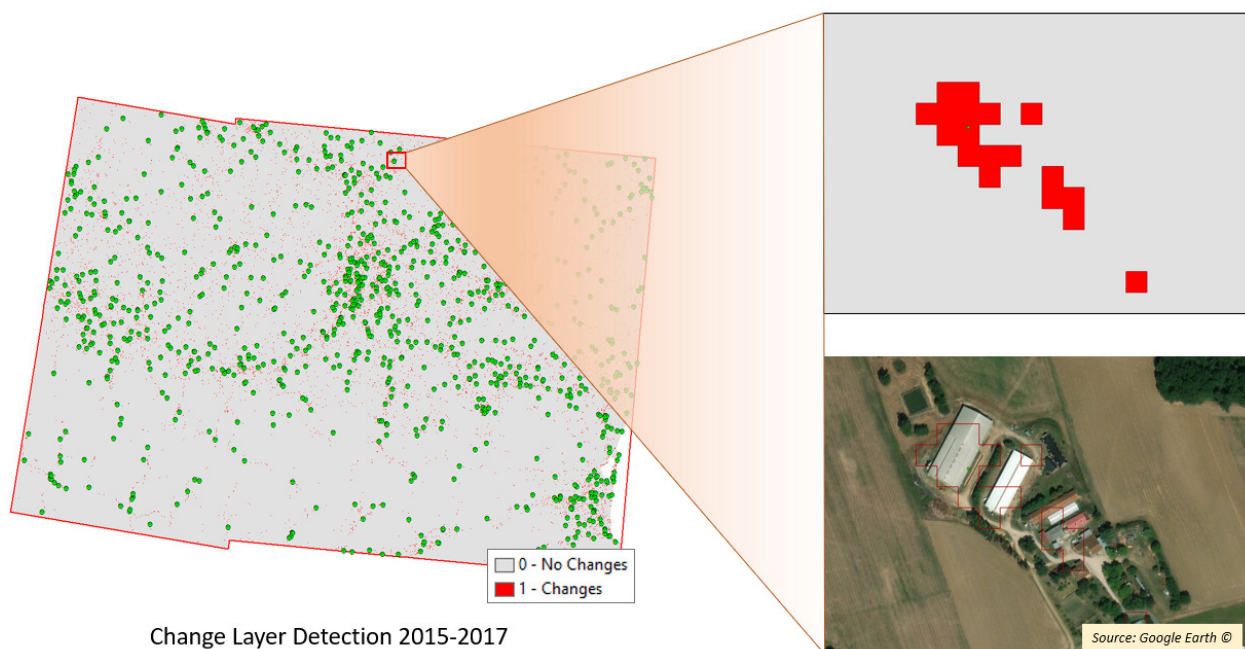


Figure 5-13: Example of omission errors in 2015 (undetected built-up in 2015)

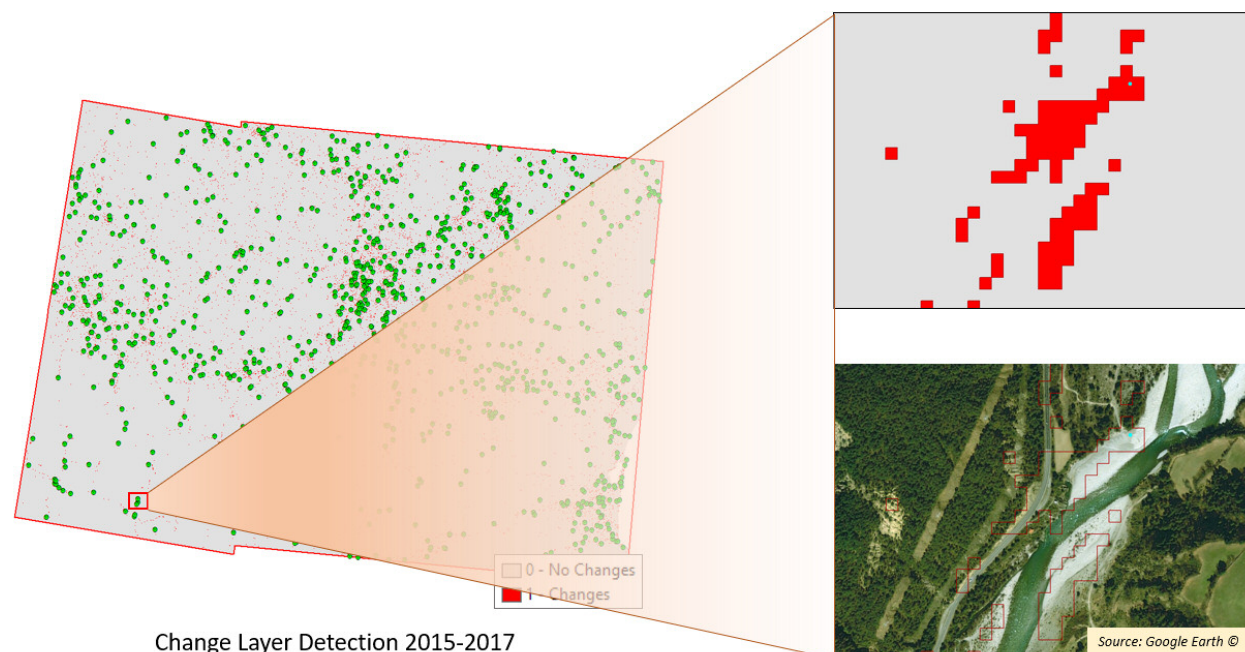


Figure 5-14: Example of commission errors in 2017, false built-up in 2017

5.2 Prototype of a potential Future HRL Forest

This section shows the prototypical implementation of the Forest Prototypes (both the improved status layer DLT and the incremental update layer TCC). Firstly, the data and processing setup is described (section 5.2.1), followed by presenting the classification results and validation (section 5.2.2), and lastly the demonstration of the change detection and incremental update results and validation (section 5.2.3).

5.2.1 Data and Processing Setup

In the following, relevant steps to prepare the input data are presented. Besides Sentinel-2, representing the main data source, also other data have been integrated in the workflow and specifically prepared (e.g. the Copernicus High Resolution Layers 2015). Thereafter, the conducted pre-processing steps are detailed and the experimental setup for the classification and incremental update approach is explained.

5.2.1.1 Input Data

The ECoLaSS demonstration site North in Sweden comprises six adjacent Sentinel-2 tiles (33VVF, 33VVH, 33VVG, 33VWF, 33VWH, 33VWG), for which Sentinel-2A+B data in 10m resolution have been processed. Selected scenes cover the time frame from 15-March to 15-August 2017. This period represents an extension of the successfully tested spring period (15 March to 15 June) in Task 3, which had yielded the best results in terms of accuracy and processing costs (see [AD06]). This extension became necessary due to a difficult data situation caused by frequent cloud cover, in particular in the northern tiles which were not part of the test site for benchmarking in Task 3 (cf. Figure 5-15).

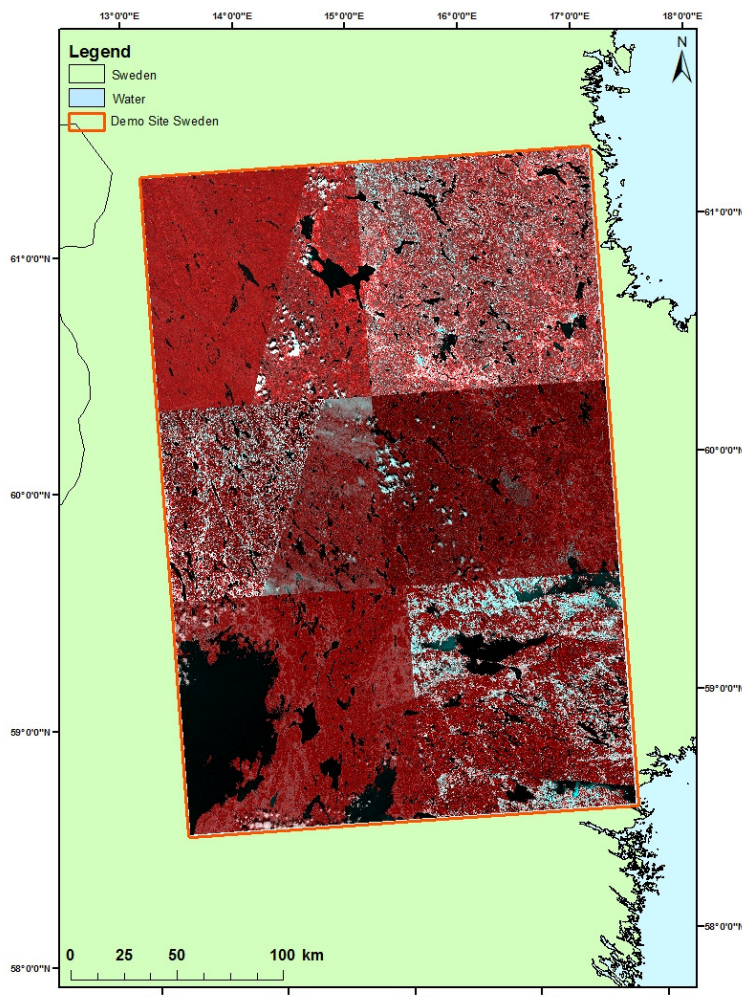


Figure 5-15: Sentinel-2 coverage of the ECoLaSS demonstration site North in Sweden.
(contains modified Copernicus Sentinel data [2017]; © EuroGeographics for the administrative boundaries)

In total, 90 Sentinel-2A+B images were used to produce the forest prototypes. Figure 5-15 shows the coverage of selected scenes for each of the six MGRS Sentinel tiles. As the cloud cover conditions in the northern countries are generally rated as difficult, the maximum allowable cloud cover threshold has been set to 60% to ensure the feasibility of calculation of complex time features by the application of a temporal sliding window (the concept of simple and complex time features is described in [AD07]). The number of available scenes with less than 60% cloud cover per tile is presented for each tile in Figure 5-16. A detailed tile-specific view of the cloud cover per individual images is given in Figure 5-17.

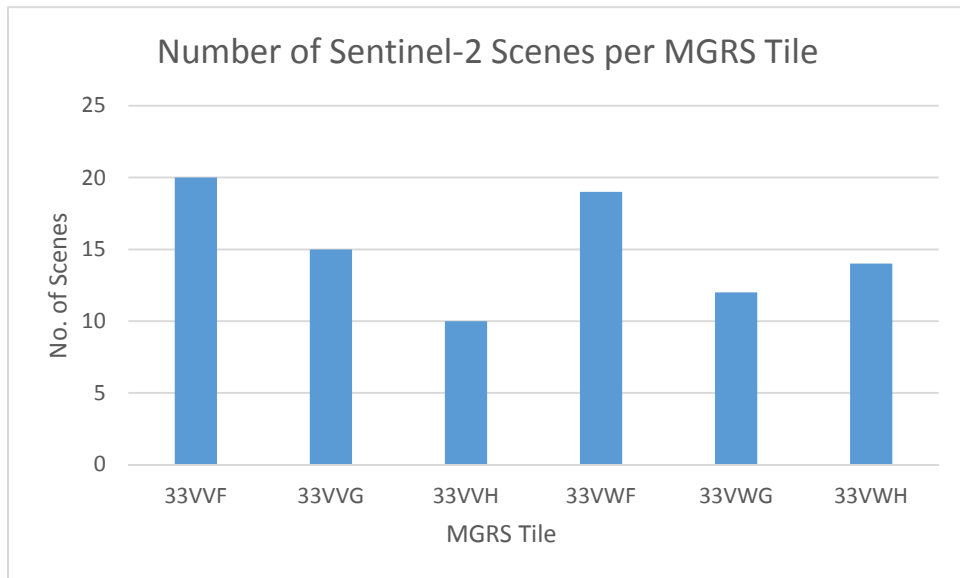


Figure 5-16: No. of Sentinel-2 scenes with maximum 60% cloud cover from 15-March to 15-August 2017 in the demonstration site North

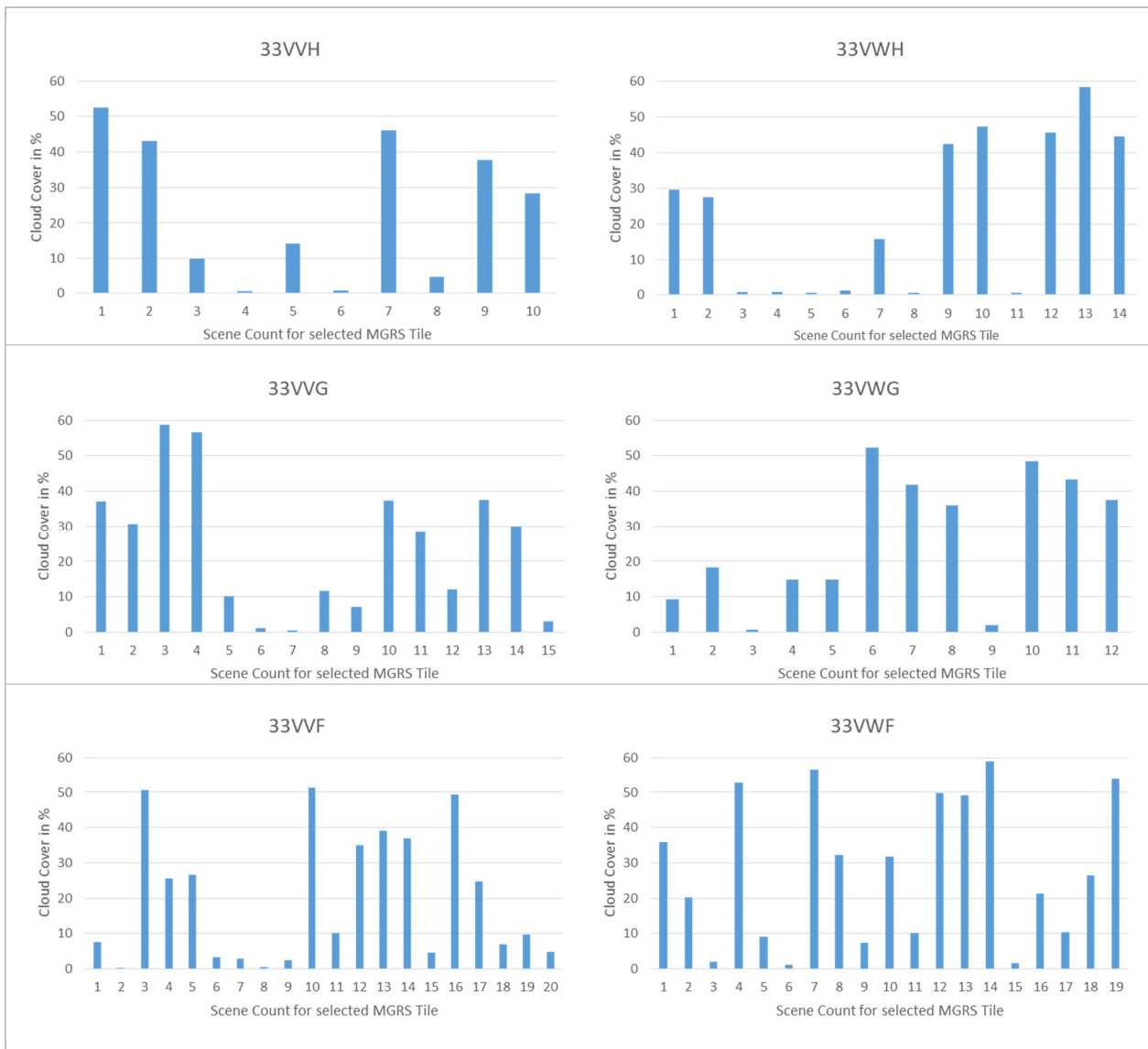


Figure 5-17: Cloud cover percentages (y axis) per scene count (x axis) for relevant MGRS tiles

From the Scene Classification Layer (SCL) obtained through Sen2Cor, scene-specific pixel-based cloud masks have been calculated. Figure 5-18 shows the respective data score (inverted cloud score) for each pixel in the demonstration site North, which is the number of available cloud-free Sentinel-2 observations per pixel, acquired within the selected time period 15-March to 15-August 2017.

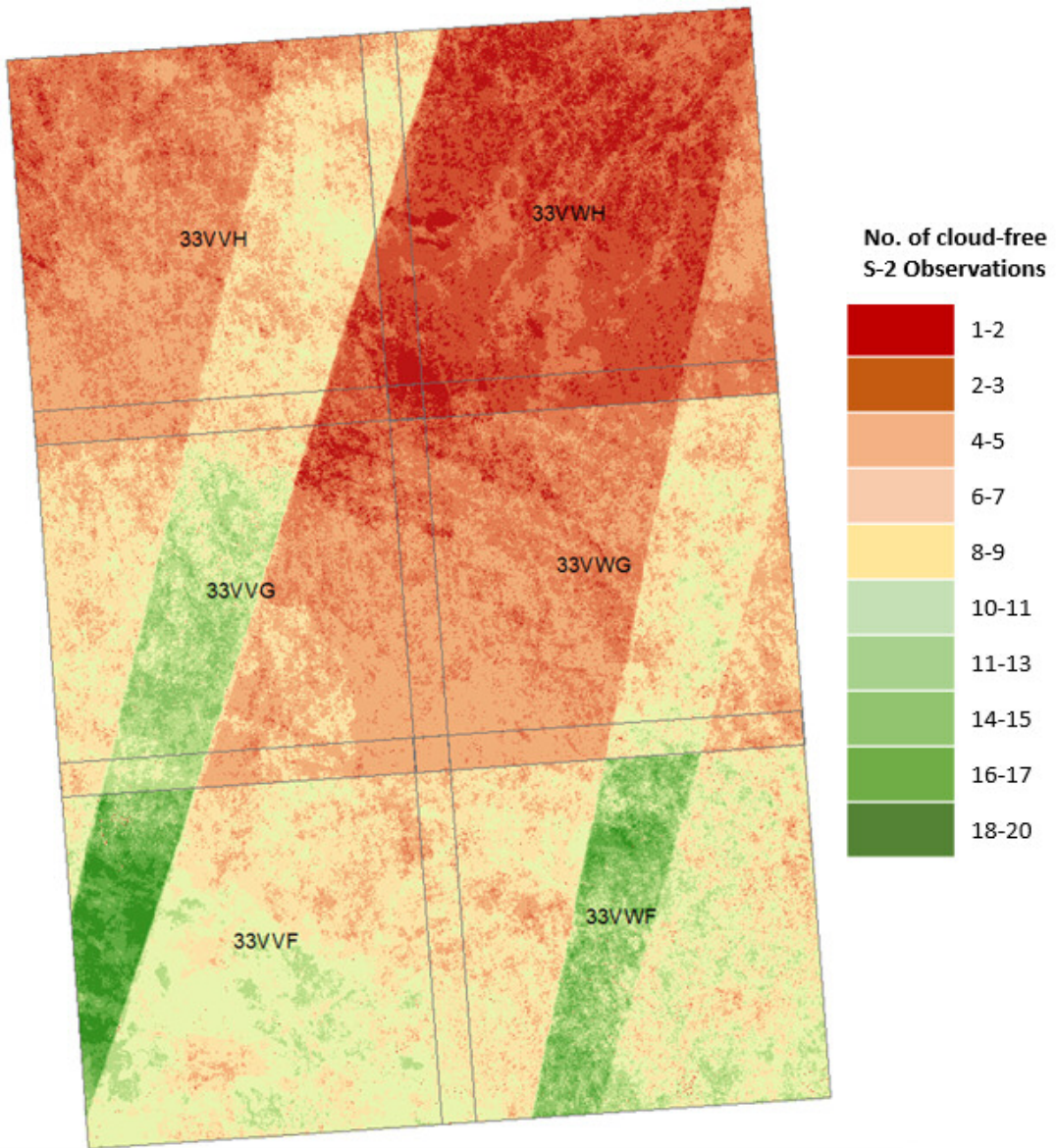


Figure 5-18: Sentinel-2 Data Score Layer (S2DSL): Number of cloud-free Sentinel-2 observations per pixel

The created Sentinel-2 Data Score Layer (S2DSL) is provided together with the products and provides information on the number of cloud-free Sentinel-2 observations per pixel. This information can be additionally used to assess the accuracy of the DLT and TCC products in areas with a poor data situation, since areas with less observations might tend to have a higher uncertainty in classification accuracy.

Additionally, the existing Copernicus High Resolution Layers 2015 (Imperviousness Degree, Dominant Leaf Type, Grassland, Water and Wetness) in 20m spatial resolution have been combined to generate a forest sample layer, which was used for the implemented automatic sampling approach. The layer has been derived by integration of the HRLs 2015 in a hierarchical order and is presented in Figure 5-19.

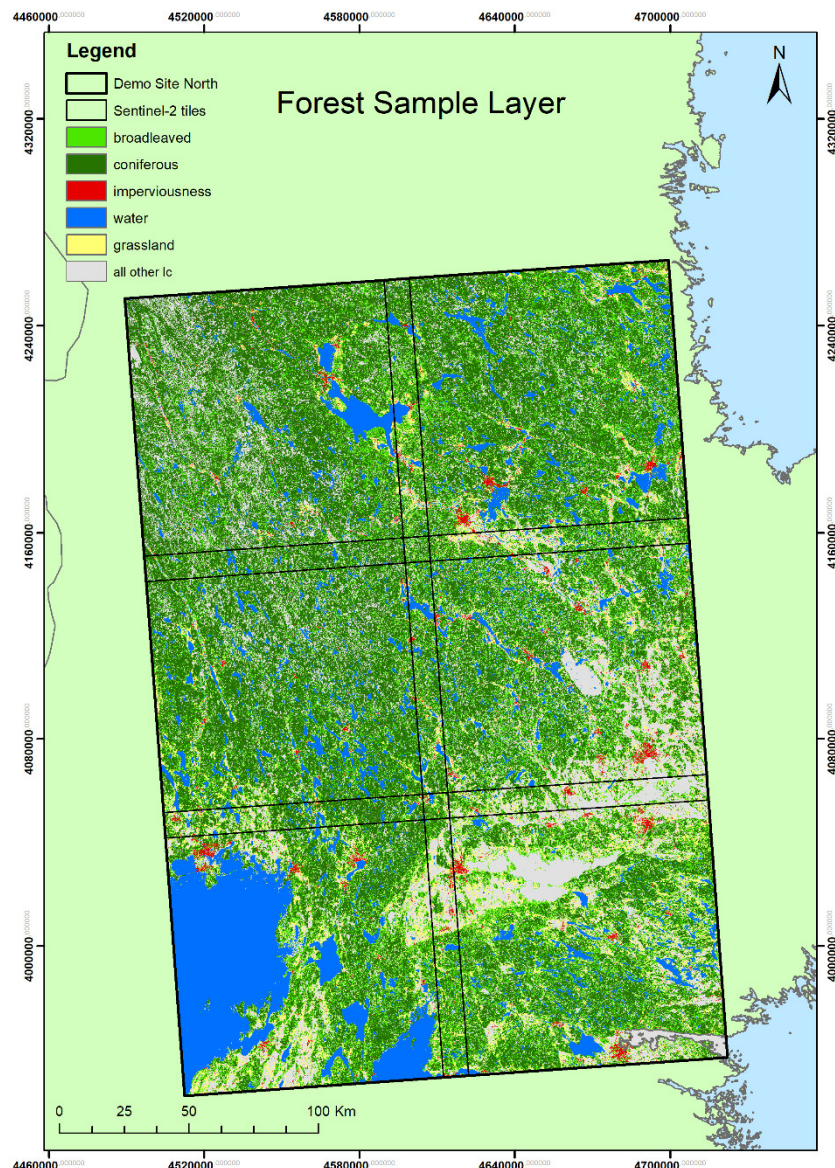


Figure 5-19: Forest sample layer derived from the integrated Copernicus High Resolution Layers 2015
 (© EuroGeographics for the administrative boundaries)

It consists of six thematic classes: broadleaved, coniferous, imperviousness, water, grassland and all other land cover. Table 5-6 provides some statistics on the derived sample layer.

Table 5-6: Land Cover statistics of the derived HRL 2015 sample layer

Class Code	Order	Class Name	Area km ²	Area %
1	3	broadleaved	12,457.50	19.15
2	4	coniferous	26,369.55	40.54
3	1	imperviousness	794.21	1.22
4	2	water	7,576.86	11.64
5	5	grassland	3,715.23	5.71
6	6	all other LC	14,130.01	21.72

Subsequently, a systematic random sampling approach has been applied to collect 1,500 samples from the generated sample layer. The aim was to automatically collect a sufficient number of samples within broadleaved/coniferous forests and in areas with no tree cover (represented by specific thematic LC classes). This pool comprises the basis for the sample selection necessary for the TCM and DLT 2017 classifications.

5.2.1.2 Pre-processing

The EO pre-processing steps include an atmospheric correction (including cirrus removal), cloud mask processing, topographic normalisation with Minnaert correction, image export in TIFF format and a subsequently performed re-projection from the native Sentinel-2 UTM projection to the European Terrestrial Reference System 1989 (ETRS89). For the atmospheric correction and topographic normalization the ESA Sen2Cor software was utilized. Details on the specific pre-processing steps of the optical Sentinel-2 data are provided in [AD06].

5.2.1.3 Experimental Setup

Methods and experiences from the previous testing and benchmarking exercise described in [AD07] have been considered to set up a classification model for the forest prototype in the demonstration site North.

For implementation of the forest prototype, a specific model has been created within a Python framework. The model aims for an automated tree cover and dominant leaf type classification using time features derived from the Sentinel time series within the period mid-March to mid of August, whereby training sample quality is of vital importance. The spring season (mid-March to mid of June) previously successfully tested within Task 3 has been extended until mid of August to address cloud cover issues in the selected optical EO data. Finally, two independent sample datasets were used for the classification and validation.

Training samples for the TCM and DLT classification have been extracted from the integrated HRL 2015 sample layer as described above.

Table 5-7 shows the distribution of sample points of the training dataset. Several measures were undertaken to reduce the number of outliers and errors within this sample pool, such as:

1. Reduction of edge effects and mixed pixels through negative buffering (20m) of the HRL DLT product classes (broadleaved trees/coniferous trees). The remaining forest patches usually represent patches of relatively homogenous leaf type;
2. Removal of patches smaller than 0.5 ha;
3. Creation of three strata: coniferous, broadleaved and non-forest (represented by the classes imperviousness, water, grassland and all other LC);
4. Equally stratified random polygon sampling (30m x 30m) within the three strata;
5. Removal of class-specific sampling errors through spectral checks in form of scatter plots;
6. Iterative resampling and visual check of samples for the broadleaved class.

Table 5-7: Sample distribution of the initial training dataset.

Class ID	Class name	Training data # polygons
0	all non-tree areas	500
1	broadleaved trees	500
2	coniferous trees	500

From the created sampling pool following the steps described above, two sample training datasets have been created for classification of the TCM and DLT. From these datasets, a final selection has been made by consulting high and very high resolution (VHR) optical satellite data as well as Google Earth Pro and Bing Maps to verify tree cover and leaf type. These validated samples were coded according to the convention

for the production of the TCM and DLT products and were finally weighted according to the estimated area proportion (derived from HRL Forest 2015).

The classification workflow comprises the following steps:

- Derivation of time features (complex and simple) from a time series of Sentinel bands/indices
- Creation of reference dataset, consisting of:
 - a set of training samples
 - a set of independently interpreted validation polygons
- Extraction of raster values at reference data locations (based on a set of samples) for the (selected) time features
- Training the classifier based on the training set, resulting in a classification model
- Generation of an accuracy report based on the independent validation data
- Prediction/mapping with the calculated raster features via the final model. This step yields the predictions (classes), class-probabilities (one layer per class), and their reliability layers (max, probability, breaking ties, entropy).

Table 5-8 provides an overview of the calculated time features based on the indices BRIGHTNESS, inverted red-edge chlorophyll index (IRECI), NDVI and Normalized Difference Water Index (NDWI), which have been used in the classification process. A full description of the calculated time features is given in [AD06].

Table 5-8: Set of calculated time features relevant for TCM and DLT 2017 classification

FEATURE NO.	SENTINEL-2 SCENE SET (START DATE TO END DATE; MAX CLOUD COVER)	BAND/INDEX	FEATURE TYPE
1	S2_2017-03-15TO2017-08-15_CC60	BRIGHTNESS	actn0t42
2	S2_2017-03-15TO2017-08-15_CC60	BRIGHTNESS	difdif3mean
3	S2_2017-03-15TO2017-08-15_CC60	BRIGHTNESS	difmax3mean
4	S2_2017-03-15TO2017-08-15_CC60	BRIGHTNESS	difmin3mean
5	S2_2017-03-15TO2017-08-15_CC60	BRIGHTNESS	max
6	S2_2017-03-15TO2017-08-15_CC60	BRIGHTNESS	maxmean3
7	S2_2017-03-15TO2017-08-15_CC60	BRIGHTNESS	mean
8	S2_2017-03-15TO2017-08-15_CC60	BRIGHTNESS	min
9	S2_2017-03-15TO2017-08-15_CC60	BRIGHTNESS	p010
10	S2_2017-03-15TO2017-08-15_CC60	BRIGHTNESS	p025
11	S2_2017-03-15TO2017-08-15_CC60	BRIGHTNESS	p050
12	S2_2017-03-15TO2017-08-15_CC60	BRIGHTNESS	p075
13	S2_2017-03-15TO2017-08-15_CC60	BRIGHTNESS	p090
14	S2_2017-03-15TO2017-08-15_CC60	BRIGHTNESS	pdiff075025
15	S2_2017-03-15TO2017-08-15_CC60	BRIGHTNESS	pdiff090010
16	S2_2017-03-15TO2017-08-15_CC60	BRIGHTNESS	std
17	S2_2017-03-15TO2017-08-15_CC60	IRECI	actn0t42
18	S2_2017-03-15TO2017-08-15_CC60	IRECI	difdif3mean
19	S2_2017-03-15TO2017-08-15_CC60	IRECI	difmax3mean
20	S2_2017-03-15TO2017-08-15_CC60	IRECI	difmin3mean
21	S2_2017-03-15TO2017-08-15_CC60	IRECI	max
22	S2_2017-03-15TO2017-08-15_CC60	IRECI	maxmean3
23	S2_2017-03-15TO2017-08-15_CC60	IRECI	mean
24	S2_2017-03-15TO2017-08-15_CC60	IRECI	min
25	S2_2017-03-15TO2017-08-15_CC60	IRECI	p010
26	S2_2017-03-15TO2017-08-15_CC60	IRECI	p025
27	S2_2017-03-15TO2017-08-15_CC60	IRECI	p050
28	S2_2017-03-15TO2017-08-15_CC60	IRECI	p075
29	S2_2017-03-15TO2017-08-15_CC60	IRECI	p090
30	S2_2017-03-15TO2017-08-15_CC60	IRECI	pdiff075025
31	S2_2017-03-15TO2017-08-15_CC60	IRECI	pdiff090010
32	S2_2017-03-15TO2017-08-15_CC60	IRECI	std
33	S2_2017-03-15TO2017-08-15_CC60	NDVI	actn0t42
34	S2_2017-03-15TO2017-08-15_CC60	NDVI	difdif3mean
35	S2_2017-03-15TO2017-08-15_CC60	NDVI	difmax3mean
36	S2_2017-03-15TO2017-08-15_CC60	NDVI	difmin3mean
37	S2_2017-03-15TO2017-08-15_CC60	NDVI	max
38	S2_2017-03-15TO2017-08-15_CC60	NDVI	maxmean3
39	S2_2017-03-15TO2017-08-15_CC60	NDVI	mean
40	S2_2017-03-15TO2017-08-15_CC60	NDVI	min
41	S2_2017-03-15TO2017-08-15_CC60	NDVI	p010
42	S2_2017-03-15TO2017-08-15_CC60	NDVI	p025
43	S2_2017-03-15TO2017-08-15_CC60	NDVI	p050

44	S2_2017-03-15TO2017-08-15_CC60	NDVI	p075
45	S2_2017-03-15TO2017-08-15_CC60	NDVI	p090
46	S2_2017-03-15TO2017-08-15_CC60	NDVI	pdiff075025
47	S2_2017-03-15TO2017-08-15_CC60	NDVI	pdiff090010
48	S2_2017-03-15TO2017-08-15_CC60	NDVI	std
49	S2_2017-03-15TO2017-08-15_CC60	NDWI	actn0t42
50	S2_2017-03-15TO2017-08-15_CC60	NDWI	difdif3mean
51	S2_2017-03-15TO2017-08-15_CC60	NDWI	difmax3mean
52	S2_2017-03-15TO2017-08-15_CC60	NDWI	difmin3mean
53	S2_2017-03-15TO2017-08-15_CC60	NDWI	max
54	S2_2017-03-15TO2017-08-15_CC60	NDWI	maxmean3
55	S2_2017-03-15TO2017-08-15_CC60	NDWI	mean
56	S2_2017-03-15TO2017-08-15_CC60	NDWI	min
57	S2_2017-03-15TO2017-08-15_CC60	NDWI	p010
58	S2_2017-03-15TO2017-08-15_CC60	NDWI	p025
59	S2_2017-03-15TO2017-08-15_CC60	NDWI	p050
60	S2_2017-03-15TO2017-08-15_CC60	NDWI	p075
61	S2_2017-03-15TO2017-08-15_CC60	NDWI	p090
62	S2_2017-03-15TO2017-08-15_CC60	NDWI	pdiff075025
63	S2_2017-03-15TO2017-08-15_CC60	NDWI	pdiff090010
64	S2_2017-03-15TO2017-08-15_CC60	NDWI	std

In the following, some examples of selected time features calculated from Sentinel-2A + B data are presented.

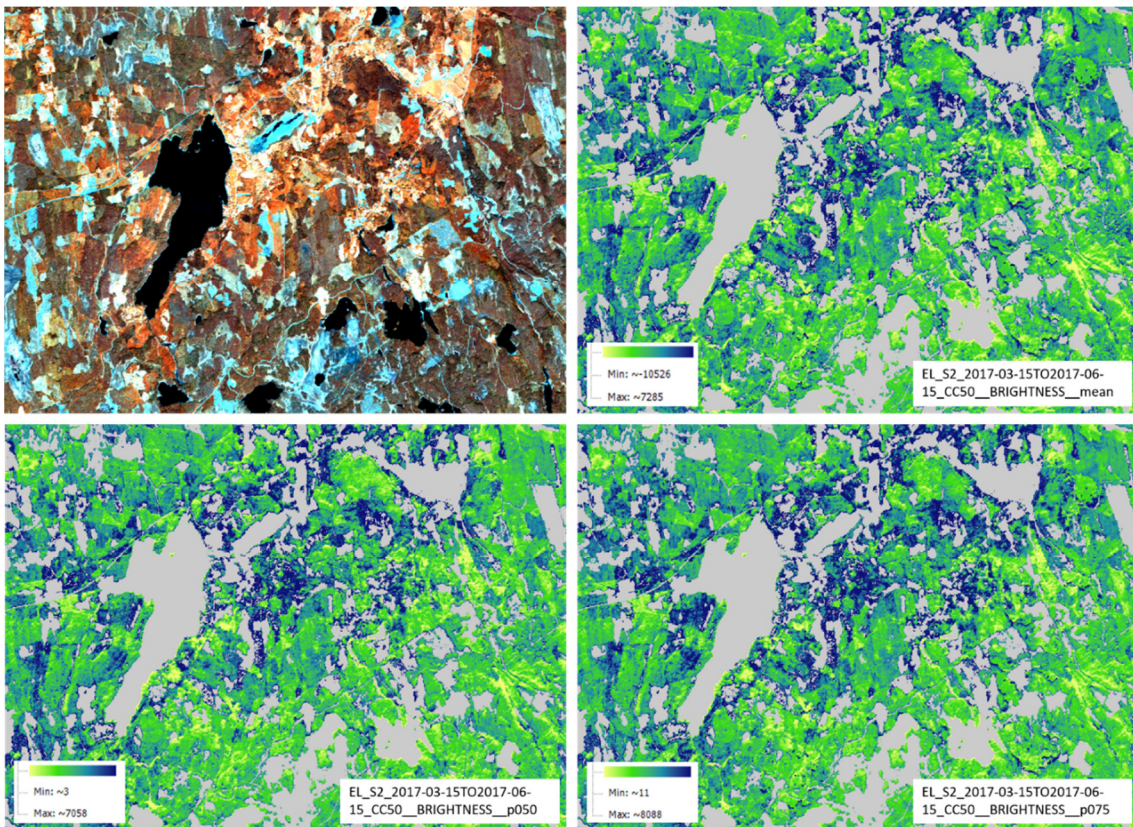


Figure 5-20: Selected time features based on the BRIGHTNESS index (mean: upper right, 50% percentile: lower left, 75% percentile: lower right). Non-tree areas are illustrated in grey. Sentinel-2 is visualized for comparison (upper left). (produced using modified Copernicus Sentinel data [2017])

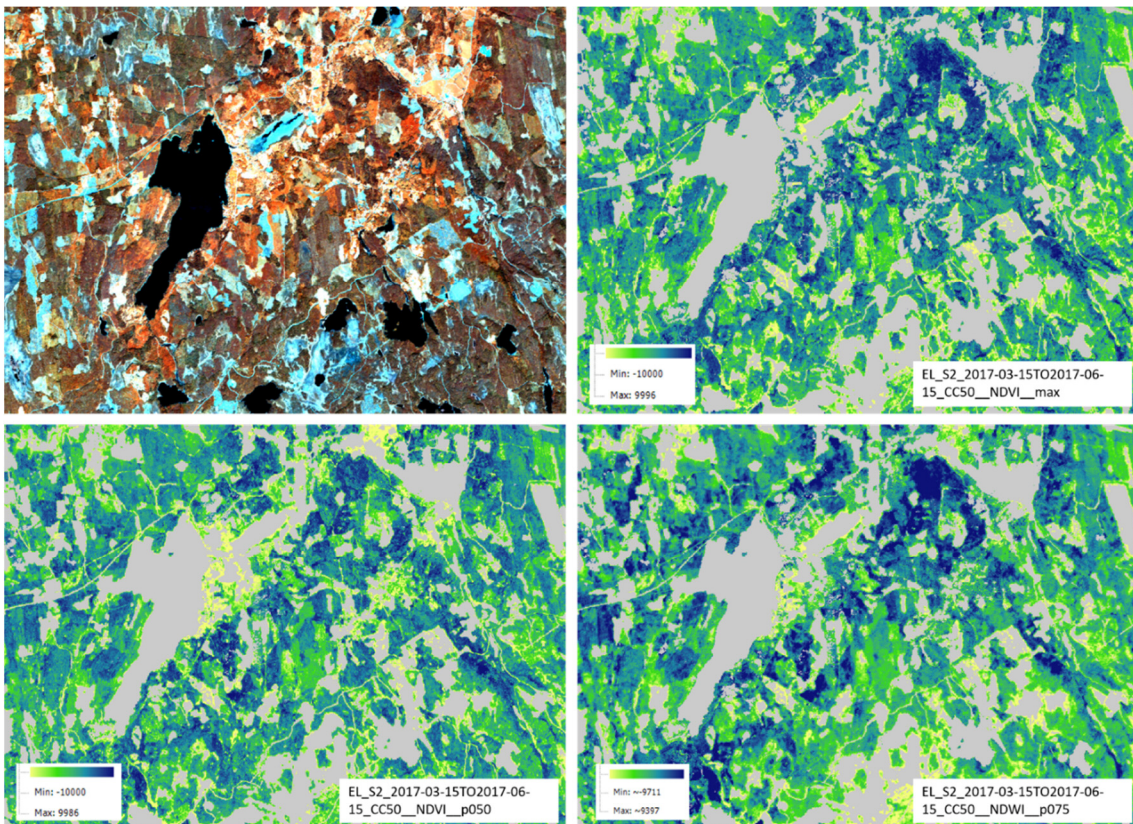


Figure 5-21: Selected time features based on NDVI (maximum: upper right; 50% percentile: lower left) and NDWI (75% percentile: lower right). Non-tree areas are illustrated in grey. Sentinel-2 is visualized for comparison (upper left). (produced using modified Copernicus Sentinel data [2017])

5.2.2 Classification Results and Validation

The classification of the TCM and DLT has been performed independently using a Random Forest classifier. The model generated has been equipped with the different sample datasets and subsequently applied on the six adjacent Sentinel-2 tiles. In total, 304 samples were included for the tree cover classification. The result is a tree cover raster with values of 0 (*no tree cover*) and 1 (*tree cover*). The internal evaluation report based of the model indicates high accuracy figures with an Overall Accuracy of 93% and a kappa coefficient of 0.86 (see Figure 5-22) for the TCM classification of all the Sentinel-2 tiles. The F1-Score is rated with 0.93.

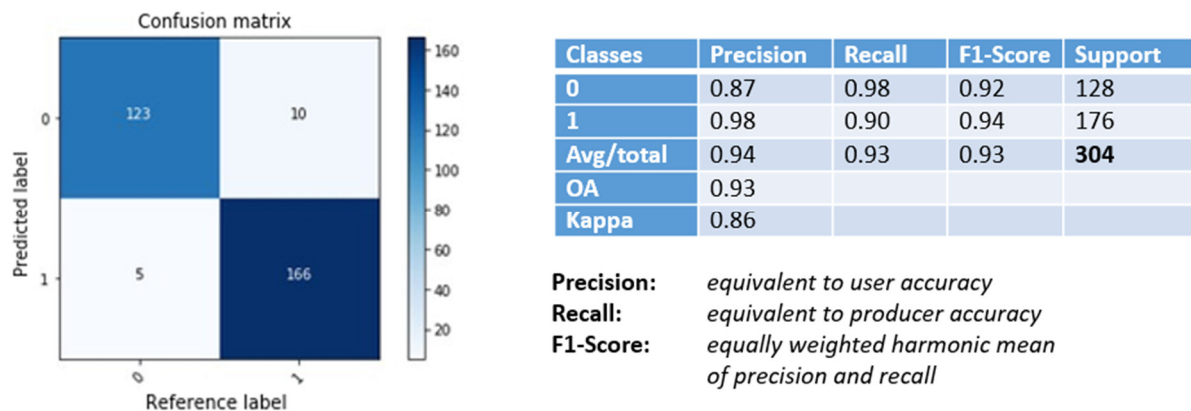


Figure 5-22: Internal evaluation model for the TCM 2017 classification

NB: the results of an independent accuracy assessment are shown further below in this section.

Generally, NDVI features have a very high influence on the TCM classification. The following six time features (out of >60) have shown the highest feature importance for the random forest classifier:

- S2_2017-03-15TO2017-08-15_CC60_NDVI_p75
- S2_2017-03-15TO2017-08-15_CC60_NDVI_p50
- S2_2017-03-15TO2017-08-15_CC60_NDVI_max
- S2_2017-03-15TO2017-08-15_CC60_NDVI_mean
- S2_2017-03-15TO2017-08-15_CC60_NDVI_90
- S2_2017-03-15TO2017-08-15_CC60_NDVI_maxmean3

The full sample of time features incorporated in the TCM classification is shown in Figure 5-23 below, ranked by their feature importance.

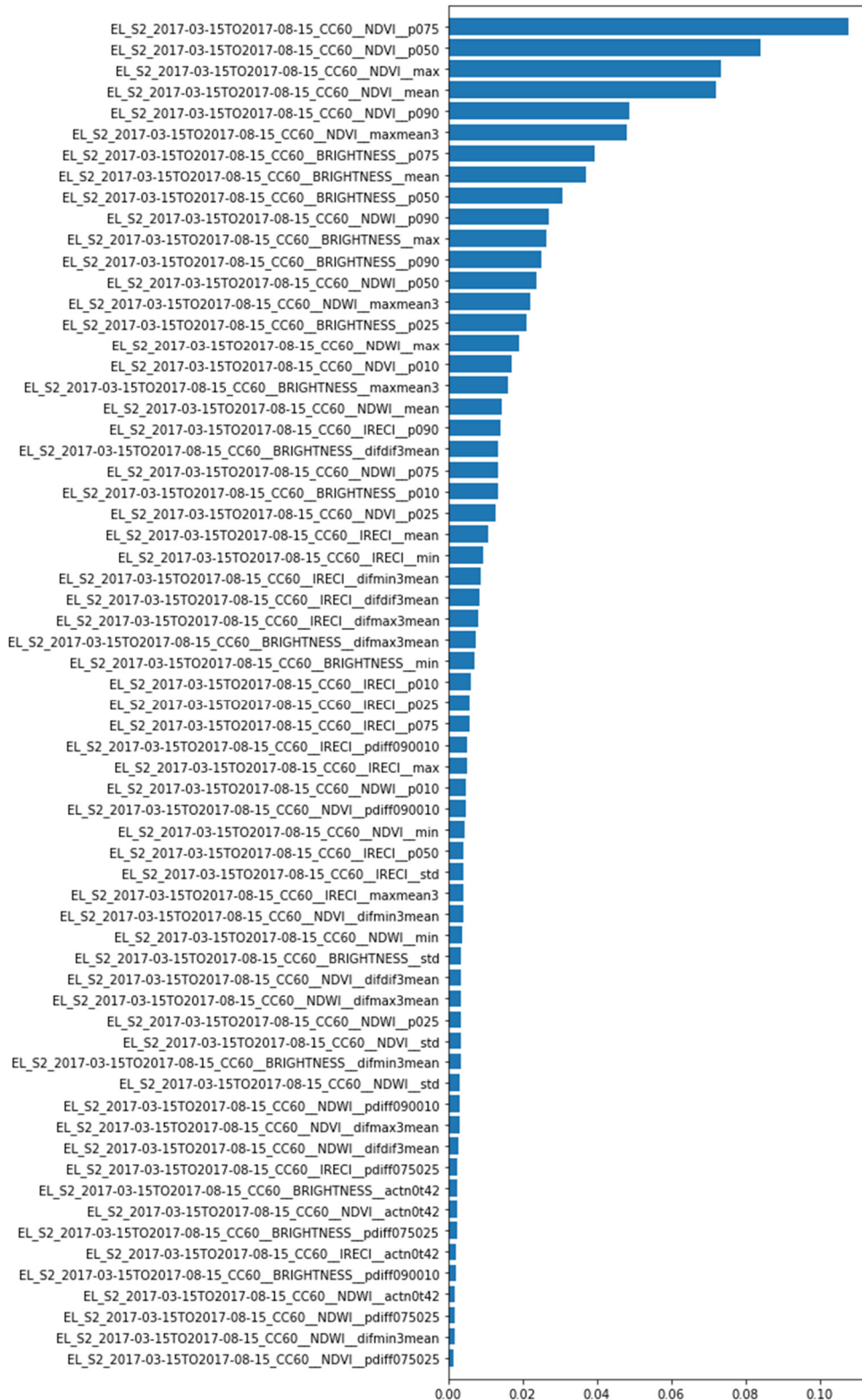


Figure 5-23: Feature importance of calculated time features for the TCM classification

The derived TCM 2017 has been slightly improved in urban areas through incorporation of the HRL Imperviousness 2015 by exclusion of pixels with an imperviousness degree from 99% to 100% from the mask. Additionally, the HRL Water and Wetness (WaW) 2015 has been utilized through the exclusion of class 1 (water) from the TCM, taking a 20m negative buffer into account. The final classification result of the TCM 2017 is illustrated in Figure 5-24.

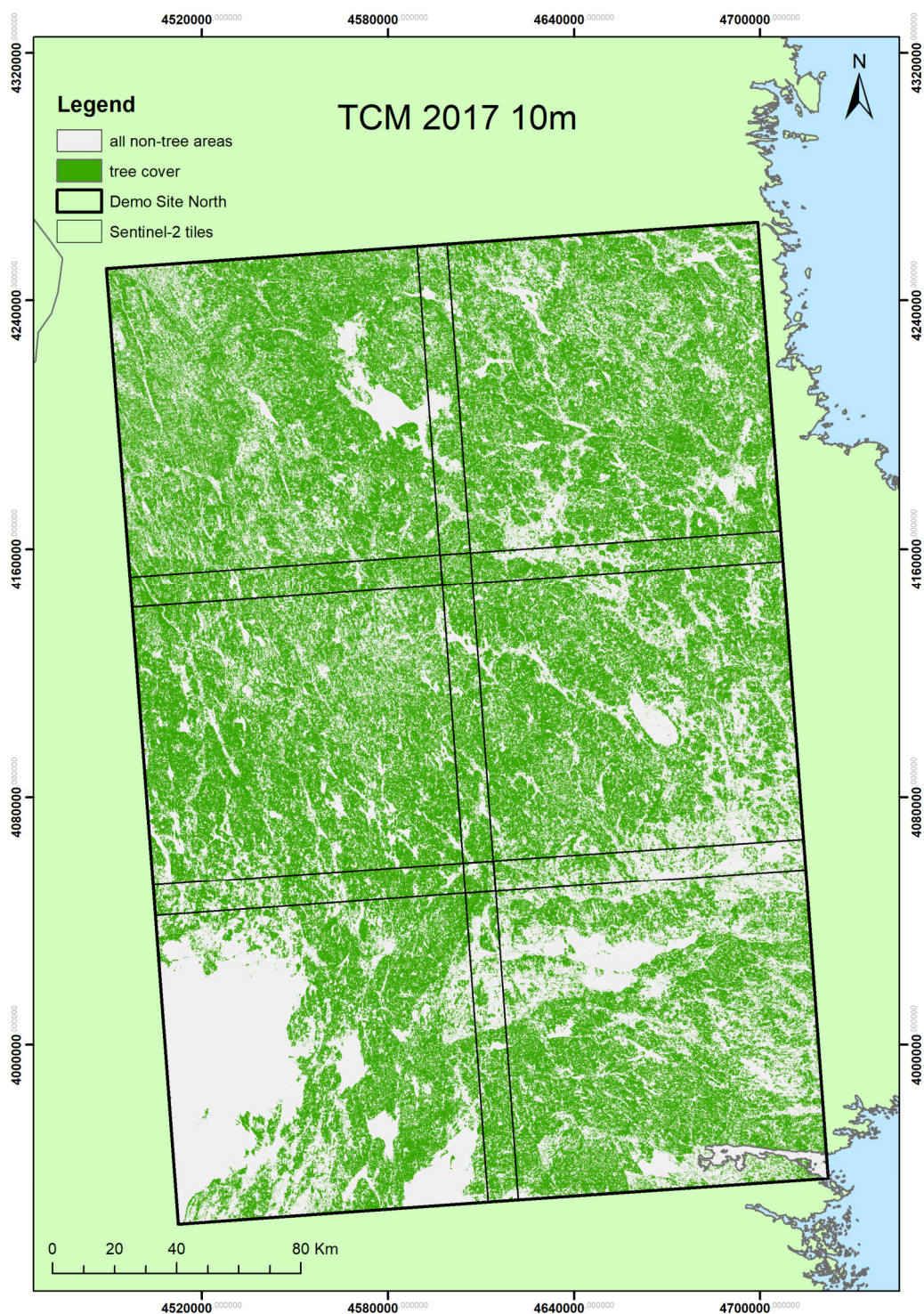


Figure 5-24: Classified Tree Cover Mask 2017 in 10m spatial resolution
(© EuroGeographics for the administrative boundaries)

Subsequently, and independently from the TCM, the classification of a dominant leaf type (DLT) layer has been performed using the derived sample dataset including 176 samples. The result is a seamless leaf type raster with values of 1 (*broadleaved trees*) and 2 (*coniferous trees*). The internal evaluation report of the model is presented in Figure 5-25. For the DLT classification it indicates an OA of 86% and a kappa coefficient of 0.69. The F1-Score is rated with 0.85. NB: the results of an independent accuracy assessment are shown further below in this section.

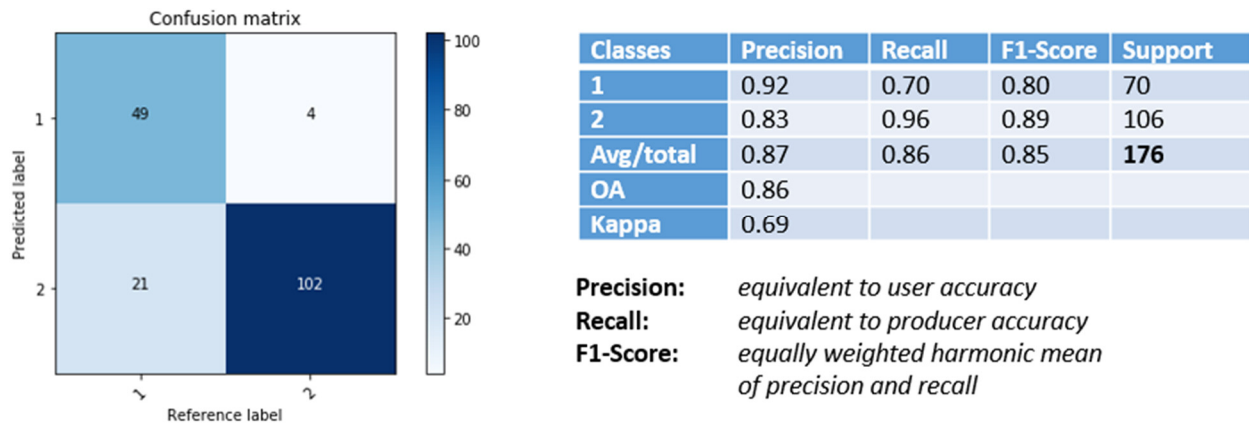


Figure 5-25: Internal evaluation model for the DLT 2017 classification

Generally, IRECI features have a high influence on the DLT classification, followed by BRIGHTNESS and NDWI features. The following nine time features (out of >60) have shown the highest feature importance for the random forest classifier to detect DLT:

- S2_2017-03-15TO2017-08-15_CC60_BRIGHTNESS_p75
- S2_2017-03-15TO2017-08-15_CC60_NDWI_p10
- S2_2017-03-15TO2017-08-15_CC60_IRECI_std
- S2_2017-03-15TO2017-08-15_CC60_IRECI_max
- S2_2017-03-15TO2017-08-15_CC60_IRECI_pdif09010
- S2_2017-03-15TO2017-08-15_CC60_IRECI_p90
- S2_2017-03-15TO2017-08-15_CC60_BRIGHTNESS_p90
- S2_2017-03-15TO2017-08-15_CC60_NDWI_p25
- S2_2017-03-15TO2017-08-15_CC60_IRECI_pdif075025

The full sample of time features incorporated in the DLT classification is shown in Figure 5-26 below.

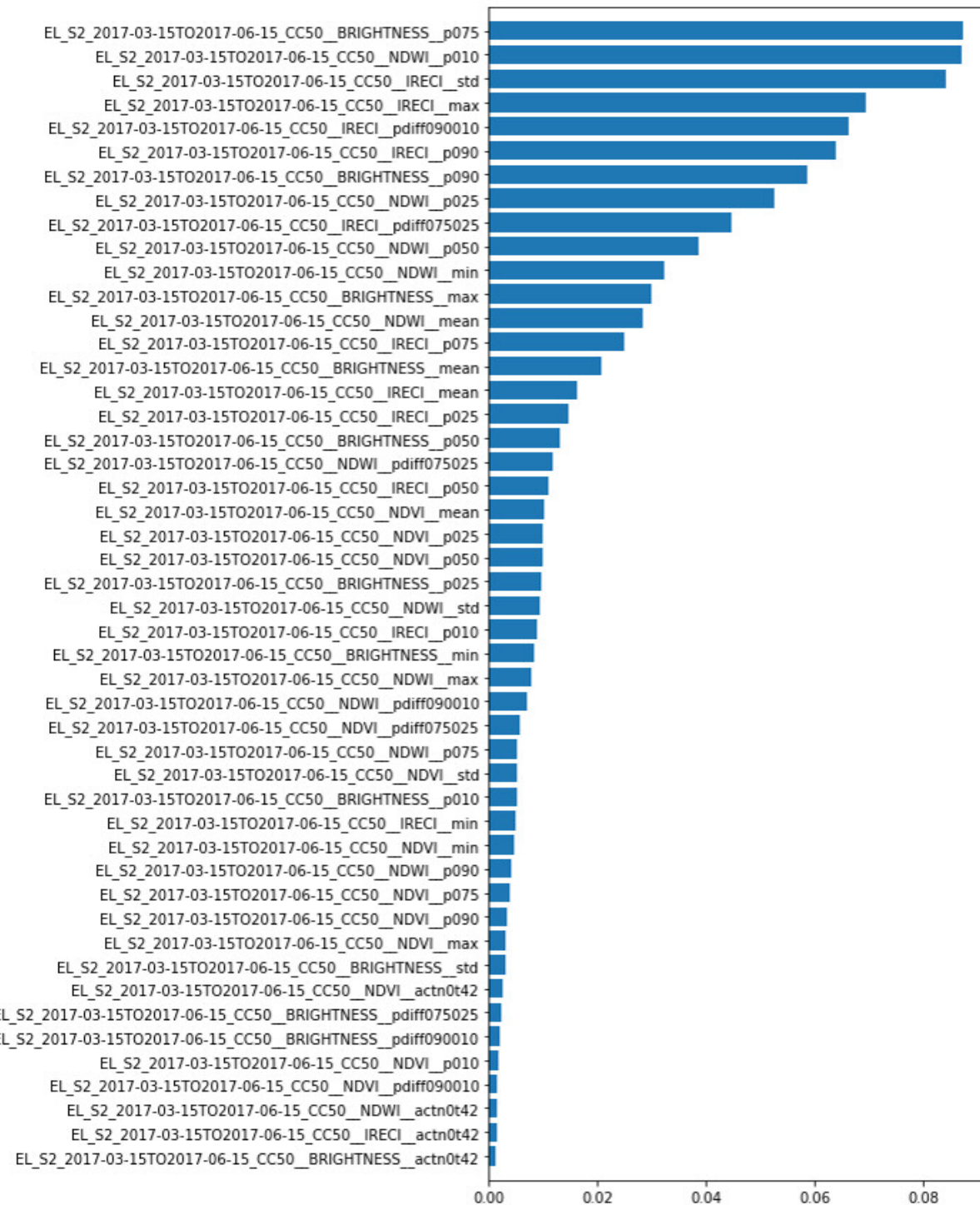


Figure 5-26: Feature importance of calculated time features for the DLT 2017 classification

Finally, TCM and DLT have been combined to create the final DLT 2017 product at 10m spatial resolution, following the prototype specifications provided in section 5.3.

Figure 5-27 presents the final DLT 2017 layer for the ECoLaSS demonstration site North.

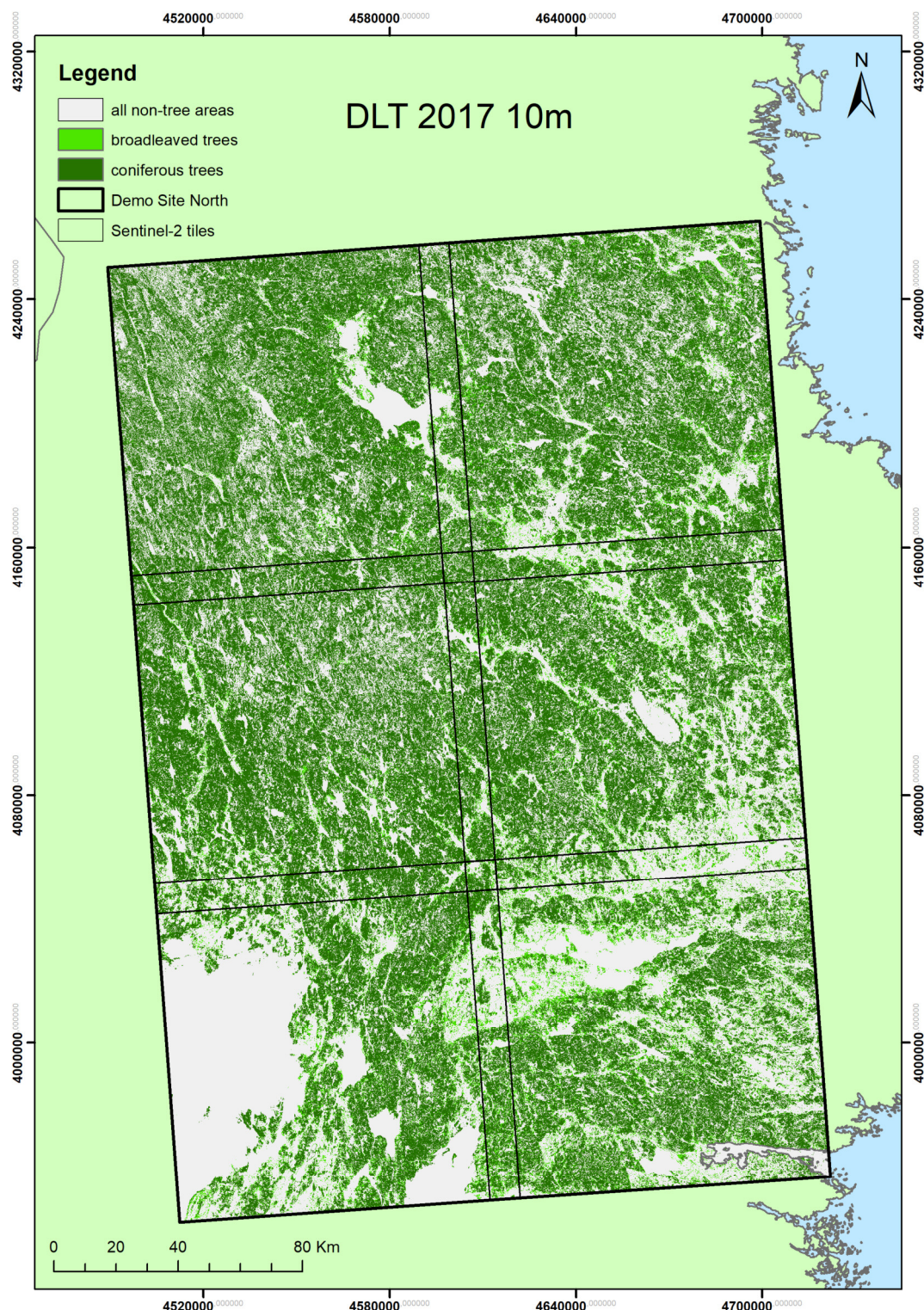


Figure 5-27: Improved Dominant Leaf Type 2017 in 10m spatial resolution
(© EuroGeographics for the administrative boundaries)

Statistics at tile-basis are presented in Figure 5-28. The areal coverage percentages of the three classes are reported individually for the six Sentinel-2 tiles and for the whole demonstration site. The class “coniferous trees” is always dominant as compared to “broadleaved trees”. In particular, “broadleaved trees” represent less than 10% of the overall area extent, with the exception of a higher proportion of broadleaved forest as well as non-forest in tile 33VWF. The highest overall forest cover proportion is reported for the tiles 33VVG (62.7%), 33V VH (60.4%) and 33VWH (58.3%).

This distribution of the two leaf types, though retrieved on the basis of the somewhat coarse Sentinel-2 tiling grid, seems to show an increasing relative proportion of broadleaved trees following a North-South axis as well as a coast-inland (East to West) direction.

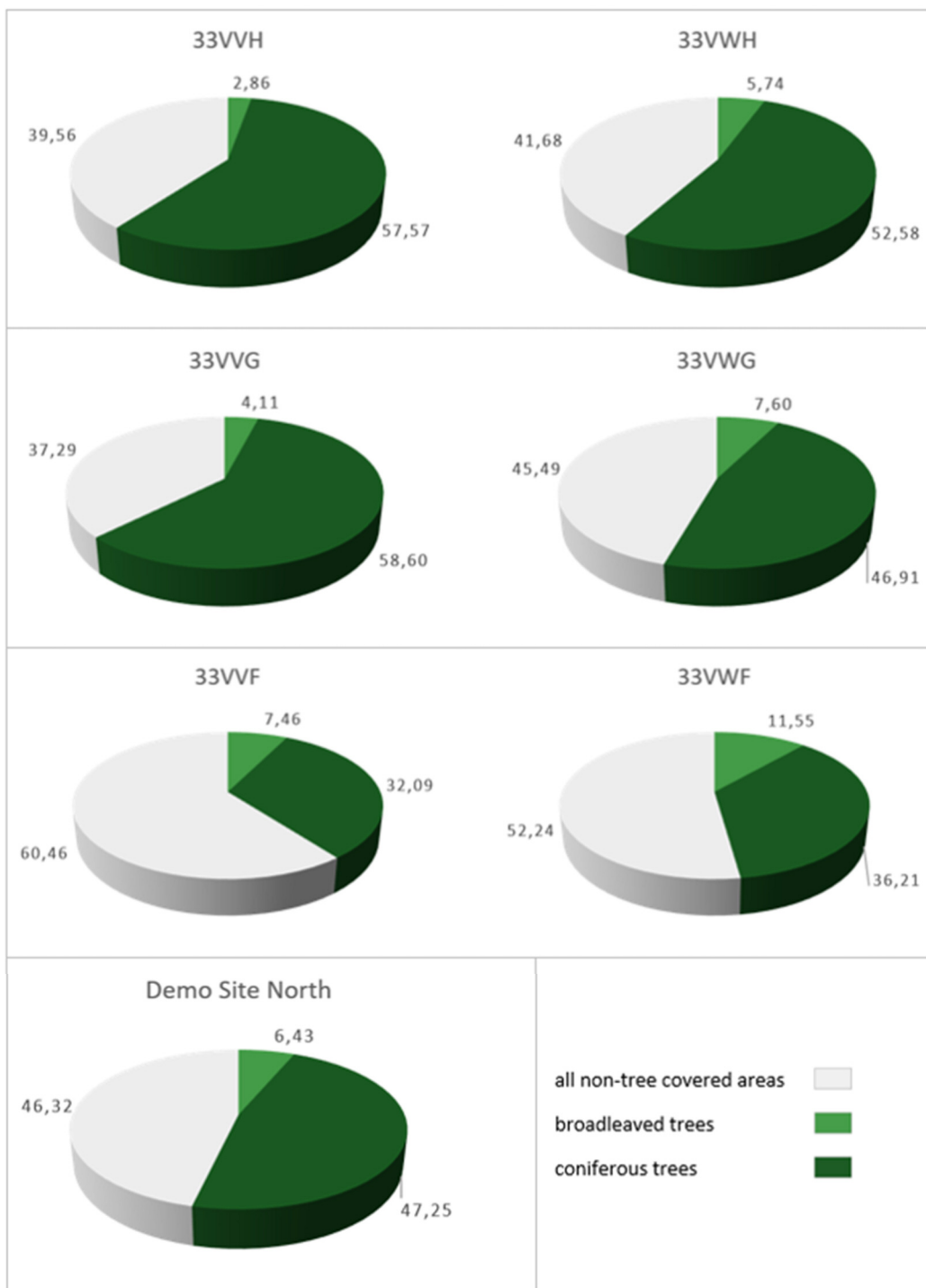


Figure 5-28: Statistics of the Dominant Leaf Type 2017 per Sentinel-2 tile and the whole demonstration site.

Figure 5-29 provides some more details on the improved DLT 2017 layer, comparing it with even higher-resolution VHR_Image_2015 data. Among a generally good leaf type discrimination, much more details as compared to the DLT 2015 product in 20m spatial resolution have been captured, which is connected to the increased spatial resolution of 10m, and presumably also due to the denser time series input data.

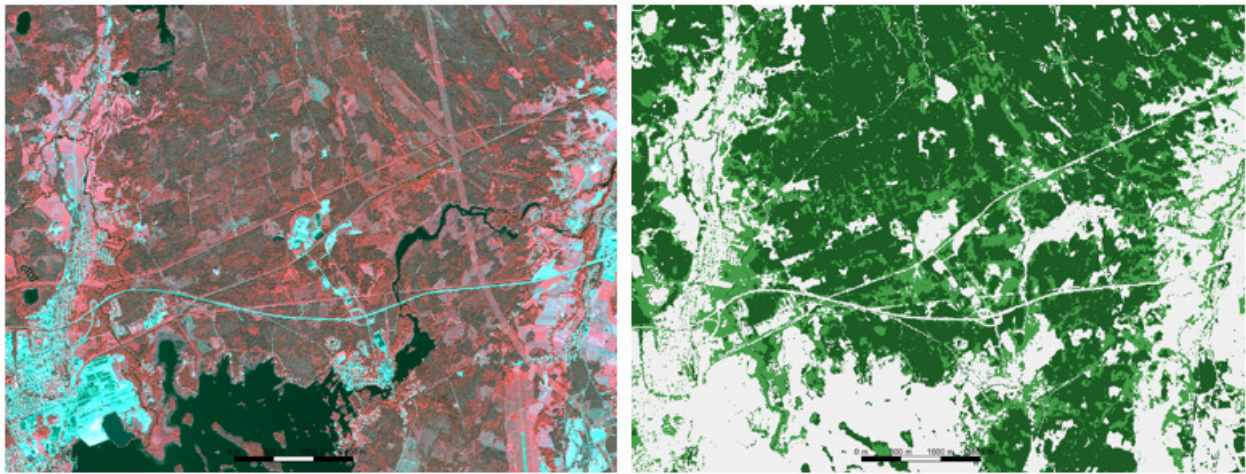


Figure 5-29: Comparison of VHR_IMAGE_2015 (left) and the improved DLT 2017 in 10m spatial resolution (right)
(© Digital Globe, Inc. 2015, all rights reserved. Produced using modified Copernicus Sentinel data [2017])

Differences in the leaf type representation and tree cover extent as well as the level of detail between the DLT 2015 in 20m spatial resolution and the improved DLT 2017 in 10m resolution are shown in Figure 5-30 and Figure 5-31.

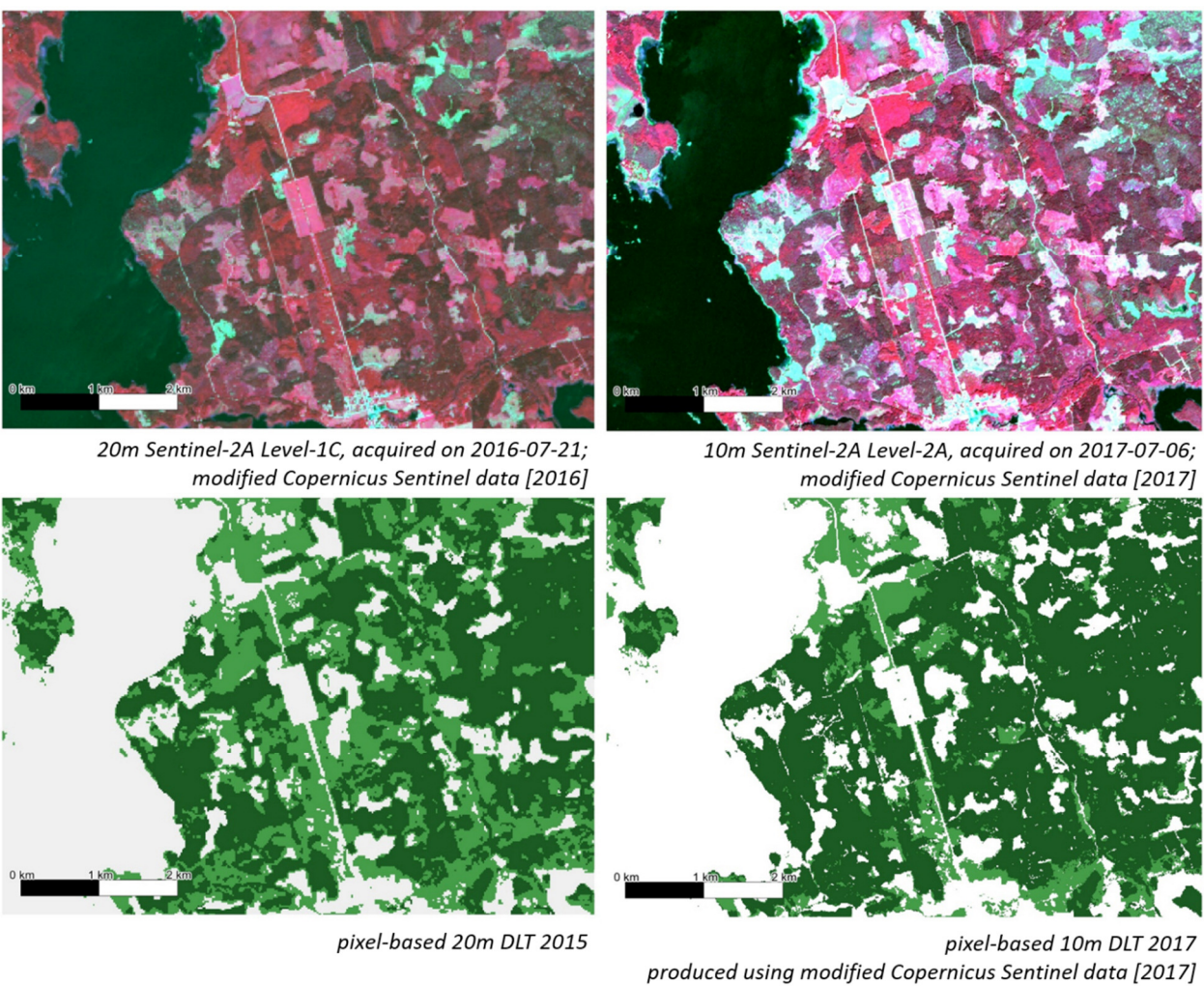


Figure 5-30: Comparison of the 20m DLT 2015 (left) and the improved DLT 2017 in 10m spatial resolution (right).
Corresponding Sentinel-2 scenes are presented in false-colour infrared (band combination: NIR-RED-GREEN).
(© European Union, Copernicus Land Monitoring Service 2015, European Environment Agency (EEA))

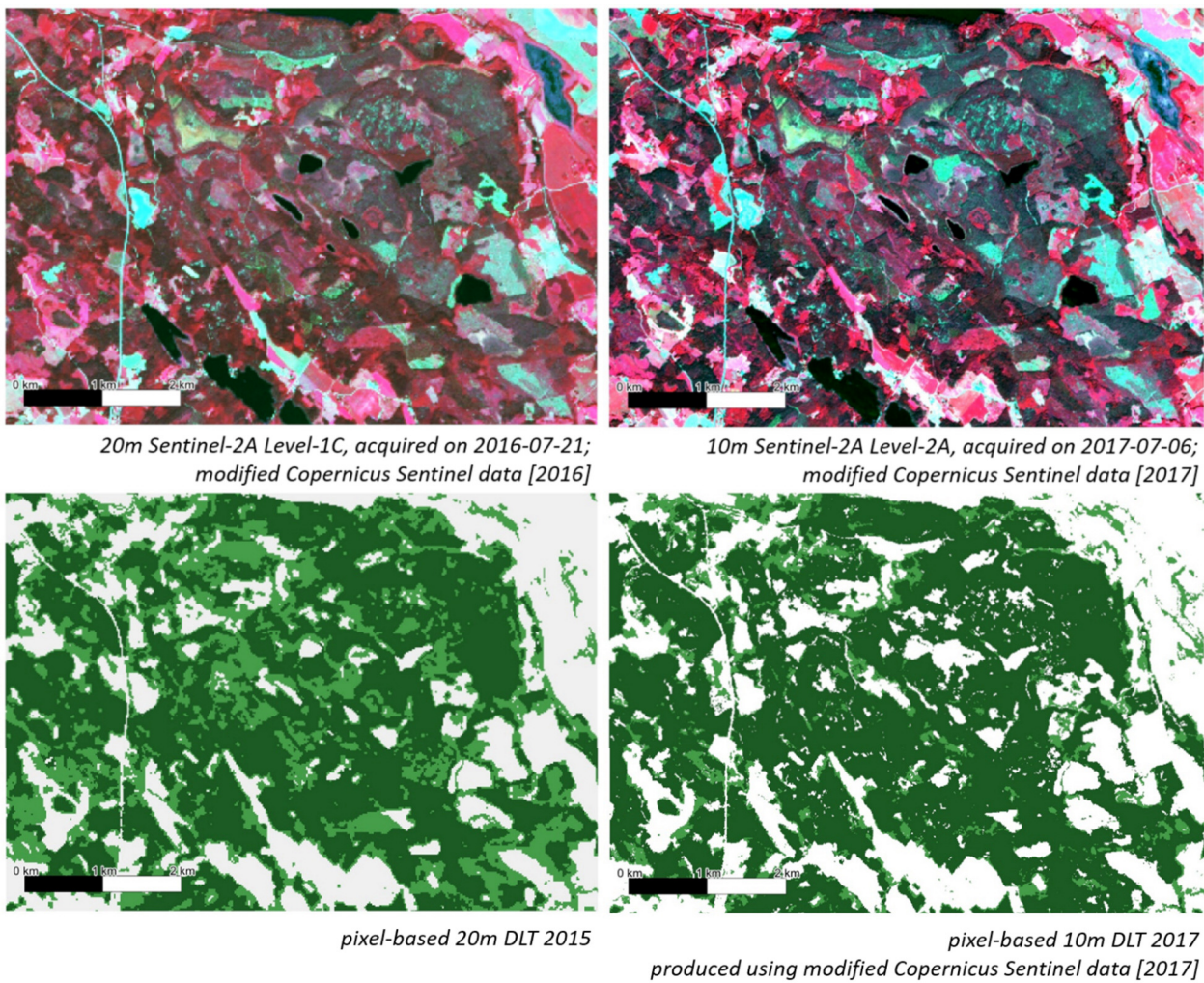


Figure 5-31: Comparison of the 20m DLT 2015 (left) and the improved DLT 2017 in 10m spatial resolution (right). Corresponding Sentinel-2 scenes are presented in false-colour infrared (band combination: NIR-RED-GREEN).
 (© European Union, Copernicus Land Monitoring Service 2015, European Environment Agency (EEA))

Compared to the 20m DLT 2015, the improved status layer DLT 2017 shows significantly less broadleaved cover. This is due to a better recognition rate of the leaf type using time features, specifically at the edge of forest patches and within young tree/forest stands. The internal validation of the 20m DLT 2015 has already confirmed a strong overestimation of broadleaved trees in some parts of the northern countries (incl. Sweden). Comparison statistics are presented in Figure 5-32.

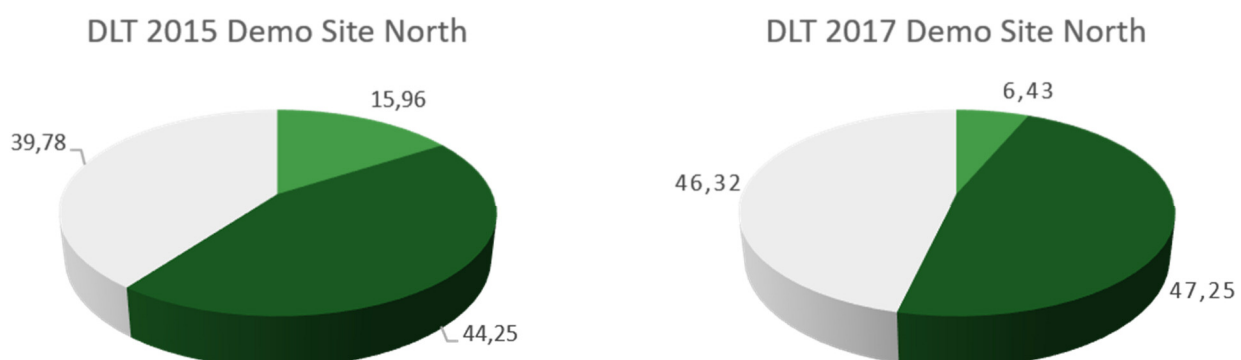


Figure 5-32: Spatial extents of the 20m DLT 2015 (left) and 10m DLT 2017 (right) for the demonstration site North

The final DLT 2017 layer has been subsequently validated using the best available (VHR) reference and (HR) guiding data. Guiding data are those that have been used in the production process and therefore act as time stamp reference in case of land cover changes, as compared to the VHR reference data. In case of the DLT, they consist of:

- Sentinel-2A+B scenes in 10m spatial resolution acquired between March and August 2017.

Reference data are any available suitable VHR data sources, namely:

- DWH: VHR_IMAGE_2015
- DWH: D2_MG2b_ECOL_011a (Archive_standard_Optical_VHR1)
- Bing Maps
- Google Earth Pro

Multispectral VHR_IMAGE_2015 data for the Large Regions 34, 35, 62 (which are partially covering the prototype site) have been mainly used for validation purposes. The overall coverage of this dataset has been significantly improved in 2018 and provides now an almost full coverage of the demonstration site (see Figure 5-33). The VHR_IMAGE_2015 completion campaign has been officially ended on 01 June 2018.

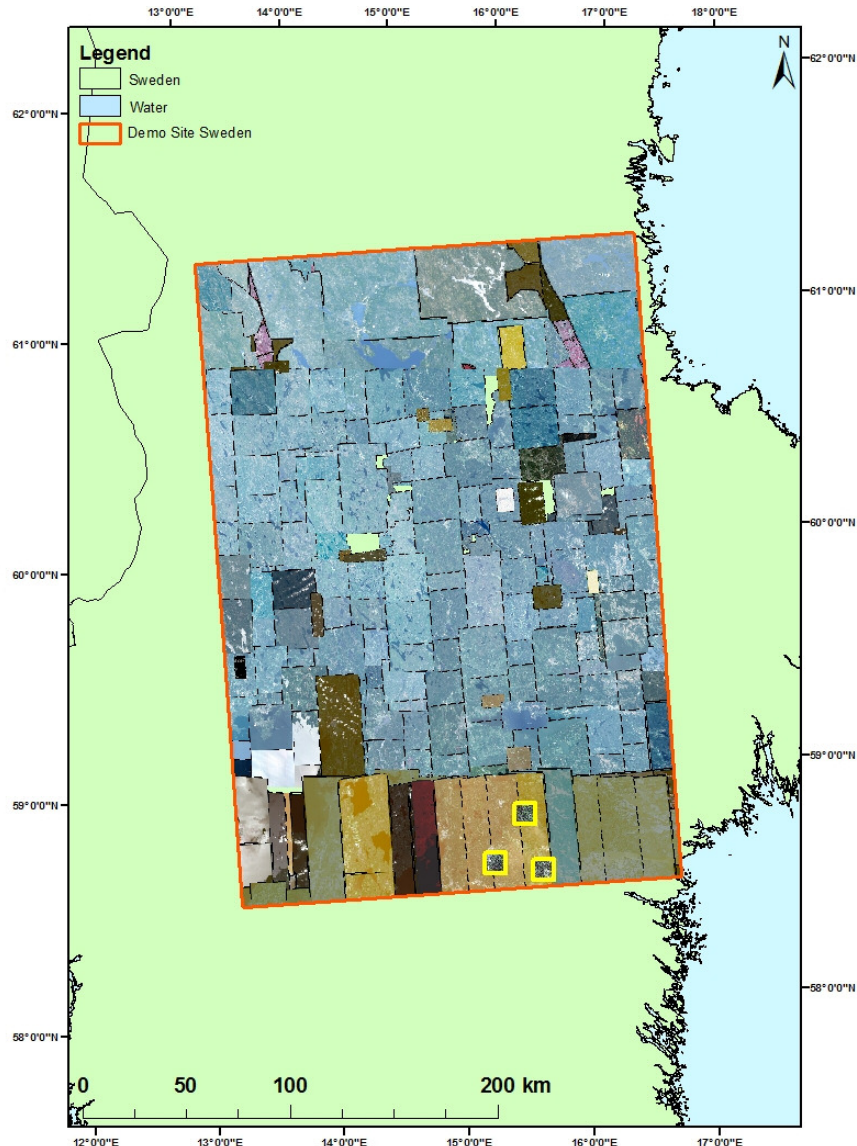


Figure 5-33: VHR_IMAGE_2015 coverage for the demonstration site North; complemented by VHR1 data from the D2_MG2b_ECOL_011a dataset (highlighted in yellow)
 (© EuroGeographics for the administrative boundaries)

Additional to the VHR_IMAGE_2015 data, VHR scenes from the ESA DWH dataset D2_MG2b_ECOL_011a have been used for validation, specifically of detected changes within the test site North. The dataset has been specifically granted to the ECoLaSS project and is providing ca. 700 km² of pan-sharpened multispectral VHR data within the test site North (as part of the demonstration site) for validation and calibration purposes (VHR1 scenes highlighted in yellow in Figure 5-33).

The accuracy assessment has been performed using a stratified random point sampling approach with 2,306 points in total. Points have been visually interpreted using the above mentioned guiding and reference data.

Thematic accuracy is presented in the form of an error matrix. Unequal sampling intensity resulting from the stratified systematic sampling approach was accounted for by applying a weight factor (p) to each sample unit based on the ratio between the number of samples and the size of the stratum considered:

$$\hat{p}_{ij} = \left(\frac{1}{N}\right) \sum_{x \in (i,j)} \frac{1}{\pi_{uh}^*}$$

Where i and j are the columns and rows in the matrix, N is the total number of possible units (population) and π is the sampling intensity for a given stratum. Overall accuracy and user's and producer's accuracies were computed for all thematic classes and 95% confidence intervals were calculated for each accuracy.

The standard error of the error rate was calculated as follows: $\sigma_h = \sqrt{\frac{p_h(1-p_h)}{n_h}}$ where n_h is the sample size for stratum h and p_h is the expected error rate. The standard error was calculated for each stratum and an overall standard error was calculated based on the following formula:

$$\sigma = \sqrt{\sum w_h^2 \cdot \sigma_h^2}$$

In which w_h is the proportion of the total area covered by each stratum. The 95% confidence interval is +/- 1.96 σ .

Results of the accuracy assessment are presented in Table 5-9.

Table 5-9: Accuracy assessment results for the improved Primary Status Layer DLT 2017

		Reference Data				
		CLASS	0	1	2	Total
DLT 2017	0	1,015	15	32	1,062	95.57
	1	13	129	2	144	89.58
	2	7	6	1,087	1,100	98.82
	Total	1,035	150	1,121	2,306	
	Prod.	98.07	86.00	96.97		<i>Overall Accuracy: 96.75%</i>
	95% CI	0.89	5.89	1.05		

The overall look & feel of the fully automatically derived product is rated as good and the product provides much more detail as its 20m pendant from the HRL Forest 2015. The achieved thematic accuracy of the product exceeds the expected minimum Overall Accuracy of 90%. Producer's and User's accuracies for the two leaf type classes are in a range of 86-98% and exceed the minimum requirements of 90% by taking the confidence interval into account. The distribution of the validation samples is presented in Figure 5-34.

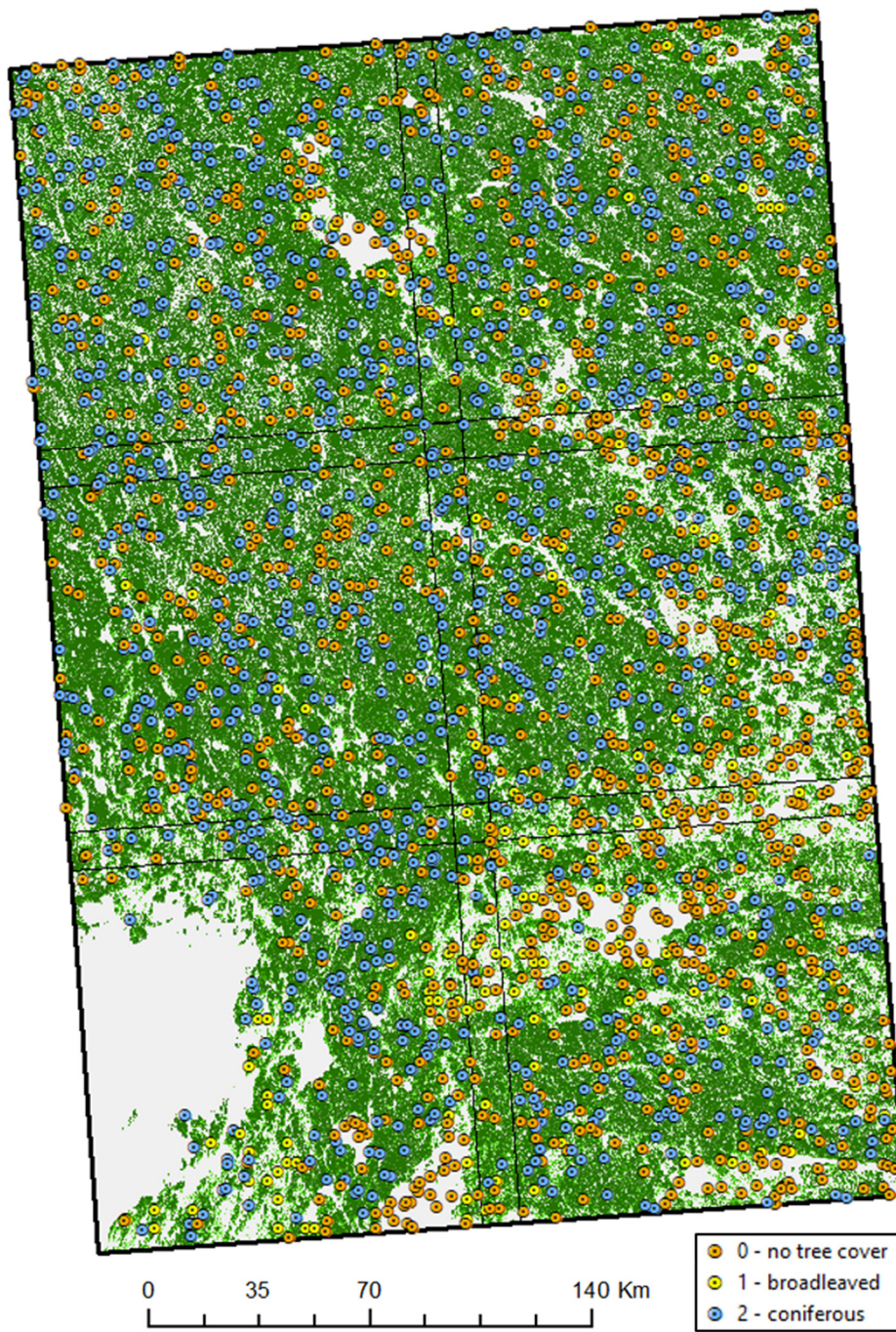


Figure 5-34: Distribution of validation samples for the DLT 2017

Typical sources of omissions are tree stands of sparse density and areas heavily influenced by clouds. Commission errors are mainly related to agricultural areas, clear cuts with a dark vegetation underground and areas influenced by a higher degree of soil moisture.

The accuracy might be further increased, when relevant sources for omission and commission errors are fully analysed and understood. Plausibility analyses and manual enhancements have proven as effective tools to increase the accuracy, but are generally accompanied with higher production costs and tend to increase the production time.

5.2.3 Change Detection and Incremental Update Results and Validation

To achieve a harmonization and continuity between the historic HRL Forest Tree Cover Mask 2015 (derived from DLT 2015) and the newly created TCM 2017, a map-to-map change detection approach has been applied using the TCM 2015 (from HRL Forest 2015 production) as basis for comparison. This method has been described in WP 34 (see [AD08]) and was finally applied in WP 42 to create an Incremental Update on an annual basis.

The Incremental Update layer is capturing Tree Cover Change (TCC) in terms of forest loss on an annual basis, whereas forest increase has to be mapped on the mid- to long-term (e.g. every 3-6 years). As the time difference between the TCM 2015, which has been mainly produced on 2016 EO data, and the DLT 2017 is only around 12 months, any indication of detected forest increase would have to be handled with special care. As already stated in [AD07], for capturing meaningful increases in tree cover (density), longer observation periods of actually ≥ 5 years should be considered. However, this is actually not feasible within the runtime of the ECoLaSS project.

From a technical point of view, any so “measured” short-term tree cover increase would represent predominantly “technical changes” (i.e. either tree cover omissions in 2015; or commissions in 2017) rather than real forest regrowth. For the abovementioned reasons, it is not taken into account for the present prototype, but could be potentially used to improve historic products in a focused enhancement step (e.g. by visual/manual enhancement steps of omission and commission errors in the reference years of the two time steps).

In the demonstration site North, the TCM 2015 has been combined with the newly created TCM 2017 to derive any changes between the reference periods. As explained above, this step does not only reveal 2015-2017 tree cover changes, but it also detects potential commission and omission errors in the TCM 2015 as well as potential commission and omission errors of the new TCM 2017.

To underpin the importance of the incremental update towards forest cover loss, trees in urban context and under agricultural use have been excluded from the change observation in the current demonstration site, taking the Forest Additional Support Layer (FADSL) 2015 into account.

The raw (yet unfiltered) “loss” is in the range of 8%, which is unrealistically high and cannot be explained by intensive forest management activities. Lots of small “changes” are introduced by geometrical imprecisions between the EO data used to generate the two masks. In this context, it should be also noted that the change of EO data spatial resolution between the HRL Forest 2015 (20m) and the prototypes in ECoLaSS (10m) is by a factor of 4, resulting in a substantial number of “technical changes”, especially at the fringe of forest patches and transport networks (see Figure 5-35).

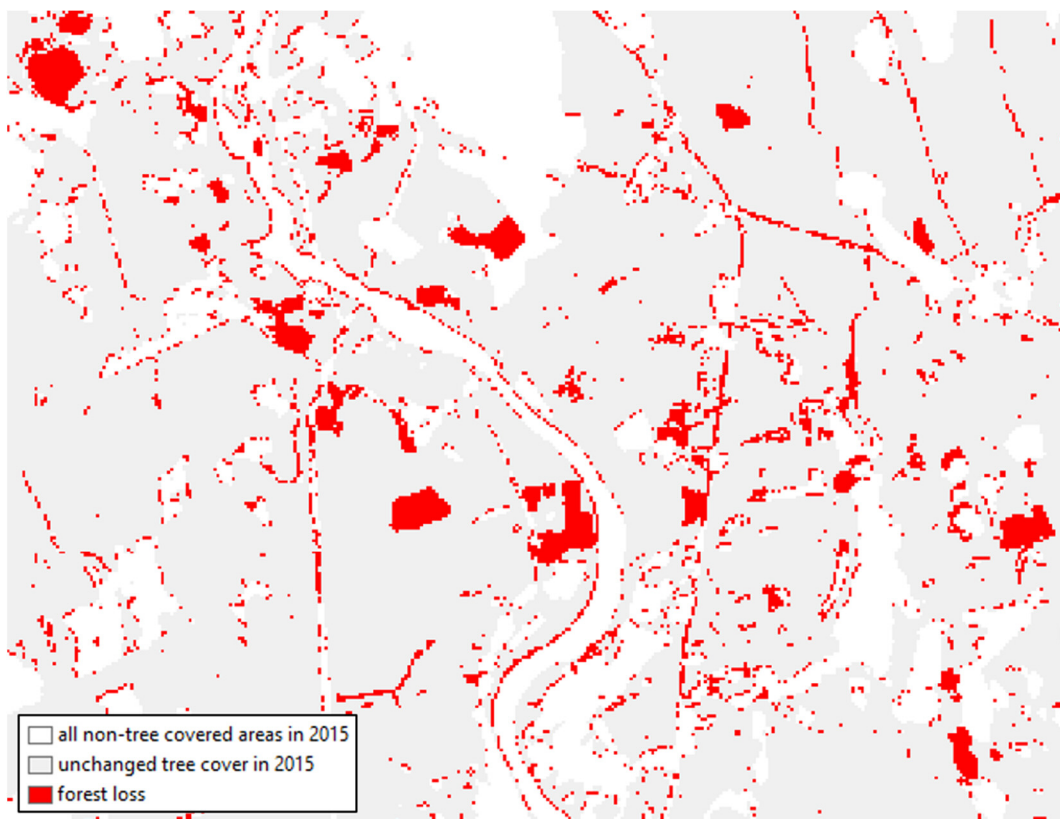


Figure 5-35: Pixel-based raw (yet unfiltered) changes in tree cover caused by both, geometric imprecisions, edge effects and forest management activities.

Further technical changes are introduced by an overestimation of tree cover in the TCM 2015 product, especially at the edges of forest patches and transition to water bodies, and by data issues within specific Sentinel-2 tiles that were used for the TCM 2017 production, which is separately discussed below.

To achieve more reliable results towards a sustainable update layer, different Minimum Mapping Units ranging from 0.5ha to 5ha have been tested. In the frame of a qualitative assessment, MMUs of 0.5ha, 1ha, 2ha, 3ha and 5 ha have been investigated towards their change significance. For this purpose, 24 Areas of Interest (AOI) (four frames per tile) have been specified across the demonstration site and visually checked using Sentinel-2 data from 2015/2016 and the most recent 2017 acquisitions used in the 2017 classification (see Figure 5-36).

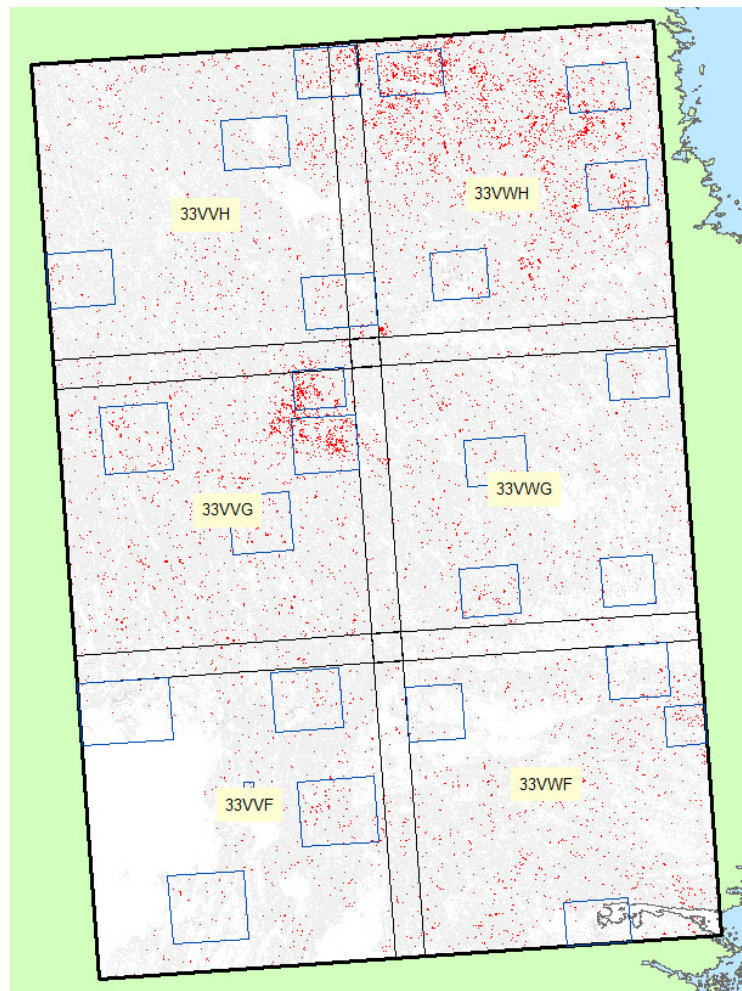


Figure 5-36: Distribution of the 24 AOIs for qualitative assessment of suitable MMUs for forest loss
© EuroGeographics for the administrative boundaries

Figure 5-37 provides an example of different MMUs within one of the selected AOIs of tile 33VWF.

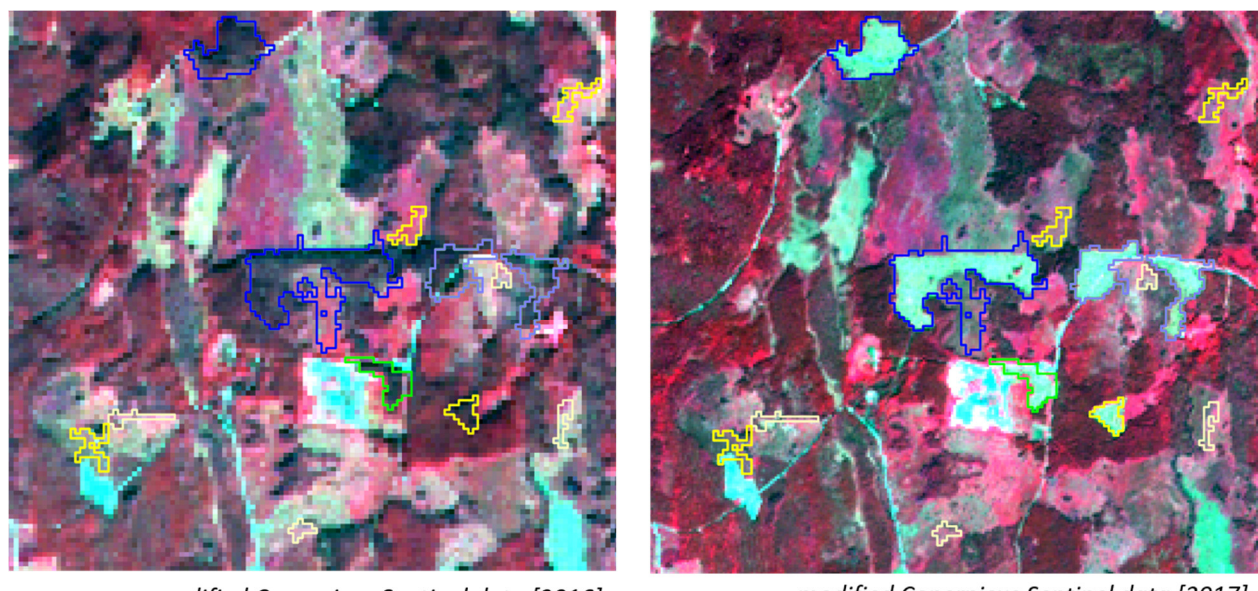


Figure 5-37: Different MMUs ranging from 0.5 ha (beige), 1 ha (yellow), 2 ha (green) and 3 ha (light blue) to 5 ha (dark blue)

A MMU of 3ha finally turned out to be best-suited for reliably capturing only the real forest loss. This MMU has been rated the best trade-off between detected real changes and technical changes which have been introduced by:

- a) fundamental differences in the methodological approach and overall data situation between HRL production 2015 and ECoLaSS,
- b) geometric differences between the TCM 2015 (derived from 20m satellite imagery) and the TCM 2017 (derived from 10m Sentinel-2 Level-2A time series),
- c) commission errors in the TCM 2015 as well as omission errors in the TCM 2017.

Figure 5-38 shows the same extent as Figure 5-35 above, but with the selected 3 ha MMU filter applied. It appears likely that a significant reduction of this MMU size will become possible, as soon as further improvements to the processing chain will have been implemented in the second project phase.

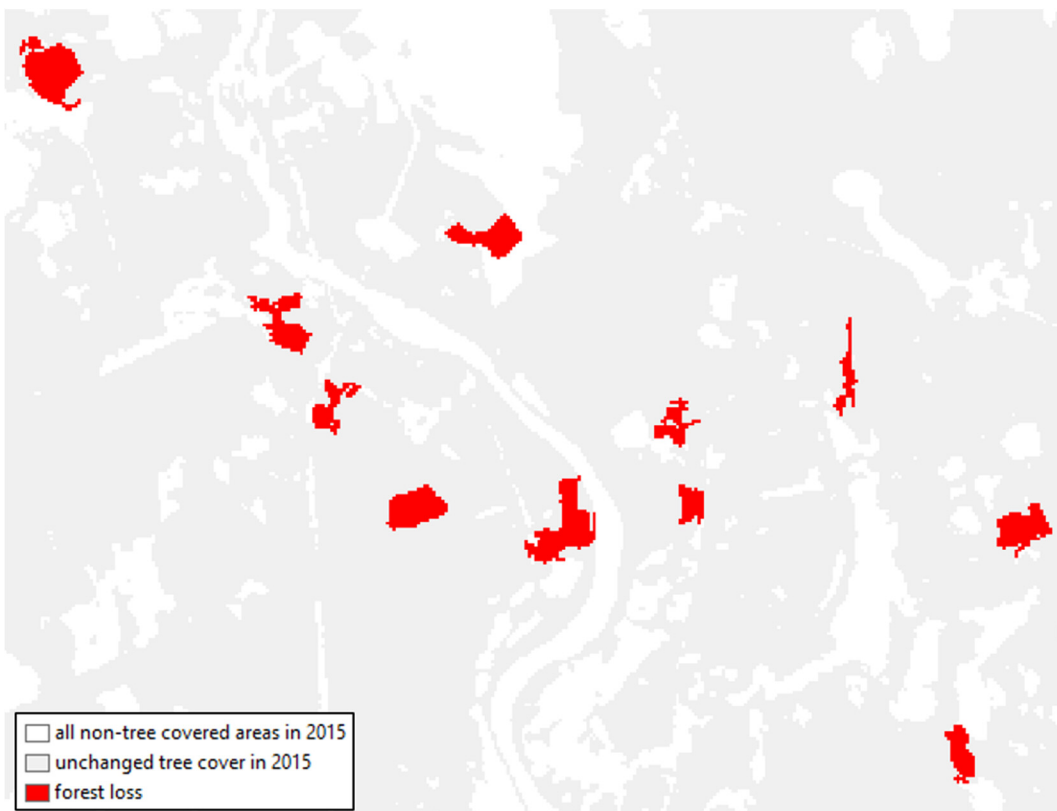


Figure 5-38: Pixel-based and MMU filtered Tree Cover Change product

Examples of so-detected forest loss between the reference years 2015 and 2017 are shown in Figure 5-39 below.

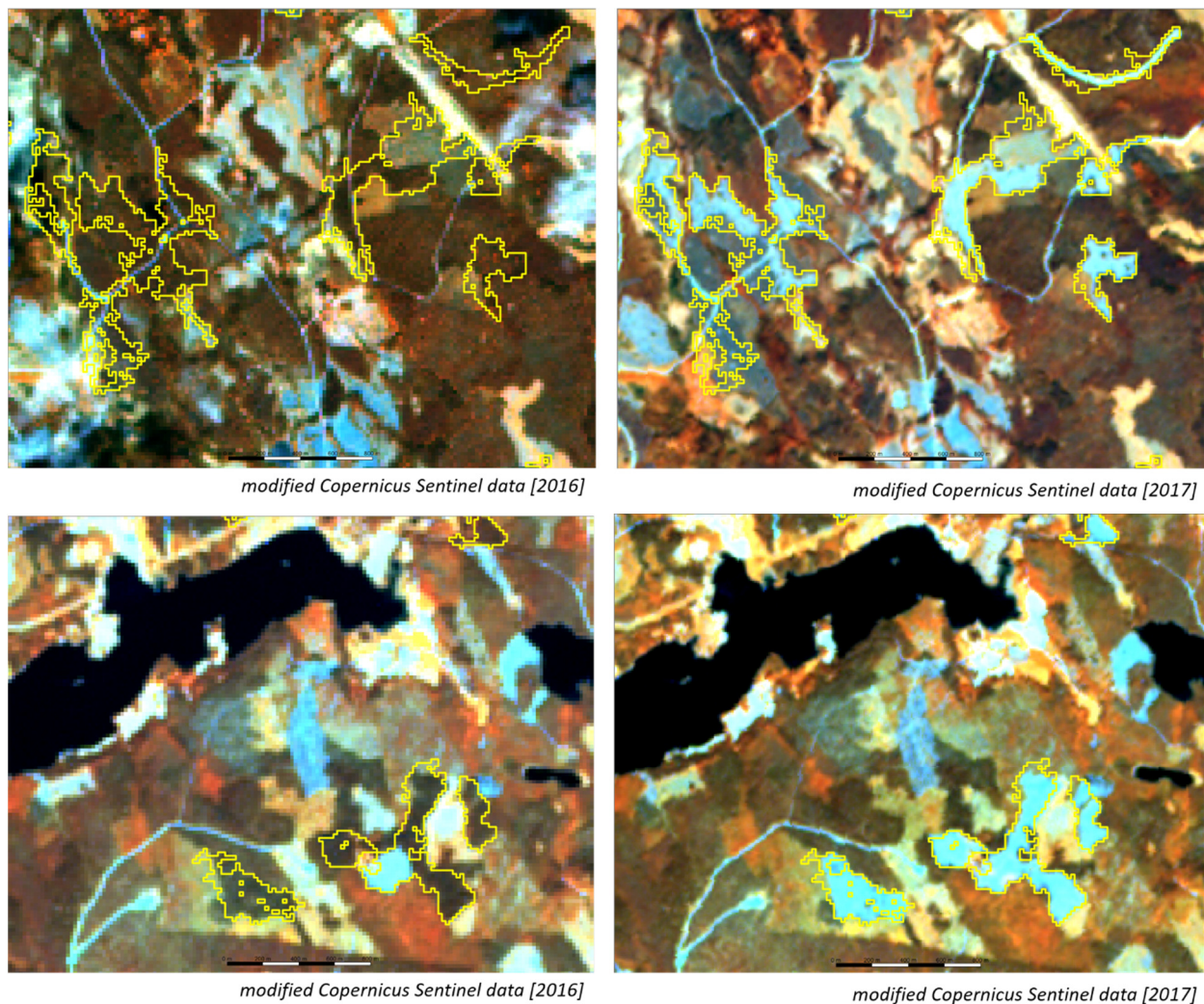


Figure 5-39: Examples of forest loss provided by the prototypic Incremental Update layer. Left: 20m Sentinel-2A scene from June 2016; right: Sentinel-2B scene from July 2017.

Figure 5-40 presents the final Incremental Update layer for the ECoLaSS demonstration site North.

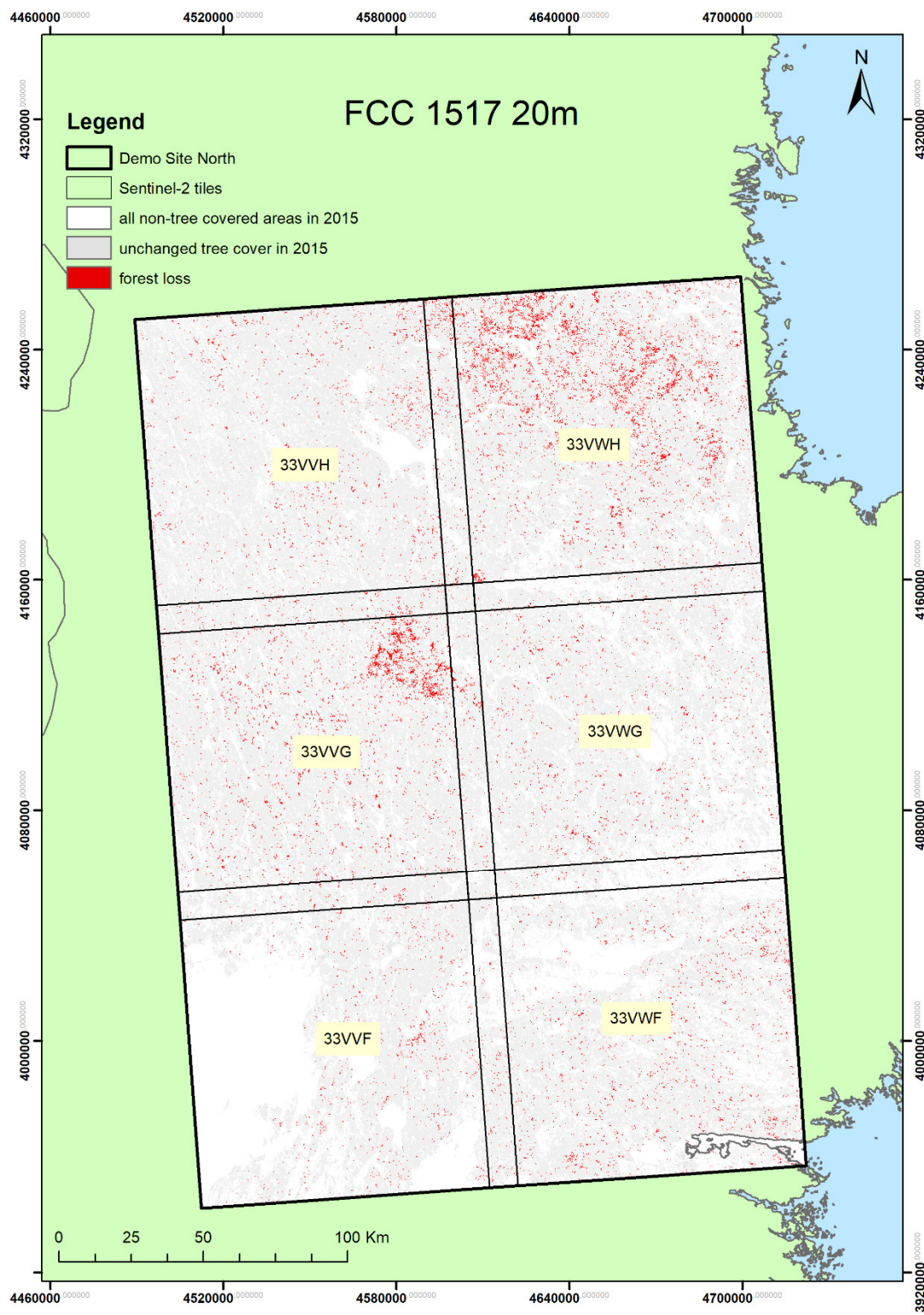


Figure 5-40: Incremental Update Layer Tree Cover Change 2015-2017 in 20m spatial resolution
 (© EuroGeographics for the administrative boundaries)

Final statistics of the Incremental Update layer for the demonstration site North are presented in Figure 5-41.

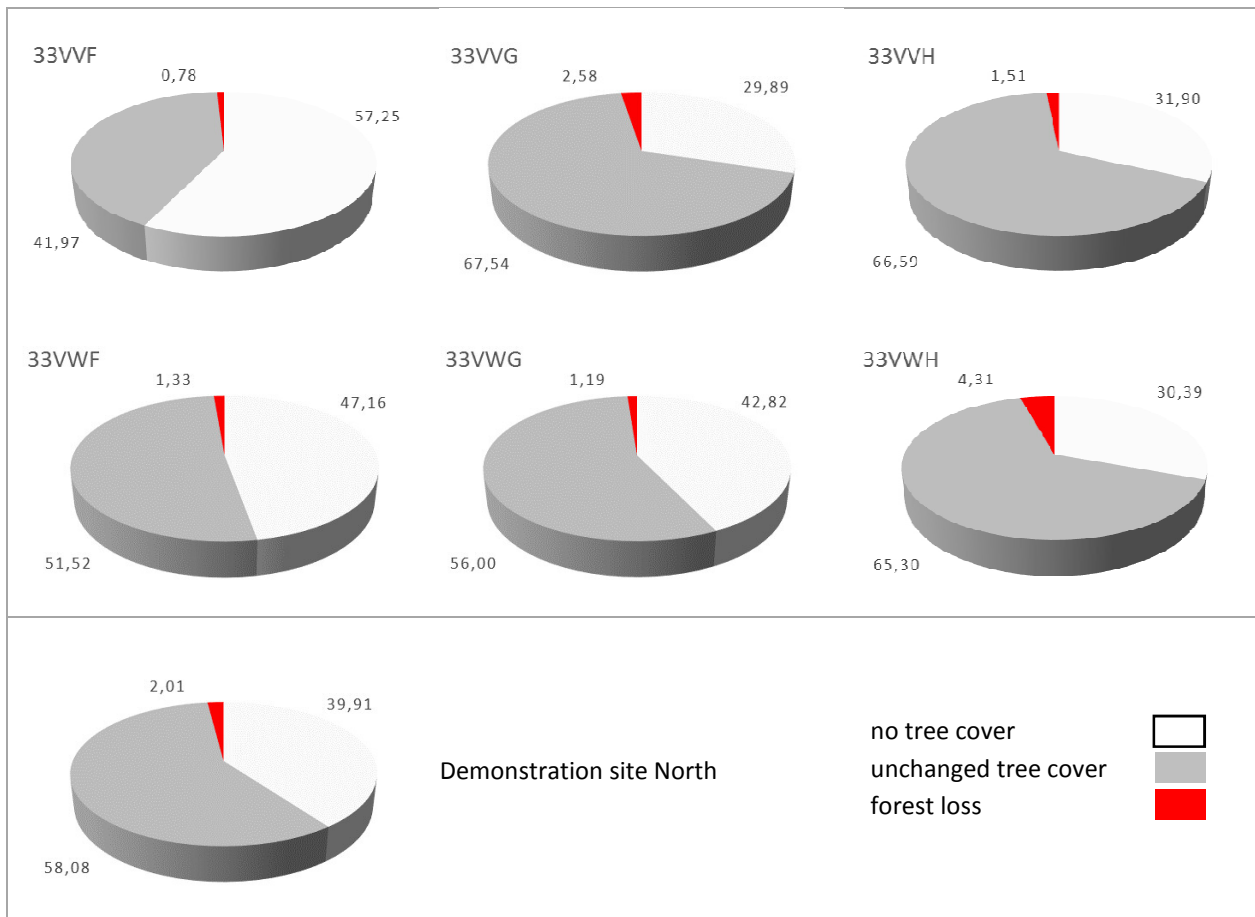


Figure 5-41: Final statistics of the TCC layer per Sentinel-2 tile and for the whole demonstration site North

In total, more than 15,900 areas of forest loss $\geq 3\text{ha}$ have been detected, most of them in the northern part (tile 33VH) and in the centre part (tile 33VVG) of the demonstration site. Within these tiles, the pattern of detected losses strongly corresponds to the availability of cloud-free images, as indicated by the Sentinel-2 Data Score Layer, see Figure 5-42 below. Tile 33VVF shows the lowest proportional change with 0.87%, whereas the tiles 33VVG, 33VH, 33VWF and 33VWG are within a range of 1.2% to 1.6%. Tile 33VWH is the one with the second highest forest proportion and shows the highest loss rate with 4.31%.

It becomes quite obvious, that the number of cloud-free observations had a strong influence on the quality of the derived TCM 2017 for certain areas within specific tiles (33VH and 33VVG). 1-2 cloud-free observations at pixel level within the acquisition period March to August 2017 were evidently not sufficient to capture the tree cover in sufficient detail. The revealed commission errors in the TCC, introduced by omission errors in the TCM 2017, are the main source of falsely detected changes within these tiles and need to be addressed in future improvement approaches.

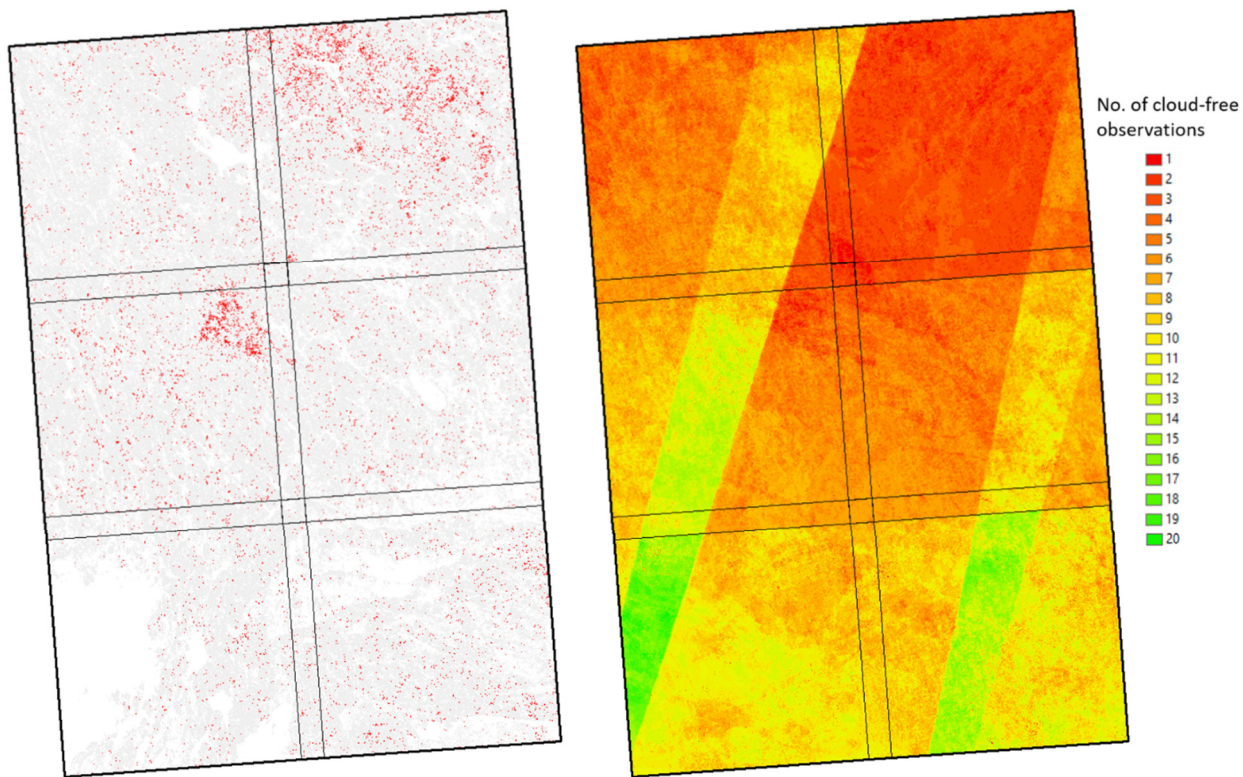


Figure 5-42: Detected losses within TCC layer in red (left) and number of cloud-free observations (right)

The final TCC 1517 layer has been subsequently validated using the best available reference and guiding data. Guiding data are those that have been used in the production process and consist of:

- Sentinel-2A+B scenes in 10m spatial resolution acquired between March and August 2017

Reference data are any available suitable EO data sources, namely:

- Sentinel-2A and Landsat 8 from 2015/2016
- DWH: VHR_IMAGE_2015
- DWH: D2_MG2b_ECOL_011a (Archive standard Optical VHR1)
- Bing Maps
- Google Earth Pro

The accuracy assessment has been performed using a stratified random sampling approach with 2,341 segments. Segments have been visually interpreted using the guiding and reference data listed above. The analysis procedure is the same as for the DLT 2017 described above. The Distribution of the segments is illustrated in Figure 5-43 below.

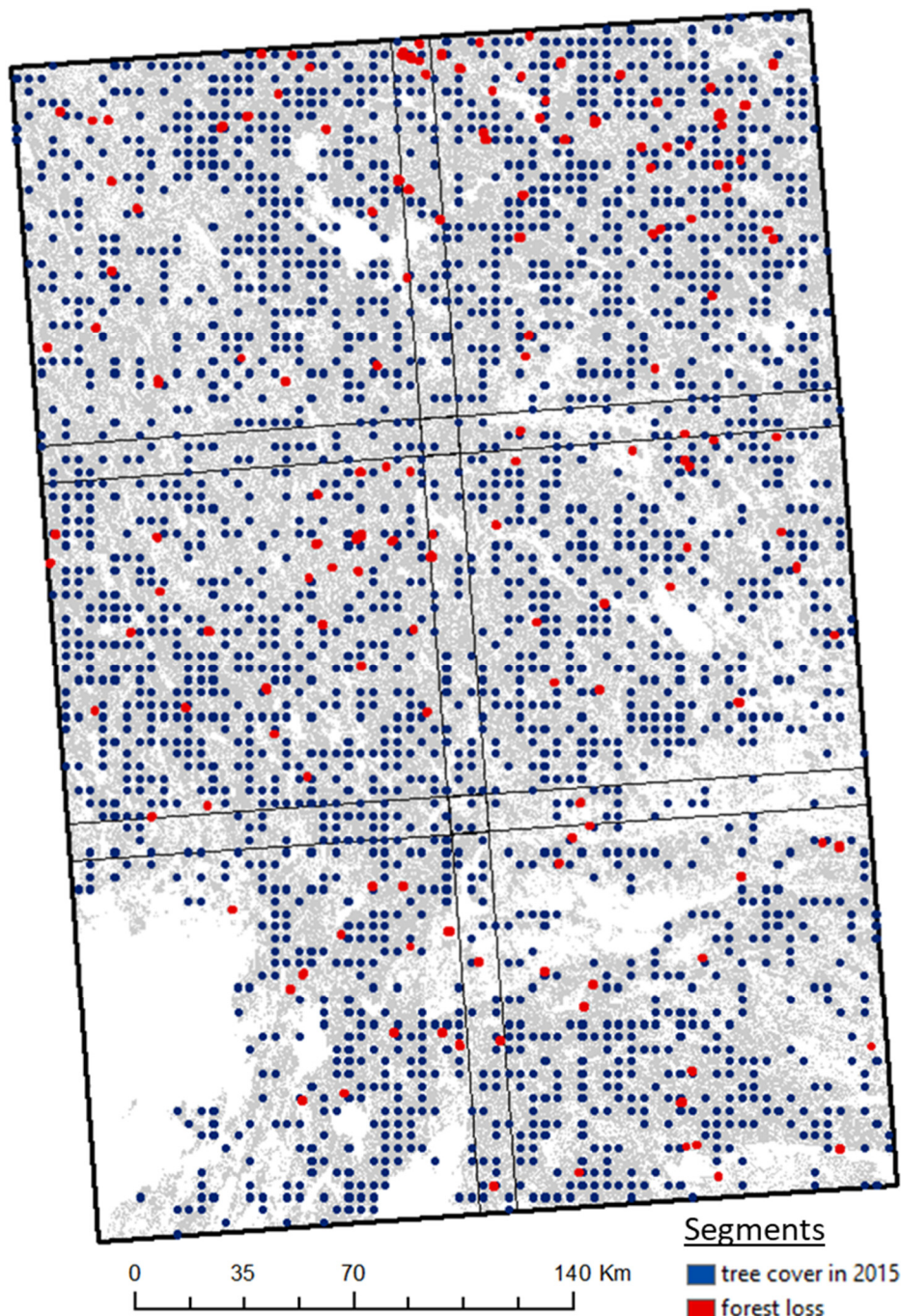


Figure 5-43: Distribution of validation segments for the TCC layer.

Results of the initial accuracy assessment are presented in Table 5-10.

Table 5-10: Initial accuracy assessment results for the Incremental Update Layer TCC

		Reference Data					
		CLASS	10	12	Total	User	95% CI
TCC 1517	10	2,166	23	2,189	98.95	0.45	
	12	95	57	152	37.50	8.03	
	Total	2,261	80	2,341			
	Prod.	95.80	71.25		Overall Accuracy: 94.96%		
	95% CI	0.85	10.54				

The Incremental Update shows a very high OA of 94.96%, which is due to the overall high proportion of (correctly classified) unchanged areas (class 10) compared to the identified forest loss (class 12). In the “unchanged” class (class code 10), a producer’s accuracy of 95.80% and a user’s accuracy of 98.95% has been reached. However, the assessment also reveals a strong overestimation of forest loss (class code 12). The producer’s accuracy is at 71.25% which means that the majority of real forest losses has been automatically captured (with a 28.75% omission error), however the user’s accuracy reaches 37.50% only (i.e. a very high commission error of 62.5%), which is far below expectations and the envisaged target accuracy.

Typical errors in the forest loss class which lead to an overestimation of the forest loss area are due to commission errors within the TCM 2015, specifically within peatbog areas, which have spectrally similar characteristics as coniferous forest stands. Omission errors in the TCM 2017 contribute (although to a lesser extent) to the overall forest loss class error rate (see Figure 5-44).

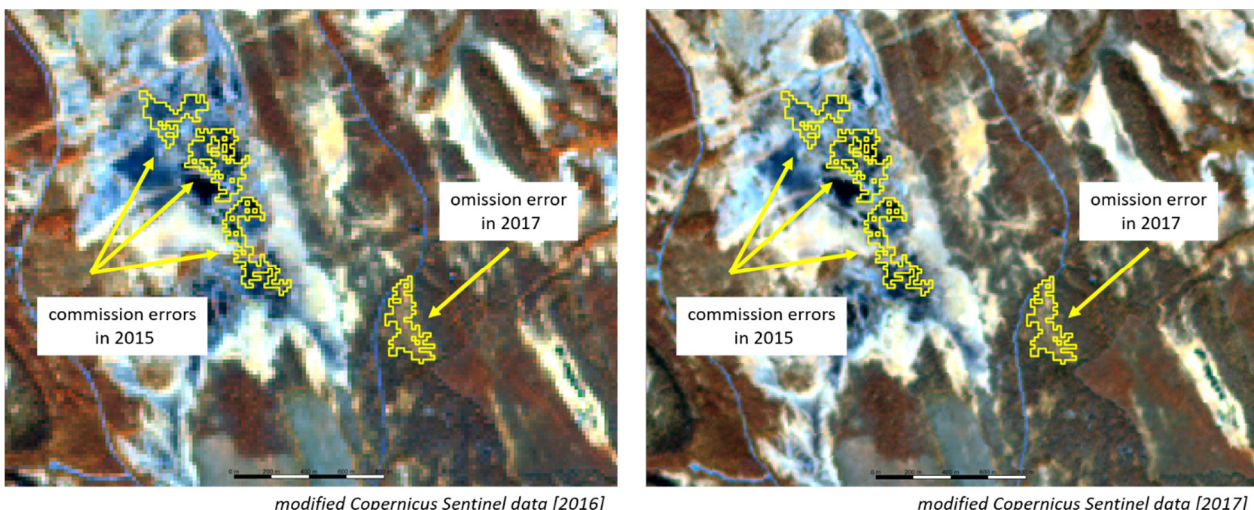


Figure 5-44: Example for omission and commission errors of forest loss within the same plot in the TCC layer.
Left: 20m Sentinel-2A scene from June 2016; right: Sentinel-2B scene from June 2017.

Commission errors of the forest loss class have been analysed in detail, and the following reasons have been identified:

- 43 segments show commission errors in the TCM 2015 (as derived from DLT 2015),
- 52 segments show omission errors in the TCM 2017, all of which are within areas with 1 or 2 EO data observations only.

The latter case has evidently a tremendous influence. In order to simulate a more realistic scenario of a future fully operational implementation phase, i.e. taking into account further EO data sources (such as Sentinel-1, Landsat-8) for gap-filling, a second test scenario has been assessed. In this test, the actual cloud cover (and resulting lack of coverages) issue is put aside, by substituting the affected segments with new randomly sampled segments in areas with good EO data time series situation. The results of an associated modified accuracy assessment are presented in Table 5-11 below.

Table 5-11: Final accuracy assessment results for the Incremental Update Layer TCC

		Reference Data					
		CLASS	10	12	Total	User	95% CI
TCC 1517	10	2,170	19	2,189	99.13	0.41	
	12	66	86	152	56.58	8.21	
	Total	2,236	105				
	Prod.	97.05	81.90				
		95% CI	0.72	7.84	Overall Accuracy: 96,73%		

This new assessment shows significantly better accuracies for the forest loss, applicable for both, the producer's and user's accuracy. The producer's accuracy is now at 81.90% and the user's accuracy increased by 19% to a value of 56.6%. Again, commission errors have been visually checked and assessed:

- 30 segments show commission errors in the TCM 2015,
- 36 segments show omission errors in the TCM 2017.

This second assessment shows an approximately equal distribution of errors within the two Tree Cover Masks 2015 and 2017, which have been used to create the Incremental Update layer.

Independent from the shortcomings of the TCC in certain parts, most of the detected losses confirm an intensive forest management in this area, which had been one of the decision criteria for the final selection of this demonstration site. Even if spatially limited, the Incremental Update provides information on forest loss within a one-year cycle, which is fully in line with the proposed update frequency of 1 year. The accuracy of detected losses needs to be further increased, e.g. by incorporation of Sentinel-1 SAR data, a possible further change or extension of the observation period and/or an increase of the cloud cover threshold for time feature calculation. This will be addressed in the second project phase.

In general, the selected map-to-map change approach is working well, but is partially and significantly dependent on the quality of the available products/maps. Even though the TCM 2015 has reached the target accuracy of 90% for producer's and user's accuracy at pan-European level, it has to be stated that this represents an average value, which implicates regional differences in the thematic accuracy across Europe. The northern countries are known (together with some Mediterranean countries) as the most difficult areas in the HRL Forest 2015 production. This fact is reflected in the tree cover extent of the two masks 2015 and 2017 for the demonstration site North. Consequently, mask errors are revealed by the selected change detection approach.

From this perspective, future corrections as well as (partial) re-processing/update of historic HRL Forest products might be an option to work towards a higher significance for tree cover and forest loss, and layer consistency over time. In addition, manual enhancements of the derived changes need to be taken into account in order to meet the user expectations and requirements.

The following figures give an impression of the kind and size of negative changes (i.e. forest losses) within the demonstration site, presumably all caused by intensive forest management activities (i.e. clear-cuts). Each of the below examples shows (a) one VHR1 image from 2015 (± 1 year) before the respective clear-cut has taken place, (b) one VHR1 image from 2017 specifically acquired in the frame of the ECoLaSS DWH quota where the clear-cut is visible, and (c) the 10m-resolution Sentinel-2 based DLT 2017 product (overlaid to the 2017 VHR1 image). These typical examples provide evidence that the incremental update is able to capture the tree cover removal quite adequately, at least if a sufficient number of Sentinel data is available. The examples also show that despite the coarser 10m spatial resolution (as compared to the shown VHR1 data), the Sentinel-2 based DLT 2017 fits the delineation of changes well.

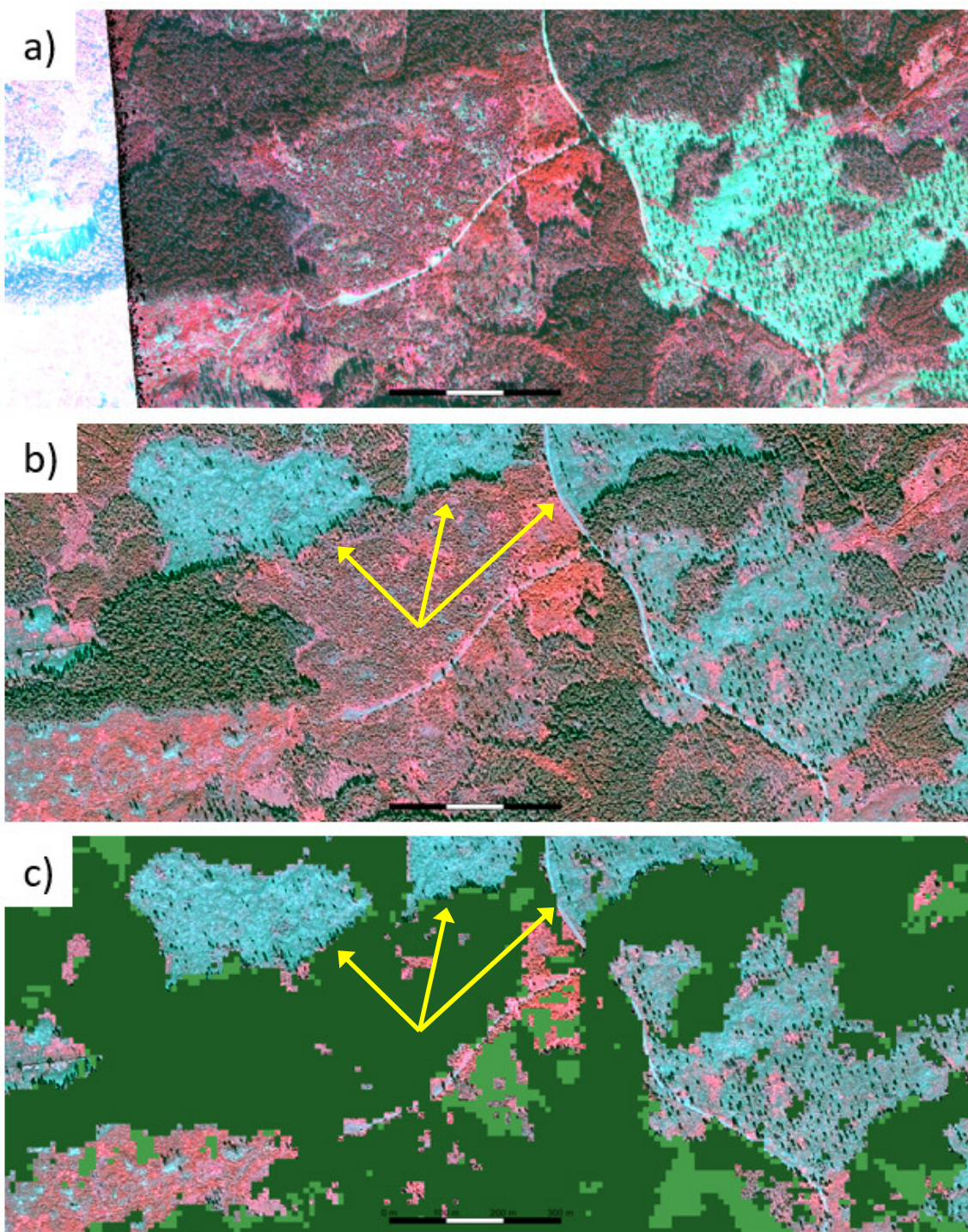


Figure 5-45: Example 1: Forest cover loss in demonstration site North: a) VHR_IMAGE_2015;
b) D2_MG2b_ECOL_011a; c) D2_MG2b_ECOL_011a overlaid with improved 10m DLT 2017

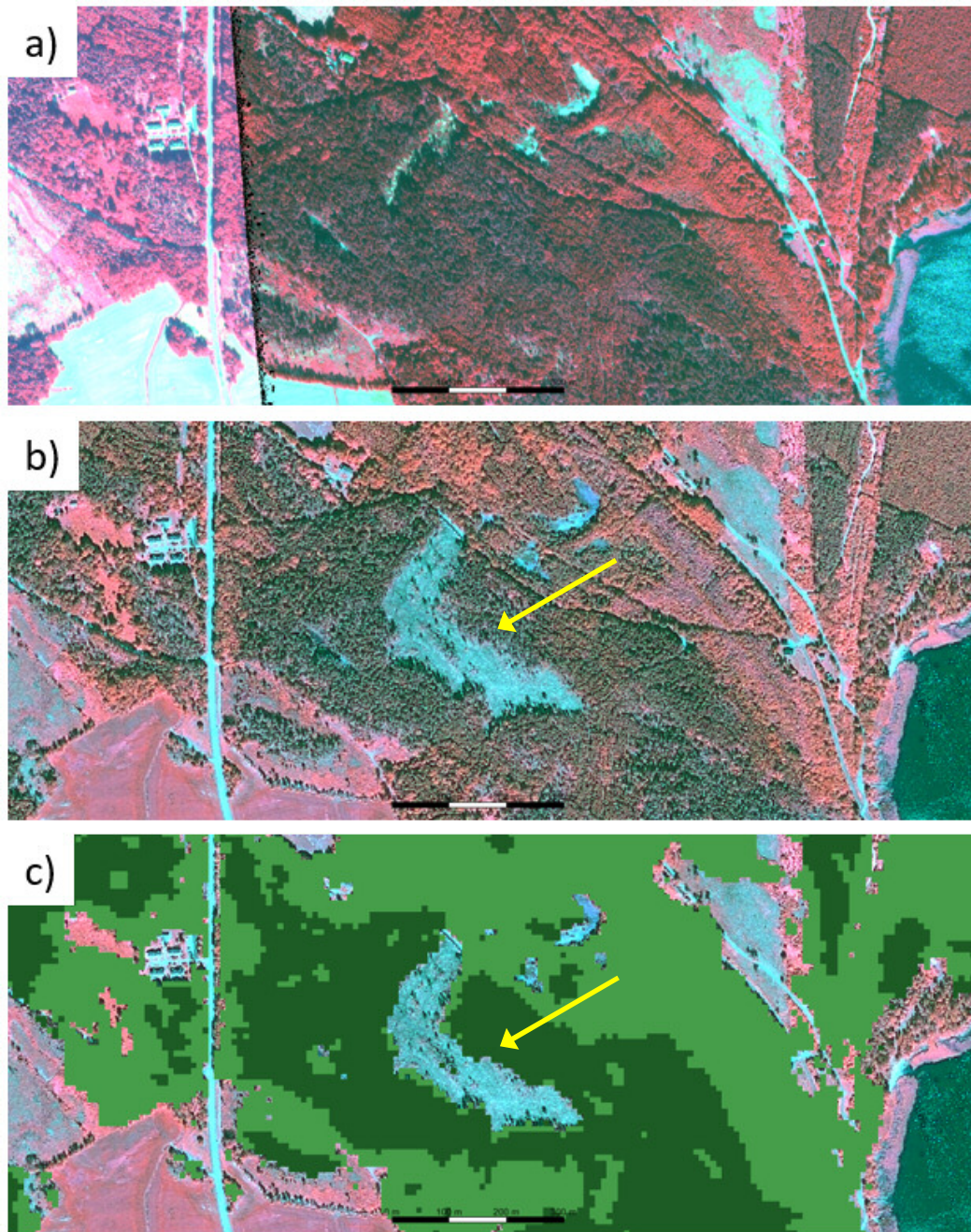


Figure 5-46: Example 2: Forest cover loss in demonstration site North: a) VHR_IMAGE_2015; b) D2_MG2b_ECOL_011a; c) D2_MG2b_ECOL_011a overlaid with improved 10m DLT 2017

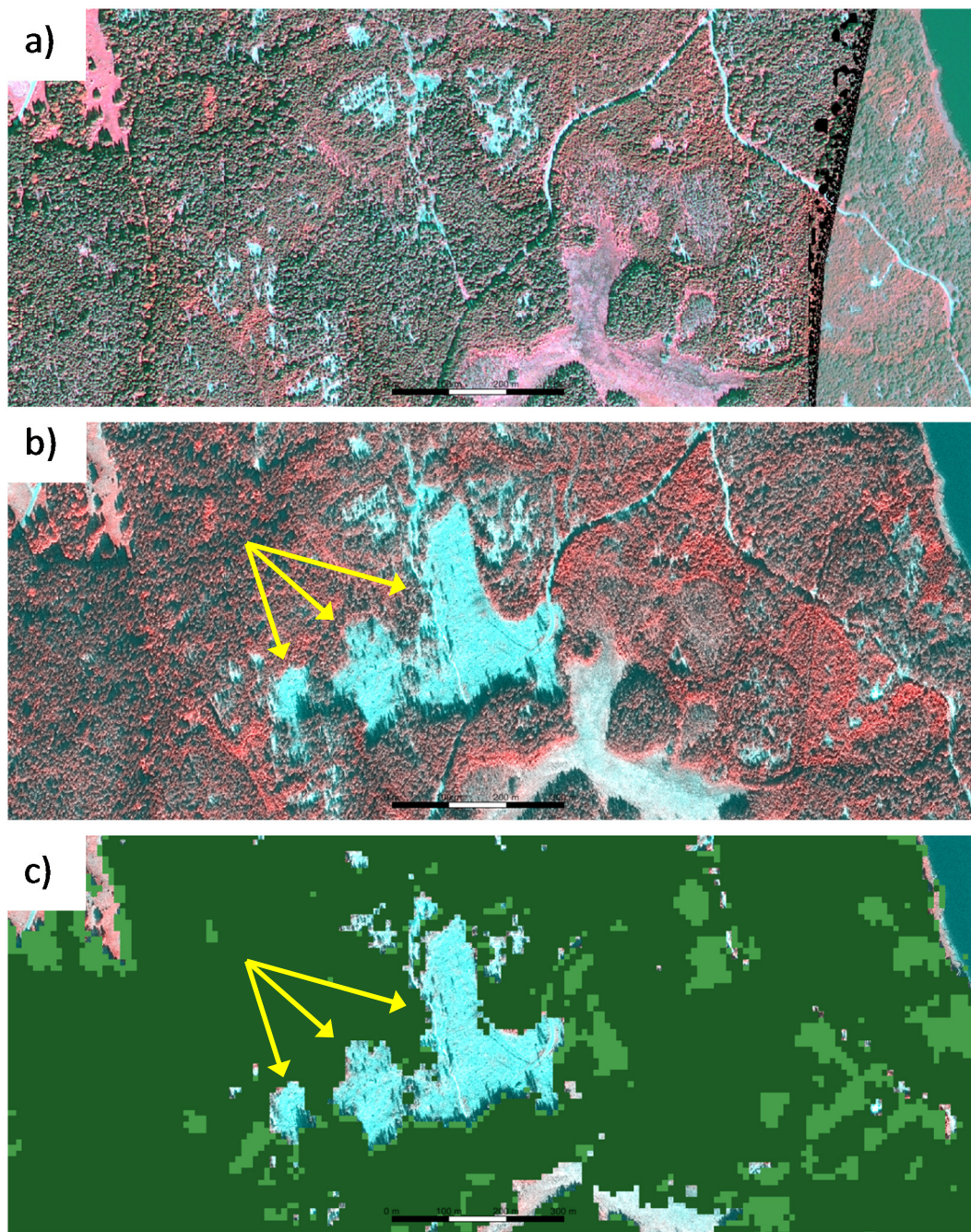


Figure 5-47: Example 3: Forest cover loss in demonstration site North: a) VHR_IMAGE_2015; b) D2_MG2b_ECOL_011a; c) D2_MG2b_ECOL_011a overlaid with improved 10m DLT 2017

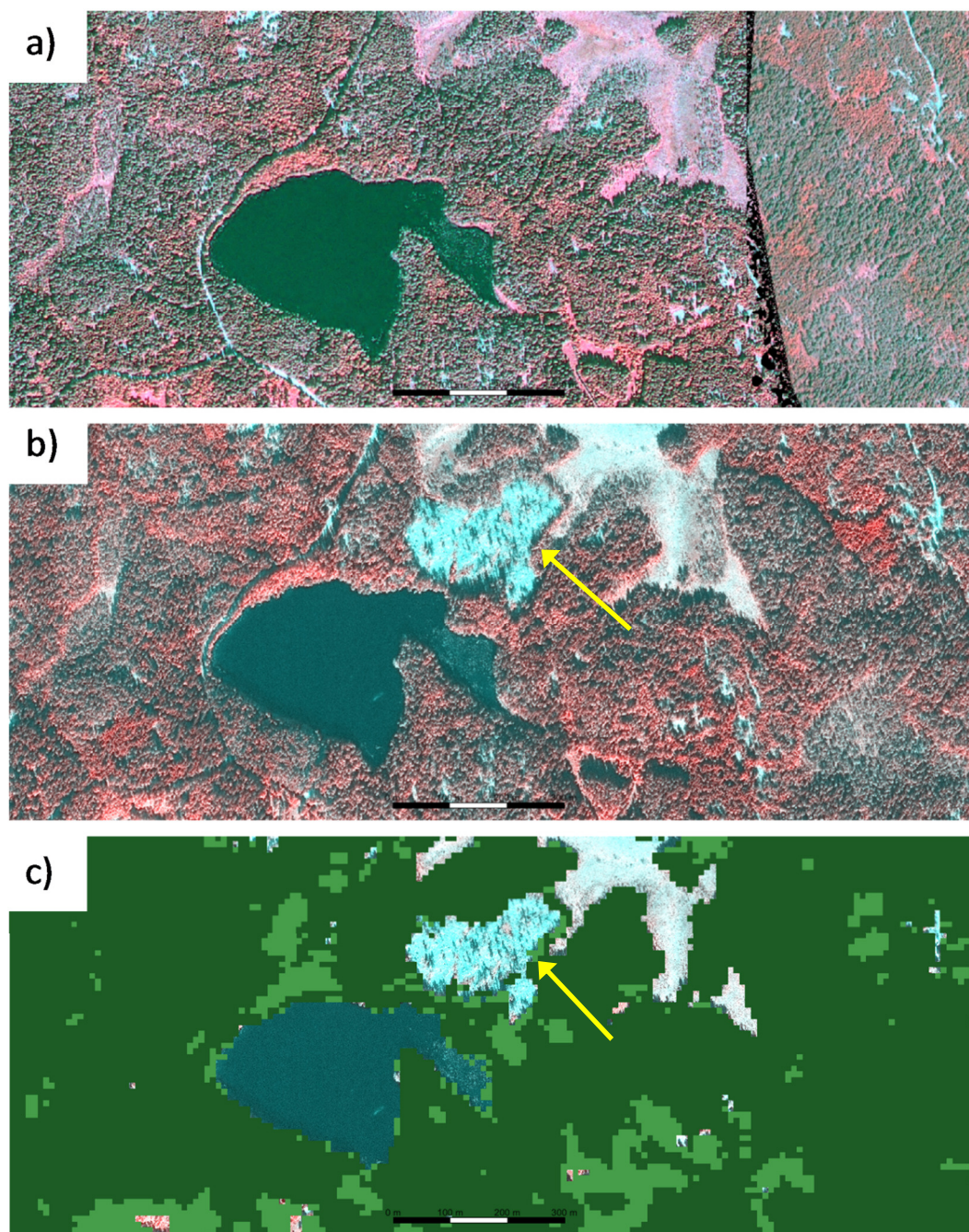


Figure 5-48: Example 4: Forest cover loss in demonstration site North: a) VHR_IMAGE_2015; b) D2_MG2b_ECOL_011a; c) D2_MG2b_ECOL_011a overlaid with improved 10m DLT 2017

5.3 Prototype Specifications

This section provides a description of the dataset properties and metadata for the implemented prototypes, also referring to “P42.2 - Data Sets of HR Layer Incremental Updates”.

Within ECoLaSS, a standardised and harmonised product file naming convention for all prototypes has been developed which is oriented along the already existing naming convention of the CLMS High Resolution Layers. The naming convention consists of the following 7 descriptors:

THEME YEAR RESOLUTION EXTENT EPSG TYPE VERSION
as follows:

THEME

3 letter abbreviation for main products (DLT (dominant leaf type), TCC (tree cover change), GRA (grassland), IMD (imperviousness degree), IMC (imperviousness change classified), CRT (crop type), CRM (crop mask) and new land cover products, to be decided.

REFERENCE YEAR

2017 in four digits; change products in four digits (e.g. 1517)

RESOLUTION

Four-digit (020m and 010m)

EXTENT

2-digit code for demonstration-sites (CE (central), NO (north), WE (west), SW (southwest), SE (southeast), SA (South Africa), ML (Mali))

EPSG

5-digit EPSG code (geodetic parameter dataset code by the European Petroleum Survey Group) “03035” for the European LAEA projection

TYPE

prototype

VERSION

3-digit code “v01”

EXAMPLE:

“DLT_2017_010m_NO_03035_prototype_v01.tif” stands for: Dominant Leaf Type, 2017 reference year, 10m, Demonstration-site North, European projection (EPSG: 3035), prototype, version 01

“TCC_1517_020m_NO_03035_prototype_v01.tif” stands for: Tree Cover Change, 2015-2017 change period, 20m, Demonstration-site North, European projection (EPSG: 3035), prototype, version 01

The raster products of the ECoLaSS prototypes are delivered as GeoTIFF (*.tif) with world file (*.tfw), pyramids (*.ovr), attribute table (*.dbf) and statistics (*.aux.xml), enabling an instant illustration and analysis of the products within Geographic Information System (GIS) software. Each product is accompanied with a product-specific colour table (*.clr) and INSPIRE-compliant metadata in XML format.

Metadata are provided together with the products as INSPIRE-compliant XML files according to the EEA Metadata Standard for Geographic Information (EEA-MSGI). EEA-MSGI has been developed by EEA to meet

needs and demands for inter-operability of metadata. EEA's standard for metadata is a profile of the ISO 19115 standard for geographic metadata and contains more elements than the minimum required to comply with the INSPIRE metadata rules. Detailed conceptual specifications of the EEA-MSGI and other relevant information on metadata can be found at <http://www.eionet.europa.eu/gis>.

The prototype specifications for the IMD and IMC layers are listed hereafter in Table 5-12 and Table 5-13, followed by the specifications for the DLT (Table 5-14) and TCC (Table 5-15).

Table 5-12: Detailed specifications for the improved primary status layer Imperviousness 2017

Imperviousness Degree 10m	Acronym	Product category
	IMD	Improved Primary Status Layer
Reference year		
2017		
Extent		
Demonstration site South-West		
Geometric resolution		
Pixel resolution 10m x 10m, fully conform with the EEA reference grid		
Coordinate Reference System		
European ETRS89 LAEA projection		
Geometric accuracy (positioning scale)		
Less than half a pixel. According to ortho-rectified satellite image base delivered by Theia.		
Thematic accuracy		
Minimum 90% user's / producer's accuracy in general for status layers for a (derived) built-up/non built up map. Threshold to be applied in transforming imperviousness to built-up mask at 1%.		
Data type		
8bit unsigned integer raster with LZW compression		
Minimum Mapping Unit (MMU)		
Pixel-based (no MMU)		
Necessary attributes		
Raster value, count, class name		
Raster coding (thematic pixel values)		
0: all non-impervious areas		
1-100: imperviousness values		
254: unclassifiable (no satellite image available, or clouds, or shadows)		
255: outside area		
Metadata		
XML metadata files according to INSPIRE metadata standards		
Delivery format		
GeoTIFF		
Colour table		
ArcGIS *.clr format		

Class Code	Class Name	Red	Green	Blue	
0	all non-impervious areas	240	240	240	
1	1% imperiousness value	255	237	195	
50	50% imperiousness value	175	74	51	
100	100% imperiousness value	113	12	2	
254	unclassifiable (no satellite image available, or clouds, or shadows)	153	153	153	
255	outside area	0	0	0	

Table 5-13: Detailed specifications for the Incremental Update Layer Impermeability Change Classified

Imperviousness Change Classified 20m	Acronym	Product category
	IMC	Incremental Update Layer
Reference year		
2015/16-2017		
Extent		
Demonstration site South-West		
Geometric resolution		
Pixel resolution 20m x 20m, fully conform with the EEA reference grid		
Coordinate Reference System		
European ETRS89 LAEA projection		
Geometric accuracy (positioning scale)		
Less than half a pixel. According to ortho-rectified satellite image base delivered by Theia.		
Thematic accuracy		
90% user's / producer's accuracy for derived IMD changes		
Data type		
8bit unsigned integer raster with LZW compression		
Minimum Mapping Unit (MMU)		
Pixel-based (no MMU)		
Necessary attributes		
Raster value, count, class name		
Raster coding (thematic pixel values)		
0: unchanged areas with impermeability degree of 0		
1: new cover - increased impermeability density, zero IMD at first reference date		
2: loss of cover - decreasing impermeability density, zero IMD at second reference date		
10: unchanged areas, IMD>0 at both reference dates		
11: increased impermeability density, IMD>0 at both reference dates		
12: decreased impermeability density, IMD>0 at both reference dates		
254: unclassifiable in any of parent status layers		
255: outside area		

Metadata					
XML metadata files according to INSPIRE metadata standards					
Delivery format					
GeoTIFF					
Colour table					
ArcGIS *.clr format					
Class Code	Class Name	Red	Green	Blue	
0	unchanged areas with imperviousness degree of 0	240	240	240	
1	new cover - increased imperviousness density, zero IMD at first reference date	255	0	0	
2	loss of cover - decreasing imperviousness density, zero IMD at second reference date	0	100	0	
10	unchanged areas, IMD>0 at both reference dates	156	156	156	
11	increased imperviousness density, IMD>0 at both reference dates	255	191	0	
12	decreased imperviousness density, IMD>0 at both reference dates	64	178	0	
254	unclassifiable in any of parent status layers	153	153	153	
255	outside area	0	0	0	

Table 5-14: Detailed specifications for the improved primary status layer Dominant Leaf Type 2017

Dominant Leaf Type 10m	Acronym	Product category
	DLT	Improved Primary Status Layer
Reference year		
2017		
Extent		
Demonstration site North		
Geometric resolution		
Pixel resolution 10m x 10m, fully conform with the EEA reference grid		
Coordinate Reference System		
European ETRS89 LAEA projection		
Geometric accuracy (positioning scale)		
Less than half a pixel. According to ortho-rectified satellite image base delivered by ESA.		
Thematic accuracy		
Minimum 90% user's / producer's accuracy in general for status layers		
Data type		
8bit unsigned raster with LZW compression		
Minimum Mapping Unit (MMU)		
Pixel-based (no MMU)		

Necessary attributes																																				
Raster value, count, class name, area (in km2), area percentage (taking outside area not into account)																																				
Raster coding (thematic pixel values)																																				
0: all non-tree covered areas 1: broadleaved trees 2: coniferous trees 254: unclassifiable (no satellite image available, or clouds, or shadows) 255: outside area																																				
Metadata																																				
XML metadata files according to INSPIRE metadata standards																																				
Delivery format																																				
GeoTIFF																																				
Colour table																																				
ArcGIS *.clr format																																				
<table border="1"> <thead> <tr> <th>Class Code</th> <th>Class Name</th> <th>Red</th> <th>Green</th> <th>Blue</th> <th></th> </tr> </thead> <tbody> <tr> <td>0</td> <td>all non-tree covered areas</td> <td>240</td> <td>240</td> <td>240</td> <td></td> </tr> <tr> <td>1</td> <td>broadleaved trees</td> <td>70</td> <td>158</td> <td>74</td> <td></td> </tr> <tr> <td>2</td> <td>coniferous trees</td> <td>28</td> <td>92</td> <td>36</td> <td></td> </tr> <tr> <td>254</td> <td>unclassifiable (no satellite image available, or clouds, or shadows)</td> <td>153</td> <td>153</td> <td>153</td> <td></td> </tr> <tr> <td>255</td> <td>outside area</td> <td>0</td> <td>0</td> <td>0</td> <td></td> </tr> </tbody> </table>	Class Code	Class Name	Red	Green	Blue		0	all non-tree covered areas	240	240	240		1	broadleaved trees	70	158	74		2	coniferous trees	28	92	36		254	unclassifiable (no satellite image available, or clouds, or shadows)	153	153	153		255	outside area	0	0	0	
Class Code	Class Name	Red	Green	Blue																																
0	all non-tree covered areas	240	240	240																																
1	broadleaved trees	70	158	74																																
2	coniferous trees	28	92	36																																
254	unclassifiable (no satellite image available, or clouds, or shadows)	153	153	153																																
255	outside area	0	0	0																																

Table 5-15: Detailed specifications for the Incremental Update Layer Tree Cover Change

Tree Cover Change 20m	Acronym TCC	Product category Incremental Update Layer
Reference year 2015/16-2017		
Extent Demonstration site North		
Geometric resolution Pixel resolution 20m x 20m, fully conform with the EEA reference grid		
Coordinate Reference System European ETRS89 LAEA projection		
Geometric accuracy (positioning scale) Less than half a pixel. According to ortho-rectified satellite image base delivered by ESA.		
Thematic accuracy 80-85% overall accuracy		

Data type	8bit unsigned integer raster with LZW compression																																													
Minimum Mapping Unit (MMU)	3 ha (is expected to decrease)																																													
Necessary attributes	Raster value, count, class name, area (in km2), percentage (taking outside area not into account)																																													
Raster coding (thematic pixel values)	0: all non-tree covered areas in 2015 10: unchanged tree cover in 2015 11: forest regrowth (not relevant for this implementation of the TCC) 12: forest loss 254: unclassifiable (no satellite image available, or clouds, or shadows) 255: outside area																																													
Metadata	XML metadata files according to INSPIRE metadata standards																																													
Delivery format	GeoTIFF																																													
Colour table	ArcGIS *.clr format																																													
<table border="1"> <thead> <tr> <th>Class Code</th><th>Class Name</th><th>Red</th><th>Green</th><th>Blue</th><th></th></tr> </thead> <tbody> <tr> <td>0</td><td>all non-tree covered areas in 2015</td><td>255</td><td>255</td><td>255</td><td></td></tr> <tr> <td>10</td><td>unchanged tree cover in 2015</td><td>240</td><td>240</td><td>240</td><td></td></tr> <tr> <td>11</td><td>forest regrowth</td><td>28</td><td>72</td><td>201</td><td></td></tr> <tr> <td>12</td><td>forest loss</td><td>255</td><td>0</td><td>0</td><td></td></tr> <tr> <td>254</td><td>unclassifiable (no satellite image available, or clouds, or shadows)</td><td>153</td><td>153</td><td>153</td><td></td></tr> <tr> <td>255</td><td>outside area</td><td>0</td><td>0</td><td>0</td><td></td></tr> </tbody> </table>					Class Code	Class Name	Red	Green	Blue		0	all non-tree covered areas in 2015	255	255	255		10	unchanged tree cover in 2015	240	240	240		11	forest regrowth	28	72	201		12	forest loss	255	0	0		254	unclassifiable (no satellite image available, or clouds, or shadows)	153	153	153		255	outside area	0	0	0	
Class Code	Class Name	Red	Green	Blue																																										
0	all non-tree covered areas in 2015	255	255	255																																										
10	unchanged tree cover in 2015	240	240	240																																										
11	forest regrowth	28	72	201																																										
12	forest loss	255	0	0																																										
254	unclassifiable (no satellite image available, or clouds, or shadows)	153	153	153																																										
255	outside area	0	0	0																																										

6 Conclusions and Outlook

In view of a future **HRL Forest** prototype, it can be stated that the full exploitation of the Sentinel-2A+B time series of the spring to summer period 2017 using time features has generally proven a stable and reliable approach, capable to successfully differentiate between tree covered and non-tree covered areas as well as broadleaved and coniferous tree/forest stands in a seamless and consistent manner. With the selected innovative approach covering mainly a time period of six months, it could be demonstrated that an almost fully automatic DLT status layer generation is generally possible with satellite data acquired within one year and in 10m spatial resolution. This improved primary status layer has been produced without manual enhancements (unlike in previous HRL Forest implementations) and provides promising accuracy figures, which can be generally further improved by means of plausibility checks, manual enhancements, a further refinement of the classification workflow, and potentially a future SAR data integration. In general, the achieved higher degree of automation in the classification process might contribute to shorter production times in the future.

In addition, cloud coverage issues could be partially addressed by an extension of the observation period. However, this procedure has some limitations for areas with generally very high cloud cover rates (e.g. British Isles, Scandinavia and French-Guiana), as it is also the case for two out of the six tiles within the demonstration site North. Consequently, the integration of Sentinel-1 SAR data needs to be addressed in the next project phase.

With the applied change detection method, using the 20m TCM 2015 mask as benchmark, an incremental update layer could be simulated within the confines of the previous (historic) 2015 inventory at 20m spatial resolution, providing information on forest cover loss within a relatively short time frame of ≤ 12 months. Due to the reasons discussed in section 5.2.3, the achieved accuracy of the incremental update layer is still not sufficient, but can presumably be improved in the future. As this approach is to a certain degree dependent on the initial thematic quality of the input data (in form of Tree Cover Masks for certain reference years), sufficient results might be obtained, if the thematic accuracy and spatial consistency of the layers will be further improved and harmonised. On the other hand, the update approach has been demonstrated using a historic 20m mask with a specific lineage. A full comparability and update feasibility can only be finally assessed when 10m forest products will become available for at least two reference years. This will be further analysed in the second project phase with EO data from 2018.

At this stage, it should be noted, that the quite ambitious and experimental 20m Dominant Leaf Type Change product of the Copernicus HRL Forest 2015 product portfolio (covering the time period 2012 to 2015; providing 14 thematic classes, thereof 10 change classes) taking different combinations of leaf type and tree cover density changes into account, has been assessed as too complex for users. The initially defined target accuracy of 90% for producer's and user's accuracy for detected changes could by far not be achieved within the HRL 2015 production due to the complexity of the product and the specific lineage of the input data (HRL Forest products 2012 and 2015). Therefore, it is recommended to revise (simplify) the current product specifications to achieve more reliable product characteristics and accuracies for a forest change product in the HR domain. The proposed Incremental Update in form of the Tree Cover Change layer is going towards such a simplification of the change aspect and is strongly highlighting the temporal aspect.

From a data perspective, an operational roll-out of the incremental update at pan-European level seems to be feasible in a 1-year update cycle with the Sentinel-2 constellation, potentially regionally supported by Sentinel-1 data. However, the selected approach will require further research to validate the transferability towards areas of different geographic conditions and seasonal patterns. In this context, the following further improvements and additional research are envisaged for the second project phase with respect to incremental updates:

- (i) testing of further time features and consequent forward feature selection
- (ii) feature analysis of misclassified areas, applicable for both, TCM and DLT
- (iii) adding Sentinel-1 SAR time series into the incremental update layer derivation
- (iv) 10m based change detection based on other multi-temporal approaches (e.g. 2017 period vs. 2018 period)

The abovementioned development points aim to increase the overall thematic accuracy, establish a higher automation level, integrate dense time series of optical and SAR data, provide more reliable forest products at 10m spatial resolution and exploit the available temporal information in the best possible manner.

The implementation of the prototypes on the **HRL Imperviousness** led to methods now fully operational (fully obtained automatically without manual enhancement) with a change layer (IMC) produced at 20m and a status layer (IMD) at 10m. Nevertheless, results from Sentinel-1 are somewhat not as good as Sentinel-2 and need to be improved in phase 2.

The relative magnitude of actual change has been estimated to only 5.8% of the total (fully automatically derived) change areas. Thus, the errors concern the remaining 94% of the change areas detected. There is a high amount of omission errors (78.9%) coming from the reference data set (HRL IMP 2015), directly impacting the change areas detected. Nevertheless, it should be noted that the specifications of the HRL 2015 reference layer are different from the HRL 2017 input data. Indeed, for 2015 the data contains a 20-meter spatial resolution production mostly based on Landsat data, whereas the HRL 2017, based on Sentinel-2, contains a 10-meters resolution; the latter explains that most of the omission errors concern small and isolated built-up features.

The following further improvements and investigations are suggested as part of the second project phase:

- (i) Next update could be produced at 10m for both status (IMD) and change layers (IMC),
- (ii) Separation of buildings toward the flat impervious surfaces to be tested,
- (iii) Integration of Sentinel-1 times series to be implemented.

Depending on the actual specifications of the upcoming operational HRL 2018 ITT, the work plan for the WP 42 in the second phase may have to be adjusted to keep developing/further enhancing prototypes in complementarity to the 2018 operational HRL implementation. In the same line, the HRL Grassland will be re-assessed to check for the need of respective incremental update investigations.

References

- Alajlan N., Bazi, Y., Al Hichri H., Melgani F., Yager R., (2013)."Using OWA Fusion Operators for the Classification of Hyperspectral Images" in Journal of Selected Topics in Applied Earth Observations and Remote Sensing v. 6, n. 2 (2013), p. 602-614.
- Breiman, L. (2001). Random Forests. Machine Learning, 4(1), 5-32.
- Breiman, L. (1984). Classification and Regression Trees. Chapman & Hall/CRC.
- Camp-Valls, G., & Bruzzone, L. (2009). Kernek methods for remote sensing data analysis. John Wiley & Sons.
- Carlinet, E., & Géraud, T. (2014). A Comparative Review of Component TreeComputation Algorithms. IEEE Transactions on Image Processing, 23(9), 3885-3895.
- Crawford, M., Tuia, D., & Ynag, H. (2013). Active Learning: Any Value for Classification of Remotely Sensed Data? Proceedings of the IEEE, 593-608.
- Dalla Mura, M., Benediktsson, J., Waske, B., & Bruzzone, L. (2010, October). Morphological Attribute Profiles for the Analysisof Very High Resolution Images. IEEE Transactions on Geoscience and Remote Sensing, 48(10), 3747-3761.
- Florczyk, A., Ferri, S., Vasileios, S., Kemper, T., Halkia, M., Soille, P., & Pesaresi, M. (2015). A New European Settlement Map From Optical Remotely Sensed Data. IEEE Journal of Selected Topics in Applied Earth Observations and Remote Sensing, 1-15.
- Gallaun, H., Schardt, M., Linser, S., 2007. Remote sensing based forest map of Austria and derived environmental indicators. Proceedings of ForestSat.
- Henrich, V., Krauss, G., Götze, C., Sandow, C., 2012. IDB. URL: <http://www.indexdatabase.de> (Entwicklung einer Datenbank für Fernerkundungsindizes. AK Fernerkundung, Bochum)
- Lefebvre, A., Sannier, C., & Corpetti, T. (2016). Monitoring Urban Areas with Sentinel-2A Data: Application to the Update of the Copernicus High Resolution Layer Imperviousness Degree. Remote Sensing, 8(606), 1-21.
- Mas, J., & Flores, J. (2008). The application of artificial neural networks to the analysis of remotely sensed data. Internation Journal of Remote Sensing, 617-663.
- Mountrakis, G., Im, J., & Ogola, C. (2011). Support vector machines in remote sensing: A review. ISPRS Journal of Photogrammetry and remote Sensing, 66(3), 247-259.
- Pesaresi, M., & Benediktsson, J. A. (2001, March). A new approach for the morphological segmentation of high-resolution satellite imagery. IEEE Transactions on Geoscience and Remote Sensing, 39(2), 309-319.
- Pesaresi, M., G. Huadong, X. Blaes, D. Ehrlich, S. Ferri, L. Gueguen, M. Halkia, M. Kauffmann, T. Kemper, L. Lu, M. A. Marin-Herrera, G. K. Ouzounis, M. Scavazzon, P. Soille, V. Syrris & L. Zanchetta (2013) A Global Human Settlement Layer From Optical HR/VHR RS Data: Concept and First Results. IEEE Journal of Selected Topics in Applied Earth Observations and Remote Sensing, 6, 2102-2131.
- Tan, P.-N., Steinbach, M., & Kumar, V. (2006). Introduction to Data Mining. Pearson.
- Tuia D., Ratle F., Pacifici F., Kanevski M.F., Emery W.J., (2009). "Active Learning Methods for Remote Sensing Image Classification,"., IEEE Transactions on Geoscience and Remote Sensing, vol.47, no.7, pp.2218,2232, July 2009 doi: 10.1109/TGRS.2008.2010404.
- Tuia D., Volpi M., Copa L., Kanevski M., Munoz-Mar Jordi, (2011). A survey of active learning algorithms for supervised remote sensing image classification. IEEE Journal of Selected Topics in Signal Processing 5(3):606 - 617 · July 2011.

Wulder, M., Franklin, S. E., 2012. Remote sensing of forest environments: concepts and case studies. Springer Science & Business Media.

Zhang, L., Zhu, X., Zhang, L., & Du, B. (2016). Multidomain Subspace Classification for Hyperspectral Images. IEEE Transactions on Geoscience and Remote Sensing, 54(10), 1-13.